TECHNISCHE UNIVERSITÄT MÜNCHEN

Lehrstuhl für Systembiologie der Pflanzen

Sutent-Sensitive Kinases as Targets for
Anti-Diabetic Therapy Development

Mathias Alexander Falcenberg

Vollständiger Abdruck der von der Fakultät Wissenschaftszentrum Weihenstephan für Ernährung, Landnutzung und Umwelt der Technischen Universität München zur Erlangung des akademischen Grades eines

Doktors der Naturwissenschaften

genehmigten Dissertation.

Vorsitzender: Univ.-Prof. Dr. K. Schneitz
Prüfer der Dissertation:
                  1. Univ.-Prof. Dr. C. Schwechheimer
                  2. Hon.-Prof. Dr. h.c. A. Ullrich
                     (Eberhard-Karls-Universität Tübingen)

Die Dissertation wurde am 05.11.2012 bei der Technischen Universität München eingereicht und durch die Fakultät Wissenschaftszentrum Weihenstephan für Ernährung, Landnutzung und Umwelt am 08.03.2013 angenommen.

TABLE OF CONTENT

1 ABSTRACT

The observation that patients suffering from cancer as well as diabetes and being treated with tyrosine kinase inhibitors like sunitinib became independent of insulin injections led to the hypothesis that diabetes-relevant signaling systems must include negatively regulating kinases. Thus we tested the multi-targeted receptor tyrosine kinase inhibitor sunitinib, which has been approved for the treatment of metastatic renal cell carcinoma (mRCC), imatinib-resistant gastrointestinal stromal tumor (GIST) and pancreatic neuroendocrine tumors (NET) for its anti-diabetic impact *in vitro.* Therefore we analysed C2C12 myoblast, 3T3-L1 pre-adipocytes as well as the insulinoma cell lines RIN-5AH-T2B (rat) and beta-TC6 (mouse). We demonstrated that sunitinib leads to an enhanced formation of adipocytes in 3T3-L1 pre-adipocytes within a narrow concentration window. Moreover, we monitored a concentration dependent increase of PPARγ expression upon sunitinib treatment, which mimics the activation of PPARs by already available drugs like thiazolidinedione. Subsequently, sunitinib could be a starting point for the development of further therapeutic anti-diabetic PPARγ treatments. In parallel, sunitinib led to an increased insulin release in insulinoma-derived cell lines. In order to reveal new negatively regulated kinases that display an increased insulin release after inhibition, we performed a kinome wide siRNA screen in beta-TC6 cells. Hence, we present new negatively regulating kinases, in particular Scyl1, Grk5, Adck1 and EphA4, as new potential therapeutic targets for triggering insulin release. Here, Grk5 is the most promising target, which does not only increase the release of insulin but also improves the uptake of a glucose analogue after reduction of target gene expression. Furthermore, we identified compound structures that bind and inhibit the kinases candidates Scyl1 and Grk5, respectively. The identified Scyl1 competitors as well as Grk5 inhibitors display an insulin independent increase of 2-NBDG glucose analogue uptake as well as an improved and concentration dependant insulin release. In conclusion, sunitinib as well as the newly identified targets Scyl1, Grk5 and their respective inhibitors are paving the way for the development of new anti-diabetic drugs imitating the effect of thiazolidinediones, metformin or sulfonylurea.

2 ZUSAMMENFASSUNG

Die Beobachtung, dass bei Patienten, die sowohl an Krebs als auch an Diabetes litten, nach Einnahme von Tyrosinkinase-Inhibitoren wie Sutent keine Injektion von Insulin mehr benötigten, führte zu der Hypothese, dass diabetes-relevante Signalwege negativ regulierende Kinasen beinhalten. Dies veranlasste uns, den Rezeptor-Tyrosinkinase-Inhibitor Sunitinib, welcher zur Behandlung fortgeschrittener, metastasierter Nierenzellkarzinome (mRCC), imatinib-resistenter gastrointestinaler Stroma-Tumore (GIST) und metastasierter maligner neuroendokriner Bauchspeicheldrüsentumore (NET) zugelassen ist, auf anti-diabetische Eigenschaften zu prüfen. Dafür verwendeten wir C2C12 Myozyten, 3T3-L1 Pre-Adipozyten sowie auch insulinsekretierende Insulinoma-Zelllinien aus Mäusen (beta-TC6) und Ratten (RIN-5AH-T2B). In Rahmen dieser Studie konnten wir zeigen, dass Sunitinib *in vitro* innerhalb eines engem Konzentrationsfensters nicht nur zu der verstärkten Bildung von Adipozyten führt, sondern auch die Expression von PPARγ erhöht und somit der Wirkungsweise bereits zugelassener Medikamente wie Thiazolidinediones ähnelt. Zusätzlich konnten wir nachweisen, dass eine Behandlung mit Sunitinib *in vitro* eine gesteigerte Sekretion von Insulin in beta-TC6- und RIN-5AH-T2B-Zellen zur Folge hat. Basierend auf den Eigenschaften von Sunitinib als Tyrosinkinase-Inhibitor suchten wir weiterhin mittels eines kinomweiten siRNA Ansatzes nach negativ regulierenden Kinasen, welche nach Reduktion der Genexpression die Sekretion von Insulin erhöhen. Die Analyse führte zu neuen negativ-regulierenden Kinasen wie Scyl1, Grk5, Adck1 und EphA4, welche wir als potentielle anti-diabetische Ziele für therapeutische Ansätze hervorheben. Das Hauptaugenmerk liegt dabei auf der Kinase Grk5, die nicht nur zu einer verbesserten Insulinsekretion führt, sondern auch zur gesteigerten Aufnahme eines Glukose-Analogon. Weiterhin identifizierten wir Inhibitoren für Scyl1 und Grk5, die in zellbasierten Experimenten den gleichen Phänotypen zeigten, wie die Reduktion der Zielgenexpression. Zusammengefasst präsentieren wir neben einem möglichen anti-diabetischen Wirkungsmechanismus von Sutent, die beiden Kinasen Scyl1 und Grk5, sowie deren Inhibitoren, die innovative anti-diabetische Therapien ermöglichen.

3 INTRODUCTION

3.1 INSULIN – A MILESTONE OF MEDICINAL HISTORY

Insulin is a peptide hormone of 51 amino acids that regulates carbohydrate and fat metabolism in the body. In 1869, Paul Langerhans identified some previously unnoticed tissue scattered throughout the whole of the pancreas, today known as Islets of Langerhans, with at the time unknown function [1]. Later, in 1921, the important role of the islets of Langerhans and their relation to insulin had been put forward for the first time by Douard Laguesse. However, Nicolae Paulescu, a professor of physiology at the University of Medicine and Pharmacy in Bucharest, was the first scientist able to isolate insulin, which he called pancrein [2]. Frederick Banting, who became aware of this discovery, tried to improve the technique of insulin isolation in order to get a purer extract by causing atrophy in the greater part of the pancreas while keeping the islets of Langerhans intact. Together with J.J.R. Macleod, Charles Best and Frederick Banting succeeded in isolating an islet extract, which they called "isletin" [3]. A few months later, in December 1921, the biochemists James Collip succeeded in purifying the islet extract for use in medicine. Frederick Banting and J.J.R. Macleod were accordingly awarded the Nobel Prize in Medicine in 1923 for this outstanding discovery of insulin. Ever since, insulin for medicinal treatment was produced by extracting it from pancreas of cattle and pigs.

About 18 years later, the locus of insulin on chromosome 11 as well as the structure of insulin was revealed [4]. In the era of recombinant DNA research, the laboratories of the Harvard University, the University of California (UCLA) and scientists at Genentech Inc. were the most important participants in the race to clone a human gene for the first time – the hormone insulin.

The postdoctoral researcher Axel Ullrich (UCLA) was the first scientist to insert complementary DNA (cDNA) of rat insulin into the plasmid pBR322, an experiment which at the time was approved by the advisory committee but not yet certified by the director of the National Institutes of Health (NIH). In spite of this enormous breakthrough and the well-

known security advantages of the plasmid pBR332 in the scientific environment, the NIH ordered to destroy the recombinant plasmids. However, pushing straight forward, Axel Ullrich repeated his work in the plasmid pMB9 and published the cloning of the complete coding region of rat-pro-insulin I, part of the pre-pro-insulin I pre-peptide, the untranslated 3' terminal region of the rat insulin mRNA as well as sequences derived from the A chain region of rat pre-pro-insulin II in 1977 [5]. Just one year later, in May 1978, the Harvard group succeeded not only in inserting double-stranded cDNA copies of a rat pre-pro-insulin messenger RNA into E. *coli*, they also managed to switch on the insulin gene expression [6]. In parallel, scientists of Genentech and The City of Hope National Medical Center announced the successful laboratory production of human insulin A and B chain from chemically synthesized insulin gene sequences which were cloned into E. *coli* using recombinant DNA technology in December 1978 [7]. By the end of 1979, Axel Ullrich, now working at Genentech, successfully cloned human pre-pro-insulin cDNA into E. *coli* and thus enabled a new way to produce insulin [8].

Developed by Genentech, the Food and Drug Administration (FDA) permitted to market genetically engineered human insulin in 1982 and thus approved the first genetically engineered drug produced by bacteria, later to be acquired by Eli Lilly in 1985 [9]. Today, approximately 50 million people worldwide depend on this outstanding innovation [10, 11].

3.2 PRODUCTION AND IMPACT OF INSULIN

Insulin is the main regulator of carbohydrate and fat metabolism in the body. It is produced and released by the beta-cells of the islets of Langerhans. Insulin secretion is essentially mediated by oxidative metabolism of glucose that is absorbed from the blood. Caused by this uptake, elevated ATP/ADP ratio blocks the K^+_{ATP} channels, which results in membrane depolarization and subsequently increased cytoplasmic calcium levels due to voltage-gated calcium channels. Calcium in turn activates the phospholipase C (PLC), which cleaves phospholipid-phosphatidyl-inositol-4, 5-bisphosphate (IP2) into inositol-1, 4, 5-triphosphate (IP3) and diacylglycerol (DAG). IP3 additionally enhances the release of calcium from the endoplasmatic reticulum (ER) via IP3 gated channels and thus further elevates the cytoplasmic concentration of calcium, which leads to the translocation of insulin-containing secretory granules to the membrane and the release of insulin. In parallel, DAG, fatty acids, GLP-1, acetylcholine from parasympathetic as well as some other stimuli can influence the amount of insulin released by pancreatic beta-cells [12-14]. Once insulin is released into the blood, it stimulates the uptake of glucose, amino-acids and fatty-acids in the peripheral tissue by increasing the expression or activity of enzymes that mediate glycogen, lipid and protein synthesis, while inhibiting the activity or expression of those that catalyse degradation. Furthermore, it enhances the synthesis and storage of carbohydrates, lipids and proteins by inhibiting their degradation and release into the blood [15].
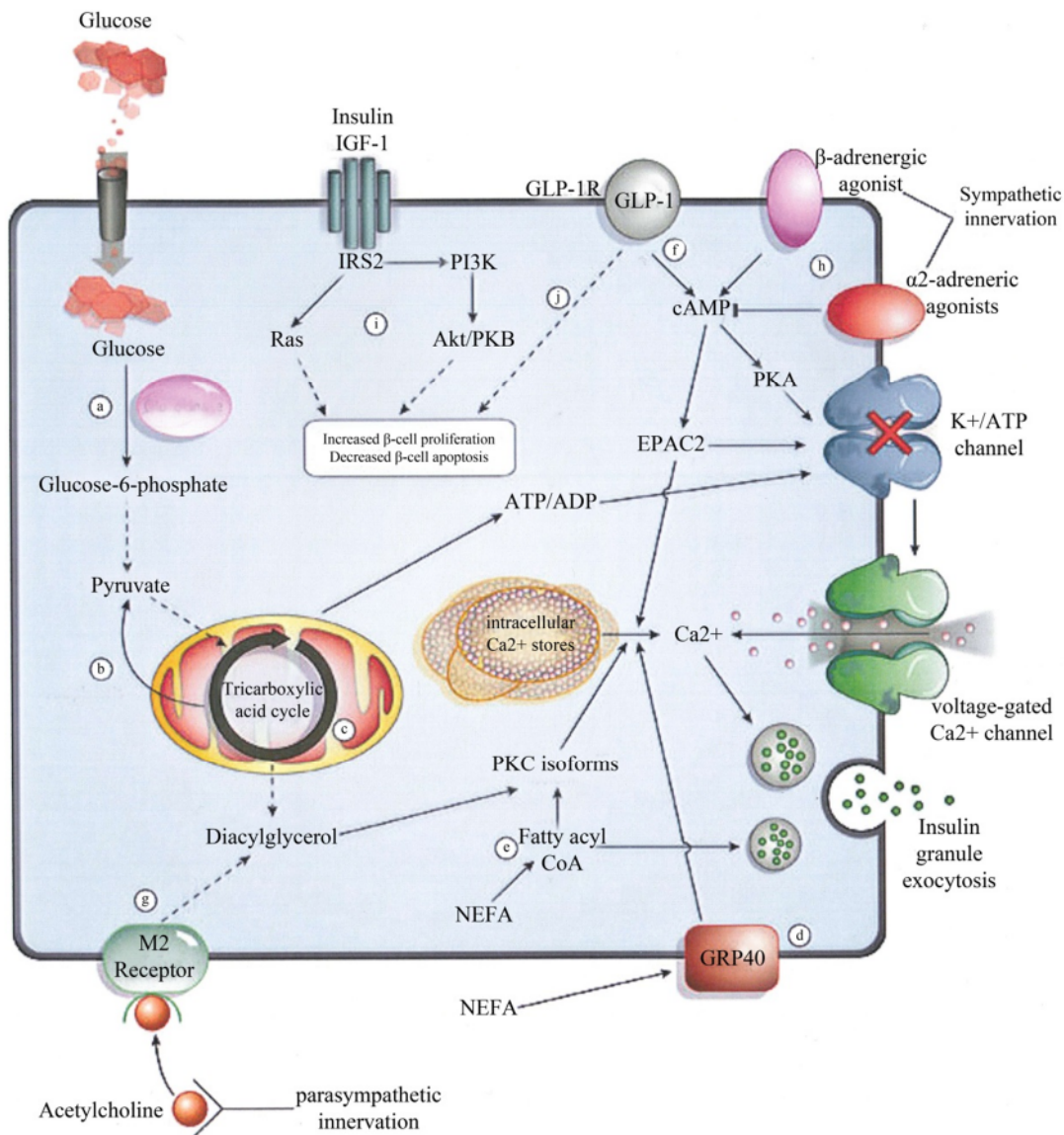
Figure 1 | *Simplified model of insulin secretion due to oxidative metabolism of glucose (a-c) and several other stimuli like non esterified fatty acids (NEFA) (d-e), incretins as glucagon-like peptide-1 (GLP-1) (f), acetylcholine from parasympathetic (g) and signals from the sympathetic nerves (h). Furthermore, activation of insulin/IGF-1 receptor (i) or GLP-1 receptor signaling (j) can positively influence the beta cell mass. Nature 444, 840-846 (Dec 2006).*

Insulin binding on the cell surface leads to auto-phosphorylation of the insulin receptor and catalyses the phosphorylation of cytoplasmic proteins, like members of the insulin receptor substrate (IRS) family, respectively GRB2-associated binding protein 1 (Gab-1), signal transduction protein Cbl (Cbl), isoforms of Shc-adaptor protein (Shc) as well as several adaptor proteins (APS) [15, 16]. The phosphorylated substrates interact with the Src-

homology-2 (SH2) domains of proteins such as phosphoinositide-3-kinase (PI3K), growth factor receptor-bound protein 2 (Grb2) or cyclin-dependent kinase6 (Cdk6/Crk2), which mediate glucose dependent gene expression or glucose transporter type 4 (GLUT4) translocation [17-21].

PI3K regulates three main types of signaling molecules: a) AGC-family members of serine/threonine protein kinases, b) guanine nucleotide-exchange proteins of the Rho-family of GTPase and c) the TEC-family of tyrosine kinases [22-24]. Moreover, it catalyses the phosphorylation of phosphoinositide to produce phosphatidylinositol-3-phosphates, especially IP3, which binds to the pleckstrin homology (PH) domains of a variety of signaling molecules like phosphoinositide-dependent kinase 1 (PDK1) or Akt/PKB [21]. Both Akt/PKB and PDK1 are important kinases in the transmission of the insulin signal. The Akt-family is divided into three genes: Akt1, Akt2 and Akt3. Whereas Akt1 appears have no effect on glucose uptake and the role of Akt3 is not clear yet, Akt2 seems to be an important signal transducer in the insulin cascade [25, 26]. Activation of Akt2 leads to a TBC1 domain family, member 4 (AS160) and TBC1 domain family member 1 (TBC1D1) mediated GLUT4 translocation which is essential for further glucose uptake and carbohydrate metabolism [27, 28]. Additionally, IP3 activated PDK1 is required for activation of atypical PKCs, like PKC-λ/ζ, which also leads to a translocation of GLUT4 vesicle [29]. In contrast, activated JNK seems to mediate feedback inhibition of insulin signaling by phosphorylation of insulin receptor substrates [30-32] and thus suppressing the insulin mediated effect. Furthermore, Akt/PKB mediated translocation of GLUT4 vesicle, glycogen-, fatty acid- and protein synthesis are regulated by several proteins based on Akt/PKB and PDK1 downstream signaling, which are not less important for a functional carbohydrate and protein metabolism.
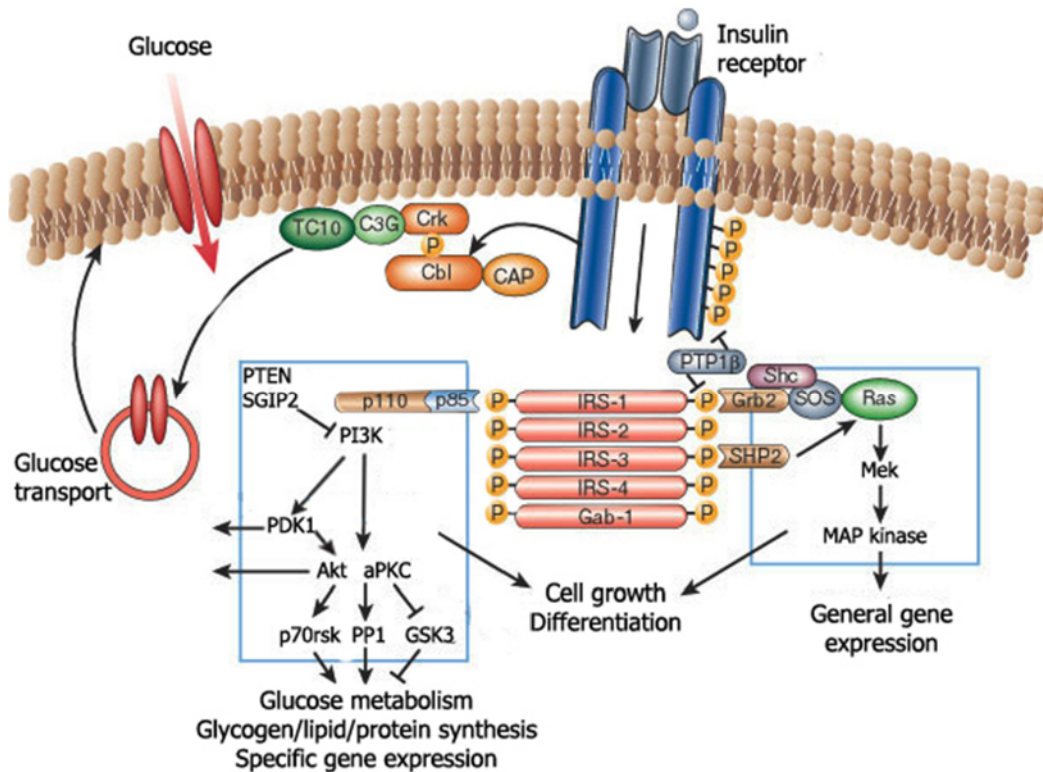
Figure 2 | *The insulin receptor undergoes auto-phosphorylation and catalyses the phosphorylation of cellular proteins such as members of the IRS family, Shc and Cbl. Upon tyrosine phosphorylation, these proteins interact with signaling molecules through their SH2 domains, resulting in a diverse series of signaling pathways, including activation of PI(3)K and downstream PtdIns(3,4,5)P$_3$-dependent protein kinases, RAS and the MAP kinase cascade, and Cbl/CAP as well as the activation of TC10. These pathways act in a concerted fashion to coordinate the regulation of vesicle trafficking, protein synthesis, enzyme activation and inactivation as well as gene expression, which results in the regulation of glucose, lipid and protein metabolism. Nature 414, 799-806 (Dec 2001).*

3.3 DIABETES MELLITUS

Diabetes mellitus is globally the fourth leading cause of death by disease and currently affects over 285 million people worldwide with almost 3 million deaths per year attributable to the disease and its secondary effects [10]. The number of people suffering from diabetes will increase due to population growth, ageing, urbanization and increasing prevalence of obesity as well as physical inactivity to approximately 385 million in 2030 [33]. Diabetes is a metabolic disease characterized by the loss of glucose homeostasis, which displays periodic or tenacious hyperglycemia. It is characterized by increased fasting plasma glucose levels

≥ 7.0 mmol/L (126 mg/dL), increased plasma glucose ≥ 11.1 mmol/L (200 mg/dL) two hours after a 75 g oral glucose, symptoms of hyperglycemia and casual plasma glucose ≥ 11.1 mmol/L (200 mg/dL) as well as an increased glycated hemoglobin (Hb A1C) level ≥ 6.5 % [34, 35].

There are three main types of diabetes: a) in *type 1 diabetes* (insulin dependent diabetes mellitus (IDDM) / *juvenile* diabetes) the defect results from insufficient insulin production by the pancreatic beta-cells due to T-cell mediated autoimmune destruction of the beta-cells, b) in *type 2 diabetes* (non-insulin dependent diabetes mellitus (NIDDM) / *adult-onset* diabetes) the defect is based on insensitivity of peripheral tissues (such as skeletal muscle, liver or adipose tissue) to secreted insulin and c) *gestational diabetes,* where women are displaying a high blood glucose level during pregnancy [36, 37]. Further forms such as maturity-onset diabetes of the young (MODY), neonatal diabetes mellitus (NDM), cystic fibrosis-related diabetes and genetic syndromes associated with diabetes, such as Down-syndrome and Prader-Willi-syndrome, are rather rare.
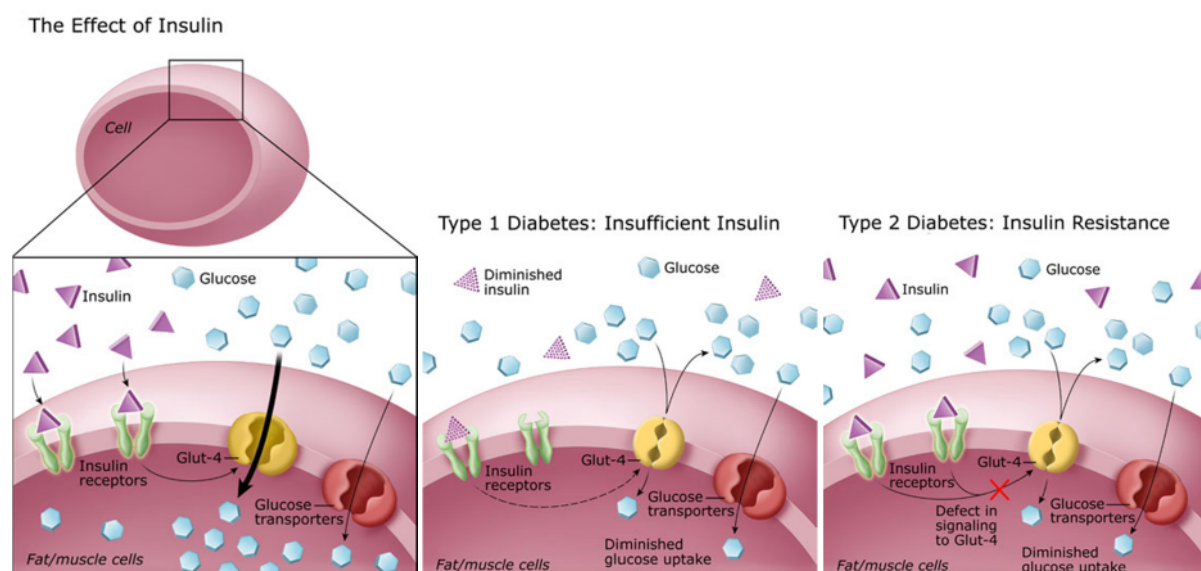
Figure 3 | *Effect of insulin on glucose uptake in fat and muscle cells for healthy and diabetic tissue. Functional glucose homeostasis is regulated by insulin of the pancreatic beta-cells, here insulin leads to GLUT4 translocation and thus to glucose uptake (left). Insufficient insulin production by the pancreatic beta cells results in hyperglycaemia mediated by reduced activation of the insulin receptor and to an impaired GLUT4 translocation (middle).*

Insensitive peripheral tissue is not able to deal with insulin. Here insulin binds the insulin receptor but errors in signal transduction diminish GLUT4 translocation and therefore glucose uptake (right). University of California, San Francisco (2010).

The traditional symptoms of diabetes are polyuria (frequent urination), polydipsia (increased thirst), polyphagia (increased hunger), blurred vision, skin irritation due to dehydration, weariness as well as ketoacidosis and an increased risk of inflammation [11, 38]. Whereas these symptoms may develop swiftly in type 1 diabetes, the progress in type 2 diabetes is much slower or, dependent on the outcome, completely absent. Over time diabetes increases the risk of cardiovascular diseases and is among the leading causes of kidney failure. Moreover, it causes neuropathy and leads to visual impairment. The overall risk of dying among people with diabetes, is at least double the risk of their peers without diabetes [11].

3.3.1 TYPE 1 DIABETES MELLITUS

Type 1 diabetes (insulin dependent diabetes mellitus (IDDM) / *juvenile* diabetes) results from insufficient insulin production by pancreatic beta-cells upon T-cell mediated autoimmune destruction of those [37]. Despite the presence of other endocrine islet cells such as alpha-cells that synthesize the hormones glucagon or somatostatin, beta-cells are the only cells that are destroyed in type 1 diabetes [39, 40]. The cause of diabetes is discussed and does not seem to be inherited in a simple pattern. Beside the genetic predisposition to the disease there seem to be some environmental triggers based on diets or infections as twin-studies revealed [41, 42]. However, the research of risk factors is still on-going and today there are 18 identified regions, each containing several genes, labelled as IDDM1 to IDDM18 [43]. The IDDM1 gene, which contains the human leukocyte antigen (HLA), which encodes immune response proteins, is by now the best studied risk factor. It is a cluster of genes on chromosome 6 that encodes a glycoprotein which is represented on the surface of most cells

and helps the immune system to distinguish between self-cells and non-self-cells [44]. Impaired detection of HLA led to a deceptive autoimmune response that attacks the body's tissues, in this case the beta-cells of the pancreas. There are two main classes of HLA proteins, categorized by the represented antigen: a) class I (A, B & C) represents peptides of digested proteins from inside the cell, here foreign peptide fragments attract cytotoxic T-cells and b) class II (DP, DQ & DR) represents antigens from outside the cell to T-lymphocytes and is most strongly linked with diabetes. In type 1 diabetes the major genetic susceptibility has been mapped to the HLA class II genes HLA-DQB1 and HLA-DRB1 [44-47]. Beside the previously mentioned antigens, several other genes are involved in immune function, also located on the HLA complex and are still under investigation.

However, there are two further non-HLA genes, IDDM2, the insulin gene, and the cytotoxic T-lymphocyte-associated protein 4 (CTLA4), which have a regulatory role in the immune response that are important predispositions [48]. The IDDM2 locus contributes about 10 % toward type 1 diabetes susceptibility [49] and is mediated by a variable number of tandem repeats (VNTRs) approximately 0.5 kb upstream of the IDDM2 origin of replication [50]. There are three classes of VNTRs in the insulin gene: a) class I 26 to 63 repeats, b) class II 80 to 121 repeats and c) class III 141 to 209 repeats. The length of VNTRs is associated with prevalence to type 1 diabetes, thereby class I alleles are associated with a higher risk of developing type 1 diabetes as longer class III alleles which seem to be protective [50, 51]. This protective mechanism is probably associated with elevated levels of IDDM2-mRNA in the thymus, where it mediates improved immune tolerance to insulin itself. The second non-HLA gene, CTLA4, is represented on the surface of T-helper-cells and mediates the interaction with co-stimulatory receptors and ligands of antigen-presenting cell (APC). CTLA4 has a negative regulatory effect on the immune system as it down-regulates T-cell activation by interfering with the signal cascade. Due to the fact that CTLA4 is only expressed in activated T-cells and there down regulates the activation of them, it is likely that CTLA4 has a role in guarding against autoimmunity [52]. The loss of this gene may result in activated T-cells

attacking self-antigens like in type 1 diabetes [53, 54]. Additionally, there are several IDDM loci (IDDM 3 to 18) that are suspected to play a role in susceptibility to type 1 diabetes and interacting on a metabolic, molecular or genetic level. However, their roles and mechanisms remain elusive.
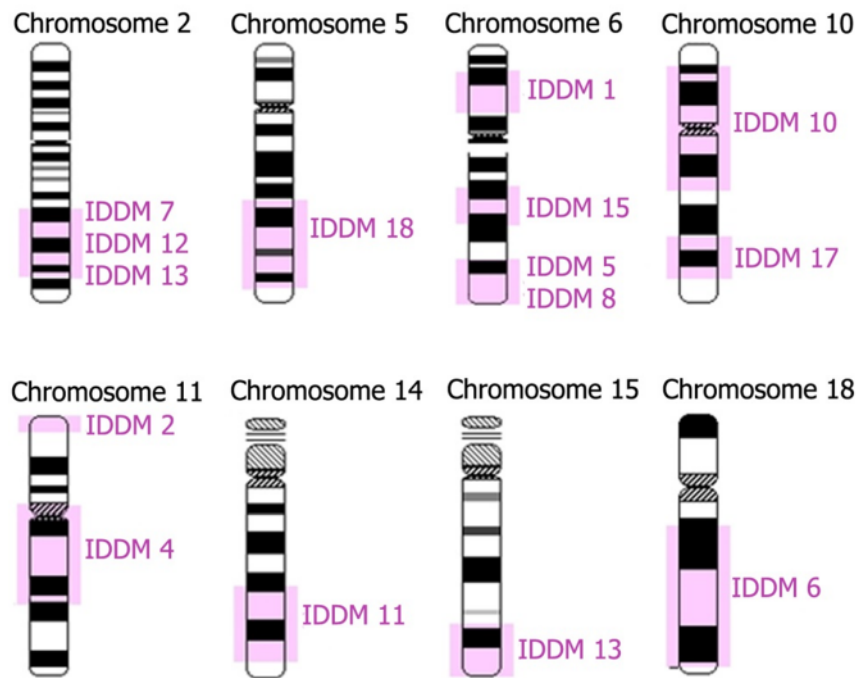
Figure 4 │ *IDDM loci in type 1 diabetes. Whereas IDDM1 and IDDM2 were both originally identified by investigating the suspected genes using case-control studies, IDDM3–IDDM18 were mainly discovered by genome scan linkage studies. Dean L, McEntyre J. The Genetic Landscape of Diabetes Bethesda (MD): National Center for Biotechnology Information (US); 2004. Chapter 2, Genetic Factors in Type 1 Diabetes. 2004 Jul 7.*

Beside the mentioned genetic predispositions, environmental and viral influences are frequently discussed and have been highlighted as triggers of type 1 diabetes. Coxsackie b viruses (CVBs), for example, mediate cell damage of target organs, that lead to a local immune response followed by the production of cytokines like type 1 and 2 interferons (IFNs), which arrest viral replication and facilitate viral clearance in mice [55]. These and other proinflammatory cytokines stimulate an immune response against the virus, but they can also initiate an autoimmune response in genetically susceptible individuals via molecular

mimicry or the mobilization of endogenous antigens, which result in immune-mediated damage and the development of an autoimmune disease [55-57].

However, the cause of type 1 diabetes is still veiled and it is not preventable with current knowledge. Insulin has to be replaced inescapably, either by subcutaneous injection or an insulin pump which delivers rapid-acting insulin continuously throughout the day using a catheter. Furthermore, the patient has to draw attention to dietary management, typically including carbohydrate tracking and careful monitoring of blood glucose levels using glucose meters. In some cases of type 1 diabetes, a pancreas transplant or islet cell transplantation, which is expected to be less invasive, may restore proper glucose regulation. In future, especially islet cell transplantation connected to stem cell research in the first instance might be a promising solution to restore insulin homeostasis in type 1 diabetes [58].

3.3.2 TYPE 2 DIABETES MELLITUS

Type 2 diabetes (non insulin dependent diabetes mellitus (*NIDDM*) / *adult-onset* diabetes), which accounts for nearly 90 % of all cases of the disease, is based on the insensitivity of peripheral tissues to secreted insulin. The number of new infections is dramatically increasing, rendering environmental factors, wrong nutrition and lack of exercise as important reasons. Furthermore, inherited factors are also important but the genes involved remain poorly defined. A number of genome-wide association studies (GWAS) revealed hundreds of genes concerning biological pathways, genes of unknown function and single-nucleotide polymorphism (SNPs) in enzymes, transporters and receptors involved in insulin metabolism that are linked to type 2 diabetes. More than 60 potential candidate genes involved in insulin action, insulin secretion and adipose metabolism have been examined in the search for type 2 diabetes susceptibility genes [59-61]. Although variants were identified in many of these genes, only a few have been shown to be associated with diabetes or impaired protein function. However, at least three genetic predispositions could be closely

connected to type 2 diabetes: a) Lys23 of KCNJ11 (potassium inwardly-rectifying channel, subfamily J, member 11), b) Pro12 of PPARγ (peroxisome proliferator-activated receptor gamma) and c) the T-allele at rs7903146 of TCF7L2 (transcription factor 7-like 2 (T-cell specific, HMG-box)) [62]. Individually, each of these polymorphisms is only moderately predisposed to type 2 diabetes [63].

The outbreak of type 2 diabetes can be triggered by environmental stimuli, lifestyle factors and metabolic changes such as pregnancy and puberty as well as ageing [64-67]. One of the most critical non-inherited factors in developing diabetes type 2 is overweight and obesity, both simply based on an energy imbalance between calories consumed and calories expended [12, 68]. Although over 80 % of people with type 2 diabetes are obese [69], the linking mechanism is not completely defined yet. Numerous factors have been suggested to play an important role in developing type 2 diabetes, highlighting cytokines, free fatty acids (FFA) as well as non-esterified fatty acids (NEFAs), hormones like resistin, leptin and adiponectine as well as tumor necrosis factor-α (TNF-α), interleukin-6 (IL-6), HNFs (Hepatocyte nuclear factors), monocyte chemo attractant protein-1 (MCP-1) and additional products of macrophages as well as other cells that populate adipose tissue [70-76].
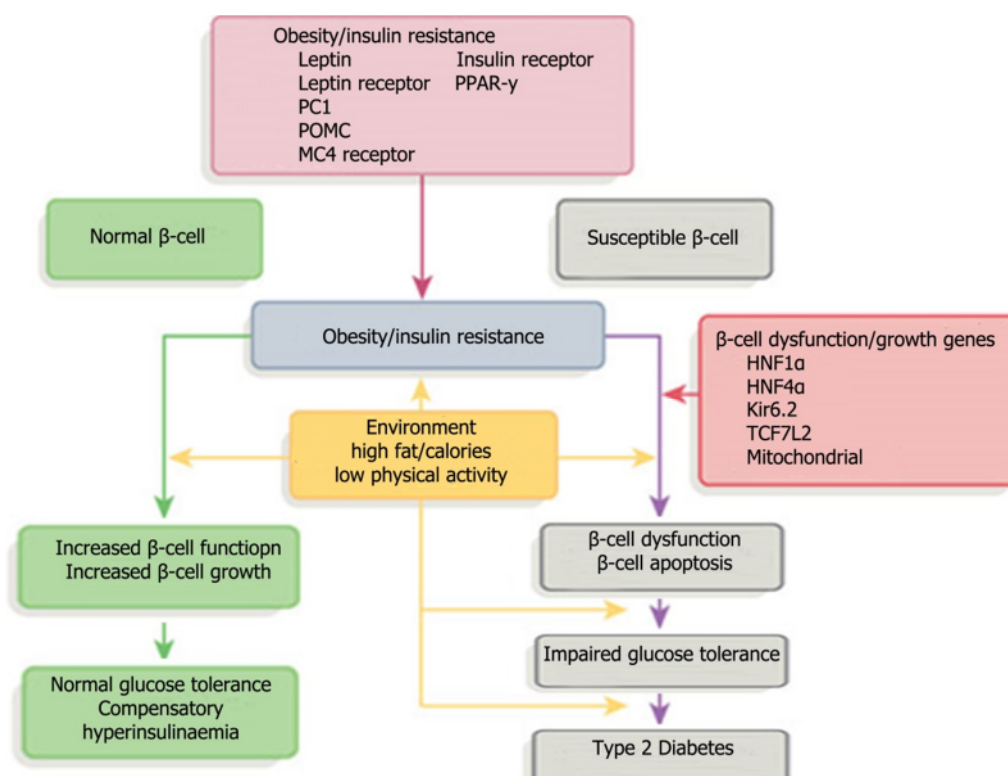
Figure 5 | *Genes responsible for obesity and insulin resistance interacting with environmental factors (increased fat/caloric intake and decreased physical activity), resulting in the development of obesity and insulin resistance. In regular beta-cells the function and mass increase in response to this increased secretory demand, leading to compensatory hyperinsulinaemia and the maintenance of normal glucose tolerance. Contrarily susceptible β-cells have a genetically determined risk and the combination of increased secretory demand and detrimental environment result in β-cell dysfunction and decreased β-cell mass, resulting in progression to impaired glucose tolerance, followed by the development of type 2 diabetes. Nature 444, 840-846 (Dec 2006).*

Today, based on various available treatments, type 2 diabetes is a chronic disease but does not remain less treacherous. Some cases cannot be managed reasonably and lead to an impaired lifestyle or even death. Onset of type 2 diabetes can be delayed or prevented through proper nutrition and regular exercise [77-79], which is more effective than the treatment with e.g. metformin [80]. Unfortunately, most patients are not eager to start or endure changes in diet and exercise to stay healthy.

Treatment in type 2 diabetic patients usually progresses from lifestyle intervention, which ranges from dietary management as well as monitoring of glucose plasma levels to the

treatment with drugs including insulin secretagogues, insulin sensitizer, apha-glucosidase inhibitors and peptide analogs. In the worst case, an insulin therapy is unavoidable [81, 82]. Despite these possible medications, diabetes is a chronic disease which claims millions of lives every year [33].

3.3.3 GESTATIONAL DIABETES MELLITUS

Gestational Diabetes Mellitus (GDM) is defined as carbohydrate intolerance with onset or first recognition during pregnancy [83]. The placenta, which supplies a growing fetus with nutrients, produces a variety of hormones to maintain the pregnancy. In some cases, these hormones, such as human placental lactogen (HPL), have a blocking effect on insulin within weeks 20 to 24 of pregnancy. If the production or release of insulin cannot equal the need of insulin by the peripheral tissue in order to overcome the effect of placental hormones, gestational diabetes mellitus is the result [84].

GDM elevates maternal blood glucose after eating (post-prandial levels) and may induce increased fetal growth which leads to a syndrome called "large for gestational age infant" (LGA). Infants with > the 90th percentile for gestational age are expected to become hypoglycemic in the first one to two hours after birth because of the state of hyperinsulinism and the sudden termination of maternal glucose when the umbilical cord is cut [85]. Therefore blood glucose levels should be closely monitored. Usually the mother's beta-cells can produce additional insulin to overcome the insulin resistance of pregnancy, but during the development of the placenta more hormones are produced and the hallmark of insulin resistance becomes more serious.

3.3.4 OTHER TYPES OF DIABETES MELLITUS

The majority of diabetes cases fall into the categories of type 1, type 2 and gestational diabetes. However, up to 5 % have further specific causes, including diabetes that results from single gene mutations. Maturity onset diabetes in the young (MODY) is caused by a mutation of a single gene that is inherited as an autosomal dominant trait. MODY usually occurs before 25 years of age and is sometimes misdiagnosed as type 1 diabetes. Genetic studies have defined a number of subtypes of MODY. For example, mutations in the genes encoding hepatic nuclear factor 4 (HNF4), glucokinase (GCK), hepatic nuclear factor 1 alpha and 1 beta (HNF1A/TCF1 and HNF1B/TCF2), insulin promoter factor 1 (IPF-1) and neurogenic differentiation 1 factor (NEUROD1) are the causes of the six known forms of MODY (MODY1-6) [86-93]. Beside this, MODY forms several disorders like Leprechaunism- and Rabson-Mendenhall-Syndrome, which display autosomal recessive disorders in the insulin receptor (InsR), as well as diseases of the endocrine system by which antagonists of insulin are dysregulated have been reported. Furthermore, diabetes can be induced by drugs like pentamidine, nicotinic acid, glucocorticoids, diazoxide or several kinds of viruses, such as oxsackie B, mumps, rubella and cytomegalovirus [94-96].

3.4 ANTI-DIABETIC MEDICATION

The aim of the anti-diabetic treatment is to lower the glucose levels in the blood by approaches such as replacement or increase of insulin release, insulin sensitization of the peripheral tissue as well as regulating the gluconeogenesis in the liver. Depending on the type of diabetes, age and the individual needs of the person, different classes of anti-diabetic drugs are prescribed. Type 1 diabetes always has to be treated with an insulin replacement therapy. In these cases, it is possible to inject insulin subcutaneously by an insulin pump or to transplant insulin producing tissue like the pancreas or isolated pancreatic beta-cells. Alongside dietary management, typically carbohydrate tracking and careful monitoring of

blood glucose levels have to be done. Transplantation of the pancreas or isolated beta-cells are rather rare but have a huge potential for coming treatments in combination with stem cell based approaches [58].
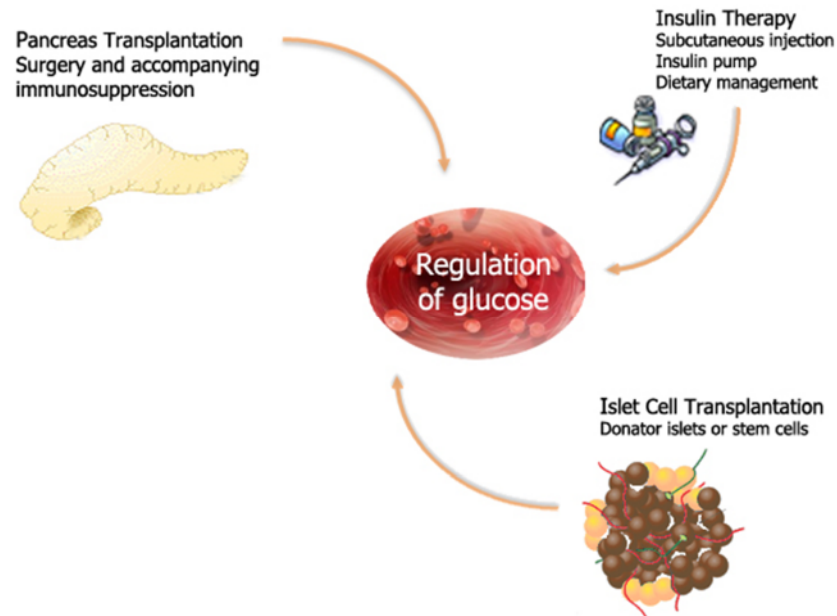
Figure 6 | *Medication of glucose homeostasis in type 1 diabetes. Besides the monitoring of nutrition and glucose plasma levels insulin therapy is the treatment of choice, whereas transplantations of islet-cells of pancreas are rather rare events.*

The treatment of type 2 diabetes is manifold, ranging from treatments with agents that increase the amount of insulin secreted by the pancreas, mediators which increase the sensitivity of the peripheral tissue to insulin and gluconeogenesis blocking drugs, to agents that decrease the rate at which glucose is absorbed from the gastrointestinal tract and insulin therapy in the worst case. Insulin sensitizers like biguanides and thiazolidinedione address the core problem by increasing the uptake of glucose by the peripheral tissue, including skeletal muscles. In the group of biguanides, metformin (Glucophage) is one of the most prescribed drugs. Metformin activates AMPK and thus improves hyperglycemia by suppressing hepatic gluconeogenesis [97-99]. Furthermore, it increases the uptake of glucose in peripheral tissues by increasing insulin sensitivity due to the activation of the

GLUT4 enhancer factor and fatty acid oxidation. Moreover, it decreases absorption of glucose by the gastrointestinal tract [100-102].

In contrast, thiazolidinedione affect the peroxisome proliferator-activated receptors (PPARs), specifically PPARγ [103]. PPARγ is a ligand-activated transcription factor that belongs to the nuclear hormone receptor superfamily. It is expressed in adipose tissue, macrophages, intestines as well as in ovaries and plays a crucial role in the regulation of energy storage, insulin sensitivity, adipocyte differentiation and lipid metabolism [104]. PPARγ activation in adipose tissue promotes adipocyte differentiation, resulting in an increase of the amount of insulin-sensitive adipocytes and a related significant decrease in serum-free fatty acid levels (FFA) and tumor-necrosis-factor alpha (TNFα) expression [105], which plays an important role in the development of insulin resistance [106, 107]. Moreover, the transcription as well as the plasma levels of adiponectine, a hormone that modulates a number of metabolic processes, including glucose regulation and fatty acid catabolism [108], are up-regulated upon thiazolidinedione treatment whereas the levels of Leptin, a key regulator of energy intake and expenditure, is down-regulated [109].

Insulin secretagogues are another approach to prevent hyperglycaemia by increasing the insulin released by pancreatic beta-cells. Sulfonylureas (e.g. tolbutamide, glipizide, glimepiride) have been the first commonly used drug. They trigger insulin release by inhibiting the K_{ATP} channel of pancreatic beta-cells, subsequently depolarize the membrane and thus open the voltage gated calcium channels which enable free calcium to translocate the insulin vesicles to the membrane [110, 111]. Meglitinides also inhibit the potassium channels as sulfonylureas do but at a different binding site [112]. There is a potential advantage in using these agents in situations in which hypoglycemia may be a significant risk, such as the elderly and renal and coronary disease patients. The short action of these agents reduces the risk of hypoglycemia, although it is not entirely eliminating it. The disadvantage of the use of these agents is the need for multiple daily doses.
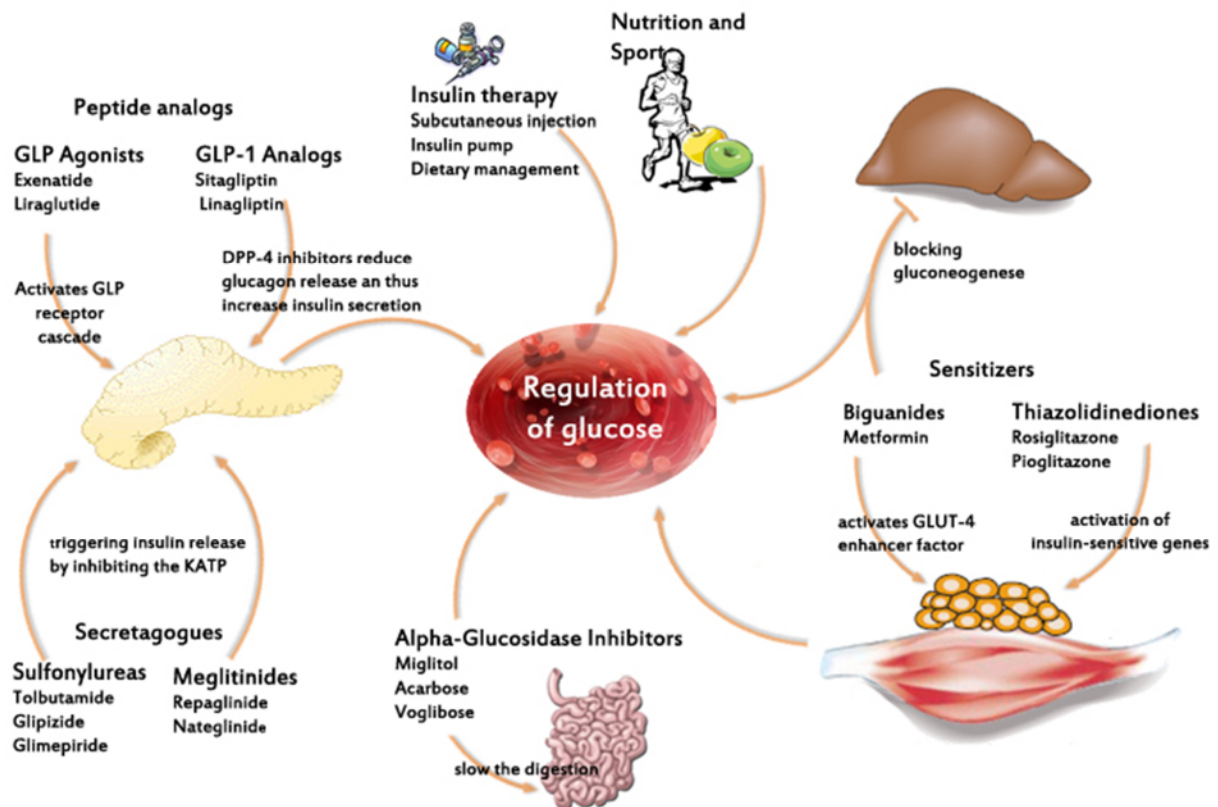
Figure 7 | *Medication of glucose homeostasis in type 2 diabetes. Beside change of nutrition and increase of sport activities, respectively, in the beginning of type 2 diabetes and insulin therapy at the very end, several possibilities to deal with the disease do exist. In general, there are two main forms of glucose regulation. Sensitizers, such as Biguanides and Thiazolidinediones, improve the impact of insulin in the peripheral tissue or the production of glucose in the liver. Furthermore, secretagogues, which increase the insulin released by the pancreatic ß-cells, are in use to treat type 2 diabetes, highlighting chemical structures like sulfonylurea, meglitinides or peptide analogs. Additionally, a rather small group of alpha-glycosidase inhibitors, which slow down the digestion and thus reduce the level of glucose in the intestine, can be used.*

Another way to induce insulin-secretion is the use of incretins and their peptide analogs. Incretins are a group of gastrointestinal hormones that cause increased insulin release, even before blood glucose levels become elevated. Today, two main candidate molecules are known for the treatment of type 2 diabetes. The glucagon-like peptide-1 (GLP-1) binds to a membrane GLP receptor and mediates the signal-transduction which leads to insulin release [113, 114]. Well known candidates of this class are exenatide and liraglutide. Because of 53 % homology with GLP (exenatide) [115] respectively peptide modifications (liraglutide)

[116], both drugs have the advantage of being more robust against the degradation by the dipeptidyl-peptidase-IV (DPP-IV) and thus increase the halftime of 1.5 – 2 minutes (GLP-1 (7-37)) up to 13 hours (liraglutide). Alternatively, DPP-IV inhibitors are used to increase the plasma concentration of GLP-1 itself by inhibiting its degradation [117].

Beside sensitizers and insulin secretagogues, the class of alpha-glycosidase inhibitors (αGI) is effective in the early stages of impaired glucose tolerance. Technically, alpha-glycosidase inhibitors are non-hypoglycaemic agents since they do not have a direct effect on insulin secretion or sensitivity, however, these agents slow down the digestion in the small intestine, thus glucose enters the bloodstream more slowly and helps to prevent hyperglycaemia.

3.5 IMPACT OF MULTI KINASE INHIBITORS ON DIABETES

Protein kinases are key enzymes that utilize signal transduction in many intracellular messaging pathways by a phosphorylation mediated modification of substrate activity. They control many cellular processes like metabolism, transcription, cell cycle progression, cell movement, apoptosis and differentiation [118]. The human kinome contains 518 protein kinases, 478 of them belong to a single superfamily whose catalytic domains are related in sequence. They can be clustered into groups, families and sub-families of increasing sequence similarity and biochemical function [118]. Highlighting tyrosine kinases, which have been implicated in several diseases like cancer, paving the way for invention of new therapy methods using small-molecule tyrosine kinase inhibitors (TKIs). Today, TKIs, e.g. imatinib (Gleevec), dasatinib (Sprycel) and sunitinib (Sutent), are used as anti-cancer drugs [119-121]. Interestingly, TKIs have been reported to cause a protective effect in diabetics as shown in several case reports [122-127]. The first published observation regarding the regression of diabetes by a TKI in 2005 depicts a case report of a nulliparous 70-year-old woman with chronic myeloid leukaemia and a long-standing type 2 diabetes mellitus, who had regression of the disease during treatment with imatinib [127]. While being treated with

imatinib, the patient's blood glucose level declined and insulin doses required were titrated down. Insulin treatment was discontinued and the diagnosis of type 2 diabetes mellitus was no longer tenable [127]. Afterwards, more case reports were published, such as "Improvement of type 2 diabetes in a lung cancer patient treated with erlotinib" [125], "Remission of diabetes while on sunitinib treatment for renal cell carcinoma" [128] as well as "Impact of sunitinib treatment on blood glucose levels in patients with metastatic renal cell carcinoma" [129]. Despite the seemingly known targets for all of the kinase inhibitors the mechanism of the anti-diabetic effect stays elusive but holds the key for a major breakthrough in the treatment of diabetes.

Table 1 | *Multi-kinase inhibitors and their impact on diabetes 2012*

TKI	Known targets	Animal models of beta-cell destruction	Animal models of insulin-resistance	Case reports
Imatinib (Gleevec®)	c-Abl, Arg, c-Kit, DDR1/2, PDGFR and NQO2	Protects against STZ-induced diabetes [130]; prevents and reverses diabetes in NOD mice [131, 132]; induces remission of diabetes in *db/db* mice [133]	Reduces high-fat diet-induced insulin resistance [134]	Remission of diabetes in CML patients [123, 127]; improved insulin sensitivity in non-diabetic CML patients [126]
Sunitinib (Sutent®)	VEGFR, c-Kit, PDGFR and Flt3	Reverses diabetes in NOD mice [135]		Remission of diabetes in renal cell carcinoma patients [122] ; lowered blood glucose levels in mRCC patients [129]
Dasatinib (Sprycel®)	c-Abl, Arg, Src, PDGFR, c-Kit, Yes, Fyn, Lyn etc.			Improved fasting glucose in a CML patient with T2D [124]
Erlotinib (Tarceva®)	EGFR			Lowered blood glucose levels in a lung cancer patient [125]
Fasudil	Rho-kinase	Prevents diabetes in insulin-resistant rats [136]		

Studies in non-obese diabetic (NOD) mice, which are considered to be phenotypically and genetically a suitable model of type 1 diabetes [137], revealed a reversed new onset diabetes after treatment in combination with imatinib and sunitinib, respectively [135]. Furthermore, imatinib induced the remission of diabetes in *db/db* mice, which developed beta-cell destruction by non-autoimmune mechanism by maybe preventing beta-cell apoptosis and elevated beta-cell proliferation [133]. Although several modes of action (MOA) have been proposed and overlapping targets of the TKIs like PDGFR and c-KIT are in focus, the protective mechanism by TKIs as well as other available drugs stays elusive. Moreover, new findings suggest that multiple target binding of TKIs - also to other kinases as referred - increases the possible targets of anti-diabetic effects, highlighting sunitinib as an example where 313 putative kinase targets were identified using a chemical proteomics approach [138].

3.6 KINASES THAT REGULATE INSULIN RELEASE

The decreased insulin sensitivity of peripheral tissues in type 2 diabetes which accounts for about 90 % of all cases of the disease is initially compensated by increased secretion of insulin by the beta-cells of the pancreas. The formally known secretion of insulin is based on the oxidative metabolism of glucose and the subsequent voltage mediated release of insulin. More triggers of insulin secretion like glucagon-like peptide-1 (GLP-1), non-esterified fat acids (NEFA), acetylcholine from parasympathetic and signals from the sympathetic nerves have been revealed over time. Furthermore, activation of insulin/IGF-1 receptor and GLP-1 receptor signaling has been connected to insulin release [*see Chap. Insulin production*]. Based on these observations, an enormous number of regulatory kinases seem to be possible, highlighting for example the insulin receptor (InsR) and the insulin-like growth factor-1 receptor (IGFR). Both are discussed most controversial with regard to insulin feedback and β-cell function in the autocrine role of insulin in insulin secretion. Published

data have led to four possible outcomes: insulin is *a)* a negative regulator, *b)* a positive regulator, *c)* essential, or *d)* not involved. However, recent reports suggest that the autocrine response of insulin in pancreatic beta cells is time and concentration dependent. Whereas basal insulin may serve as a maintenance signal that primes the β-cell to respond to the next glucose stimulus, insulin may inhibit further release at the peak of the exocytotic event, i.e. at very high local insulin concentration. It has been shown that knock-out mice of beta-cell specific insulin receptor (InsR) or insulin-like growth factor-1 receptor (IGFR) displayed a defect in glucose-stimulated insulin secretion [139, 140]. The double knockout of InsR and IGFR in beta-cells results in a hypoinsulinoma with a marked beta-cell loss and a defect in insulin biosynthesis [141]. Further downstream, insulin receptor substrate activates PI3K [142, 143] to mediate PIP2 to PIP3 conversion which activates AKT/PKB and PKC due to PDK1 [144]. Additionally, PDK1 is negatively regulated by phosphorylation upon p38δ activity [145]. Despite the poorly understood role of p38 in insulin release, p38 activity has been reported to be increased in insulin-resistant peripheral tissues from diabetic patients [146]. Likewise, *in vitro* data have revealed that p38 activation upon exposure to TNF-α, free fatty acids and oxidative stress impairs insulin signaling in adipocytes and skeletal muscle cells through mechanisms very similar to those described for JNK, which is known to be activated under diabetic conditions and to be possibly involved in the progression of insulin resistance [147-149]. Furthermore, overexpression of a dominant-negative form of c-*jun* N-terminal kinase (JNK) prevents the decrease in PDX-1 binding activity in response to oxidative stress in a c-jun-independent manner [148, 150]. Activation of JNK is a central signal transduction event, causing peripheral insulin resistance, suppressing insulin production and secretion as well as increasing apoptosis of islet cells [151, 152]. Another interesting kinase which regulates the insulin release mediated by metabolic ratios of AMP, ADP and ATP and that is already a target for metformin, is the AMP-dependent protein kinase (AMPK), a major cellular fuel sensor in a variety of cells and tissue which also affects insulin secretion and beta-cell survival [153]. The AMPK complex is a heterodimer

serine/threonine kinase which is activated by an increase in the cellular AMP/ATP ratio due to glucose deprivation, hypoxia, ischemia or inflammation. By this process AMPK protects the cells against ATP-depletion by reducing the energy consuming processes such as operation of ion transporters and secretion [153]. AMPK is activated by phosphorylation of the alpha-subunit on amino acid Thr172 by upstream kinases like the serine/threonine kinase 11 (LKB1), the calcium/calmodulin-dependent protein kinase kinase 2 (CaMKK2) or independently by a CaMKK2 dependent increase in the intracellular calcium concentration [154, 155]. Active AMPK has short- as well as long term effects on cellular energy homeostasis, insulin sensitivity and insulin secretion [156]. However, the reports about AMPK activation of insulin release are controversial discussed, either describing inhibition [157-159] or stimulation [160-162]. Beside the kinases that are linked to AMP/ADP/ATP ratio monitoring, several metabolites like ATP, GTP, cAMP, NADPH and malonyl-CoA are supposed to mediate the potentiation of insulin secretion at suitable calcium levels [163]. This is where calcium dependent kinases also play an important role in regulating insulin secretion.

CaMKK2 is a serine/threonine-specific protein kinase that is regulated by the calcium/calmodulin complex. Besides the CaMKK2 mediated activation of AMPK or PKA, CaMKK2 itself temporally correlates with insulin secretion in perfused rat islets [164, 165]. In addition, another calcium/calmodulin-dependent protein serine kinase (CASK), known for vesicle transport in neurons, forms a complex with two unidentified phospho-tyrosine proteins pp100 and pp95 in response to insulin-stimulation, though CASK is not itself tyrosine phosphorylated [166]. Furthermore, insulin decreases CASK nuclear location as well as down-regulates the expression of CASK targeted genes [166]. A further protein kinase which regulates insulin release is the multi-potential serine/threonine casein kinase 2, alpha 1 polypeptide (CK2/CSNK2A1). The regulatory mechanism of CK2 to insulin response is not clear yet, because secretion by a negative feedback [167, 168] or a positive feedback mechanism [169, 170] or no effect at all [171] have been reported. However, publications regarding this topic have a tendency to display CSNK2A1 as a negatively regulating kinase.

Furthermore, it is clear that CK2 is phosphorylating PDX-1 [172], a well-studied transcription factor that is critical to both β-cell development and function. PDX-1 together with other transcription factors regulates both, insulin gene transcription and insulin secretion [173].

One of the most recently discovered kinases involved in the network of insulin secretion is the serum/glucocorticoid regulated kinase 1 (SGK1). SGK1 seems to provide an important molecular link between salt and glucose homeostasis, as SGK1$^{-/-}$ knockout mice fed with high-salted chow demonstrated decreased SGK1-dependent cellular glucose uptake [174]. Beside SGK1 functions in trans-membrane glucose transport [175-178] and insulin signaling [179], SGK1 also plays a role in insulin secretion. In INS-1 cells SGK gene transcription and protein expression is strongly regulated and SGK1 up-regulates the activity of voltage-gated K$^+$ channels, which in turn reduce calcium influx and inhibit insulin release [180]. Another SGK1-dependent molecular mechanism in insulin secretion is the activation of Na$^+$/K$^+$-ATPase during plasma membrane repolarization [181]. Furthermore, patient studies revealed that a variance of the SGK1 gene is associated with insulin secretion in different European populations [182]. Highlighting the mentioned kinases and their possible interaction partners, the release of insulin is triggered by a huge network of more than metabolic and voltage dependent events. Based on this knowledge, the development of new target-oriented small-molecule inhibitors with anti-diabetic properties are paving the way for a potential breakthrough in the treatment of this disease.

3.7 PROTEIN KINASES

The family of protein kinases contains enzymes that catalyze the transfer of the gamma phosphate groups from ATP to serine, threonine or tyrosine hydroxyl group in target protein substrates [183] and thus activates positively or negatively signaling cascades that are regulating cellular responses. In the human kinome 518 genes encoding protein kinases are known and at least 30 % of the human proteome is phosphorylated by such protein kinases

[184]. The kinases can be clustered into groups, families and sub-families of increasing sequence similarity and biochemical function, resulting in a kinase dendrogram *(see Figure 8)* [185]. Furthermore, they can be distinguished by their phosphorylation site. Tyrosine kinases form a distinct group whose member phosphorylate proteins on tyrosine residues, whereas enzymes in all other groups phosphorylate primarily serine and threonine residues. The largest group of such enzymes contains serine/threonine protein kinases (STK) which use the phospho-group of a nucleoside triphosphate (e.g. ATP) to phosphorylate the OH-group of serine or threonine in their substrates-phosphor-acceptor-site. Prominent candidates of this group are Akt/PKB, casein kinase 2 (CK2), the protein kinase A (PKA) and protein kinase C (PKC) as well as the calcium/calmodulin-dependent protein kinases (CaMK). Their cell-localization varies through the cell membrane (receptor-tyrosine kinases (RTK)) throughout the cytoplasm to the nucleus. Their function differs also in processes, pathways and actions that are responsible for key events in the metabolism. In humans, over 100 genes encode protein TKs, here 58 encode RTKs that are distributed into 20 subfamilies and 32 encode cytoplasmic, non-receptor protein tyrosine kinases in 10 subfamilies [186, 187]. Kinases that act on serine/threonine and tyrosine are determined as dual-specificity kinases [188]. Further 40 atypical kinases have no sequence similarity to typical kinases, but are known or predicted to have enzymatic activity or to have a similar structural fold as typical kinases [186]. Recently, histidine kinases, which phosphorylate an imidazole nitrogen on a histidine residue, have also emerged as signaling enzymes [189].
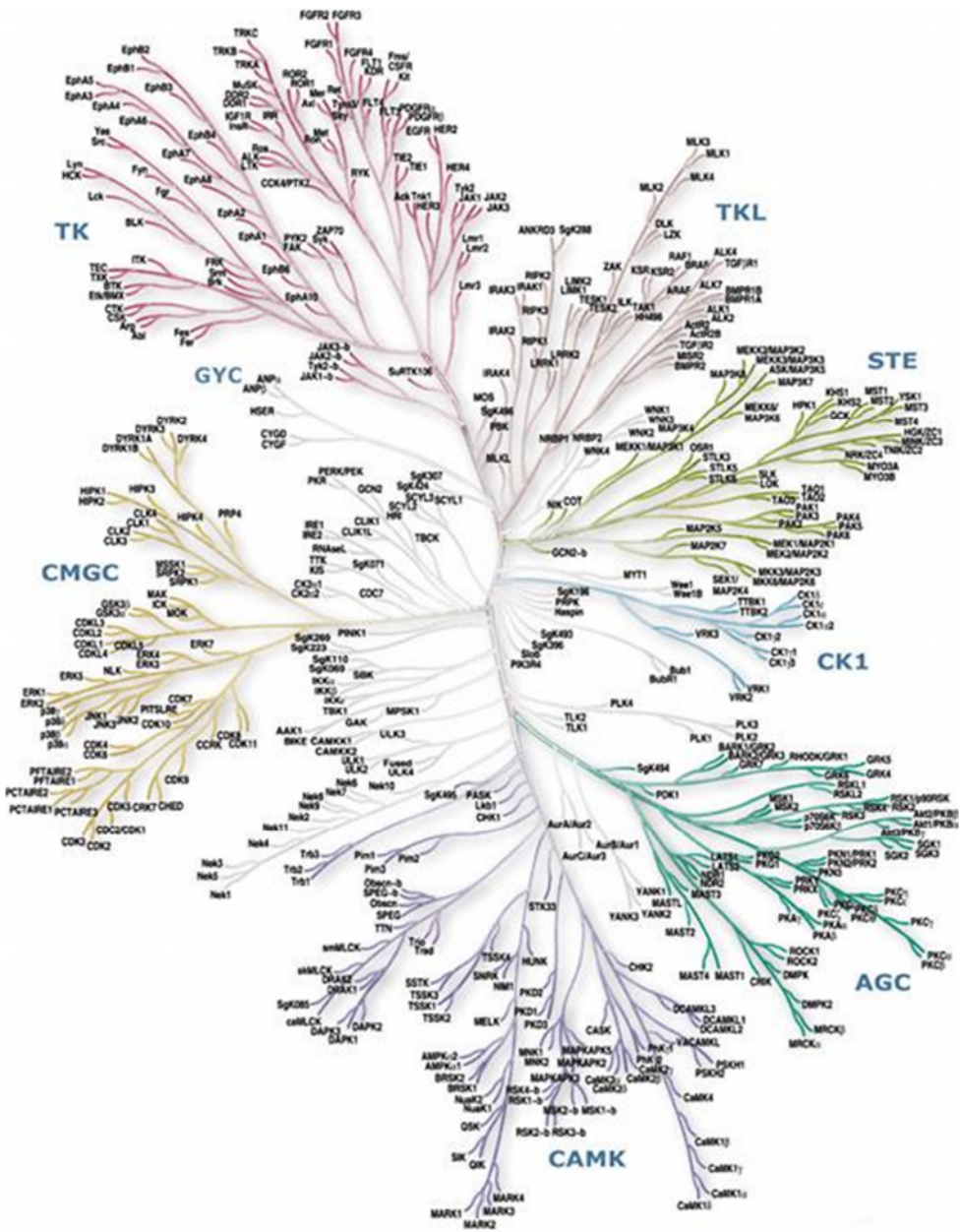
Figure 8 | *Human protein kinases. AGC containing PKA, PKG, PKC families; CAMK calcium/calmodulin-dependent protein kinase; CK1 casein kinase 1; CMGC containing CDK, MAPK, GSK3, CLK families; STE homologs of yeast Sterile 7, Sterile 11, sterile 20 kinases; TK tyrosine kinase; TKL tyrosine kinase-like. Gerard Manning, Science 2001, Sugen, Inc., South San Francisco, CA, USA.*

As indicated, protein kinases play an important role in signal transduction and thus in controlling major cellular processes, including metabolism, transcription, cell cycle progression, cytoskeletal arrangement and cell movement, apoptosis and differentiation [190]. Alterations in kinase signal transduction by mutation amplification or disorders in

general are the origin of many diseases [184]. Therefore, protein kinases are important targets in drug discovery for treating diseases, including autoimmune disorders, diabetes, neurological disorders and cancer.

Table 2 | *Diseases caused by mutations in particular protein kinases and phosphatases (Cohen, 2001)*

Disease	Kinase/phosphatase
Myotonic muscular dystrophy	Myotonin protein kinase
X-Linked agammaglobulinaemia	Bruton tyrosine kinase
Hirschsprungís disease	Ret2 kinase
Autosomal recessive SCID	Zap70 kinase
X-Linked SCID	Jak3 kinase
Chraniosynostosis	FGF receptor kinase
Papillary renal cancer	Met receptor kinase
Chronic myelomonocytic leukemia	Tel-PDGF receptor kinase
Chronic myelogenous leukemia	Abelson tyrosine kinase
Non-Hodgkins lymphoma	Alk kinase
Peutz–Jeghers syndrome	Lkb1 kinase
Coffin–Lowry syndrome	MAPKAP-K1b (RSK-2)
Ataxia-telangiectasia	Atm kinase
Li–Fraumeni syndrome	Chk2 kinase
Williams syndrome	Lim kinase-1
Leprechaunism, diabetes	Insulin receptor kinase
Wolff–Parkinson–White syndrome	AMP activated kinase
Wolcott–Rallison syndrome	eIF2A-kinase 3
X-Linked myotubular myopathy	MTM1 Tyr phosphatase

3.7.1 PROTEIN KINASE INHIBITORS

Protein-kinase-inhibitors can be separated into two functional groups: a) therapeutic antibodies, so called biologics, and b) small-molecule kinase inhibitors [191]. Both are in clinical use for cancer-specific targeted therapies for a broad spectrum of different tumor indications. Biologics interact with growth factor signaling and angiogenesis by interfering with receptor tyrosine kinases like epidermal growth factor (EGF), insulin-like growth factor (IGF) or vascular endothelial growth factor (VEGF). Various types of biologics have been pursued and include therapeutic monoclonal antibodies, vaccines and other novel oligonucleotide-based agents. Examples for monoclonal antibodies are Herceptin (Trastuzumab) [192-194], Avastin (Bevacizumab) [195] and Erbitux (Cetuximab) [196].

Immunotherapeutic vaccines are also under investigation using growth factors, RTKs or other protein kinase-derived peptides as antigens. Some encouraging trial vaccines are in clinical studies, particularly in order to improve the immune response against tumor cells [197, 198]. Oligonucleotide-based agents like aptamers that bind to specific target molecules or siRNA, which reduce the gene expression of proteins, are recently under investigation but until today only Vitravene is approved by the FDA as antisense-based drug used in the treatment of cytomegalovirus retinitis (CMV) in immune-compromised patients [199]. However, several antisense compounds are in clinical trials for non-small cell lung cancer patients [200, 201], high-grade glioma patients [202] and diabetic macular edema [203].

Small-molecule kinase inhibitors compete with ATP at its binding site and present one to three hydrogen bonds to the amino acids located in the hinge region of the target kinase, thus imitating the hydrogen bonds that are normally formed by the adenine ring of ATP [204-206]. Depending on whether the TKI interfere with the activation loop in the active or inactive conformation one distinguishes type 1- and type 2 inhibitors. Type 1 inhibitors typically consist of a heterocyclic ring system that occupies the purine binding site, where it serves as a scaffold for side chains that occupy the adjacent hydrophobic regions I and II, adenine region, the ribose region and the phosphate-binding region [205]. Although the

adenine region is always occupied by all type I inhibitors, the ability of the kinase inhibitors to present diverse functionality to other regions can form the basis for inhibitor selectivity among different kinases [207, 208].

Type 1 Inhibitor
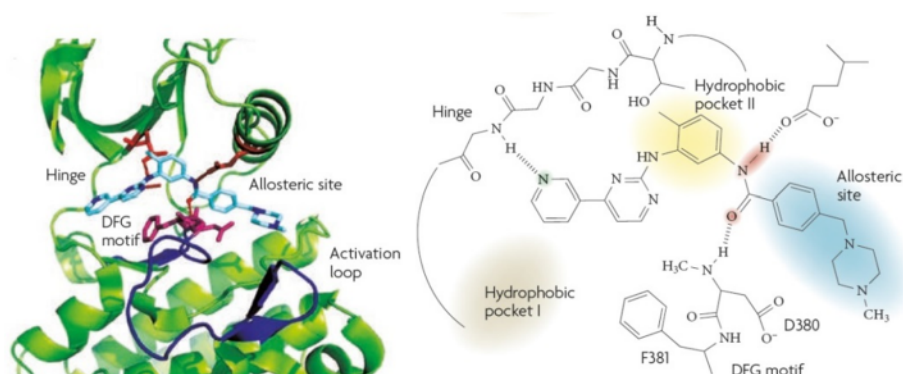
Type 2 Inhibitor
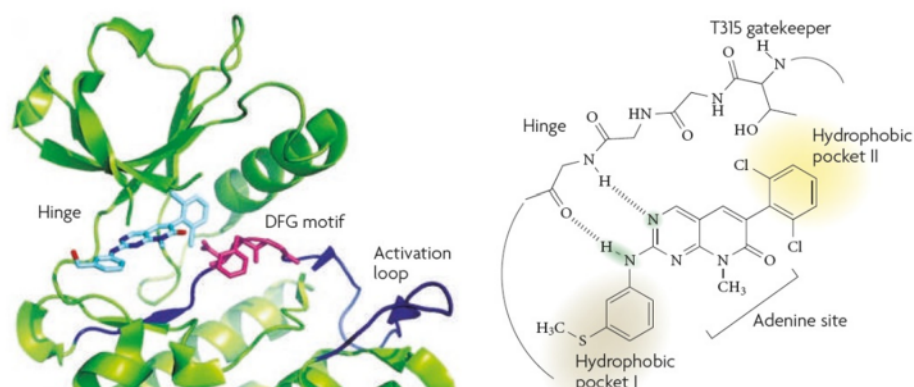
Figure 9 | *Kinase inhibitor binding modes. Kinase inhibitor–protein interactions are depicted by ribbon structures (left) and chemical structures (right). The chemical structures display hydrophobic regions I and II of ABL1 (shaded beige and yellow respectively) and hydrogen bonds between the kinase inhibitor (inhibitor atoms engaged in hydrogen bonds to hinge are highlighted in green or to allosteric site in red) and ABL1 are indicated by dashed lines. The DFG motif (pink), hinge and the activation loop of ABL1 are indicated in the ribbon representations. The kinase inhibitors are shown in light blue. Upper figure: ABL1 in complex with the type 1 ATP-competitive inhibitor PD166326 (Protein Data Bank (PDB) ID 1OPK) 104. Shown here is the DFG-in conformation of the activation loop (dark blue). Lower figure: The DFG-out conformation of the activation loop of ABL1 (dark blue) with the type 2 inhibitor imatinib (PDB ID 1IEP) 105. The allosteric pocket exposed in the DFG-out conformation is indicated by the blue shaded area (right). Zhang, Nat Rev Cancer. 2009 Jan; 9(1): 28-39.*

In contrast, type 2 kinase inhibitors recognize the inactive conformation of the kinase near the ATP binding pocket and prevent kinase activation by occupying the exclusively created conformation of the activation loop (DFG-out), which is based on a shift of the phenylalanine residue of the DFG motif [209]. Movement of the activation loop to the DFG-out conformation exposes an additional hydrophobic binding site, directly adjacent to the ATP binding site [206]. However, both drug types are orally active, have a satisfactory safety profile and can be easily combined with other forms of chemotherapy or radiation therapy.

Examples for natural products that are potent inhibitors of protein kinases include the alkaloid staurosporine, purine olomoucine and wortmannin [210-212]. Many therapeutic inhibitors of protein kinases are structurally based on these discovered natural products. To date, approximately 80 inhibitors have been advanced to some stage of clinical evaluation, the majority for the treatment of cancer. Some drugs in the group of multi-kinase-inhibitors are: Gleevec (imatinib), Tarceva (erlotinib), Sprycel (dasatinib), Nexavar (sorafinib) and Sutent (sunitinib).

3.8 SUNITINIB MALATE

Sunitinib malate (SUTENT, SU11248) is an orally available oxindol, multi-targeted receptor tyrosine kinase inhibitor that was approved by the FDA for the treatment of metastatic renal cell carcinoma (mRCC) and imatinib-resistant gastrointestinal stromal tumor (GIST) on January 26th, 2006 [213-215]. Since 2011, it is also approved for the treatment of pancreatic neuroendocrine tumors (NET) that cannot be removed by surgery or have spread to other parts of the body [216, 217]. Sunitinib was the first cancer drug simultaneously approved for two different indications [218] and has been initially developed as an angiogenesis inhibitor based on the discovery by Millauer *et al*. [215] that inhibition of Flk-1/VEGFR2 function in a mouse glioblastoma model prevented angiogenesis and inhibited tumor growth.

Sunitinib has been identified as a potent inhibitor of class III, V and XII split-kinase domain receptor tyrosine kinases like vascular endothelial growth factor receptors (VEGFR) (types 1-3), fetal liver tyrosine kinase receptor 3 (FLT3), KIT (stem cell factor [SCF] receptor), platelet-derived growth factor receptor (PDGFR) (types α and β), as well as colony-stimulating factors type 1 (CSF-1R) and glial cell-line derived neurotropic factor receptor (RET) in both biochemical and cellular assays [219-222].
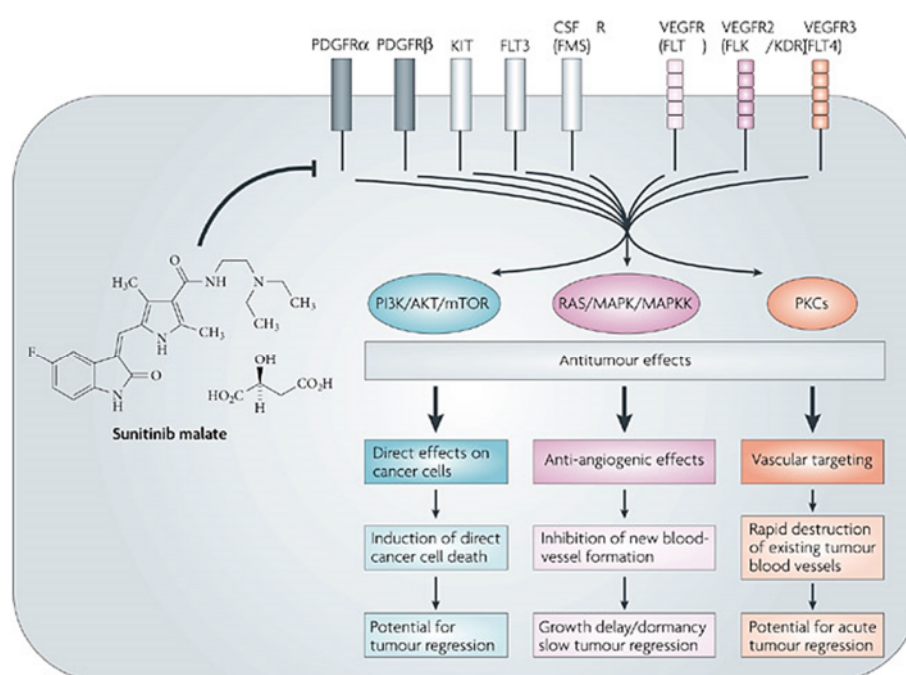
Figure 10 | *Sunitinib malate is an oxindol molecule designed to interact selectively with the intracellular ATP-binding sites of tyrosine kinase vascular endothelial growth factor receptors 1–3 (VEGFR1–3), platelet-derived growth factor receptors (PDGFRs), stem-cell growth factor receptor (KIT), fms-related tyrosine kinase 3 (FLT3) and colony-stimulating factor 1 receptor (CSF1R). Receptor inhibition has multiple effects on cellular processes including tumor cell survival, endothelial cell growth and migration, vascular permeability, pericyte recruitment and lymph angiogenesis. The final anti-tumor effects may be classified as the following: direct cytotoxic effects on tumor cells by induction of cell death; anti-angiogenic effects leading to growth delay and/or tumor regression by cytostatic inhibition of new blood-vessel formation; vascular disruption by inhibition of existing VEGF/VEGFR-dependent tumor blood vessels leading to central tumor cell necrosis and cavitation that may be associated or not with tumor regression. MAPK, mitogen-activated protein kinase; MAPKK, MAPK kinase; mTOR, mammalian target of rapamycin; PI3K, phosphatidylinositol 3-kinase; PKC, protein kinase C (Faivre et al., 2007).*

The structure SU11248 (Sutent) is based on the anti-angiogenic oxindol inhibitors SU5416 and SU6668 that had inadequate pharmacological properties for clinical development and failed in clinical trials. Furthermore, Sutent was found to be 10-30 times more potent against VEGFR2 and PDGFRα than other candidate drugs in biochemical and cell-based assays [220, 223]. Inhibition of the VEGF-dependent mitogenic response of human umbilical vein endothelial cells by sunitinib was revealed to prevent migration of these cells and attenuated capillary-like tubule formation [224]. Moreover, Osusky *et al.* depicted that *in vivo* sunitinib decreases tumor micro vessel density, prevents neovascularization in a tumor vascular-window model and attenuates the formation of lung metastasis in a Lewis lung carcinoma model [224]. The inhibition of the other Sutent targets such as FLT3, which plays a role in acute myeloid leukemia [225-227], KIT, which is related to GIST [228, 229] as well as RET, which is often deregulated or mutated in neuroendocrine tumors [230-232] and CSF-1R as a factor implicated in metastatic breast cancer [233, 234] have been predicted to be beneficial for the treatment of cancer. However, sunitinib inhibits the signal transduction of VEGF, SCF, and PDGF and induces apoptosis of human umbilical vein endothelial cells [220]. *In vivo*, sunitinib exhibited dose- and time-dependent antitumor activity in mice, potently repressing the growth of a broad variety of human tumor xenografts including renal cell-, breast-, lung-, liver- and epidermoid carcinoma as well as melanoma [219, 220, 235-239]. Furthermore, antitumor activity was observed in numerous tumor types such as RCC, GIST, NETs, non-small-cell lung cancer (NSCLC), sarcoma other than GIST, thyroid cancer, melanoma, hepatocellular carcinoma and head and neck squamous cell carcinoma in clinical studies [240-244].

At the dose of 50 mg/d (4 weeks on, 2 weeks off), Sutent displays manageable toxicity in patients, but strong reduction of intra-tumor vascularization and central tumor necrosis [244]. Most of the adverse events reported in patients receiving sunitinib in clinical studies were mild to moderate in severity and generally consistent across indications [245-248]. The

most commonly reported treatment related non-hematological adverse effects include fatigue, gastrointestinal toxicities (diarrhea, nausea, vomiting, stomatitis and dyspepsia), anorexia, hypertension, skin discoloration and hand-foot syndrome. Following administration, sunitinib is primarily metabolized by cytochrome P450-3A4 to an active N-desethyl-metabolite called SU12662. The active metabolite is also metabolized by cytochrome P450-3A4 [246, 248]. Elimination is primarily via the feces with <16 % excreted in the urine. Because SU12662 has an inhibitory profile similar to that of sunitinib *in vitro* and has similar plasma protein binding, the combination of sunitinib plus SU12662 (sunitinib + SU12662) represents the total active drug (total drug) in plasma. Pharmacokinetic investigations in both, healthy volunteers and cancer patients, have shown that following a single oral dose, peak plasma sunitinib concentrations occur between 6 and 12 hours post-dose [246, 248]. In addition, sunitinib and SU12662 have previously been shown to display linear pharmacokinetics and have prolonged half-lives of 40 and 80 hours, respectively [249].

4 MATERIALS & METHODS

4.1 MATERIALS

4.1.1 LABORATORY CHEMICALS

Agarose	Eurogentech, Belgium
Acrylamide	Serva, Heidelberg
Aprotinin	Sigma, Taufkirchen
APS (Ammonium peroxodisulfate)	Bio-Rad, München
Bisacrylamide	Roth, Karlsruhe
BSA (Bovine serum albumin)	Sigma, Taufkirchen
D(+)-Glucose	Merck, Darmstadt
FCS (Fetal calf serum)	Life-Technologie, Darmstadt
IAA (Iodoacetic acid)	Sigma, Steinheim
IBMX (3-Isobutyl-1-methylxanthin)	Life-Technologie, Darmstadt
Insulin (Bovine)	Sigma, Steinheim
L-Glutamine (GibCo)	Life-Technologie, Darmstadt
β-Mercaptoethanol	Merck, Darmstadt
MTT-Formazan	Sigma, Taufkirchen
2-NBDG (Fluorescent glucose analog)	Life-Technologie, Darmstadt
NCS (Newborn calf serum)	Sigma, Steinheim
Penilicin/Streptavidin (GibCo)	Life-Technologie, Darmstadt
PMSF (Phenyl-Methane-Sulfonyl-Fluoride)	Sigma, Taufkirchen
Ponceau S	Sigma, Taufkirchen
Propidium iodide	Roche, Mannheim
SDS (Sodium dodecyl sulfate)	Roth, Karlsruhe
Sodium azide	Serva, Heidelberg
Sodium fluoride	Sigma, Taufkirchen
Sodium orthovanadate	Sigma, Taufkirchen
TEMED (N,N,N',N'-Tetramethylethylenediamine)	Serva, Heidelberg
Triton X-100	Serva, Heidelberg
Tween 20	Sigma, Taufkirchen

All other chemicals were purchased in analytical grade from Merck (Darmstadt).

4.1.2 INHIBITORS AND AGONISTS

Akt Inhibitor II	Calbiochem, USA
Cycloheximid	Roth, Karlsruhe
Exendin-4	Sigma, Taufkirchen
GLP-1 fragment 7-36 human	Sigma, Taufkirchen
Imatinib (Gleevec)	Biomol GmbH, Hamburg
SU11248 (Sutent, Sunitinib)	ACC Corporation, USA
Tolbutamide	Sigma, Taufkirchen
Glibenclamide	Tocris bioscience, UK

4.1.3 ENZYMES

DNAse I, RNAse free	Roche, Mannheim
Trypsin (GibCo)	Life-Technologie, Darmstadt
REDTaq ReadyMix	Sigma, Taufkirchen
Reverse Transcriptase (AMV)	Roche, Mannheim

4.1.4 KITS AND OTHER MATERIALS

Cell culture materials	Greiner, Solingen
	Nunclon, Dänemark
	Falcon, UK
	Corning, USA
Enhanced Chemi Luminscent (ECL) Kit	PerkinElmer/NEN, Köln
Hyperfilm MP	Amersham Pharmacia, Freiburg
Micro BCA Protein Assay Kit	Pierce, Sankt Augustin
Mouse-/Rat Insulin ELISA	Merck-Millipore, Darmstadt
Parafilm	Dynatech, Denkendorf
Protein A-Sepharose	Amersham Pharmacia, Freiburg
Protein G-Sepharose	Amersham Pharmacia, Freiburg
Protein Marker pre-stained	New England Biolab, USA
QIAGEN Plasmid Maxi Kit	Qiagen, Hilden
QIAGEN Plasmid Mini Kit	Qiagen, Hilden
QIAGEN RNeasy Mini Kit	Qiagen, Hilden
QIAquick PCR Purification Kit (50)	Qiagen, Hilden
Sterile filter 0.22 μm, cellulose acetate	Nalge Company, USA
Sterile filter 0.45 μm, cellulose acetate	Nalge Company, USA
Transwells, 0.8 μM pore-size	BD Biosciences, Heidelberg
Whatman 3MM	Whatman, Rotenburg/Fulda

4.1.5   CELL CULTURE MEDIA

GibcoTM media and supplements were obtained from Life-Technologie (Darmstadt). Media were supplemented to the requirements of each cell line. Freeze medium contained 95 % heat-inactivated FCS and 5 % DMSO.

Transfection media for Accell technology were obtained from Thermo Scientific/Dharmacon (USA). The media for beta-TC6 cells were supplemented with D-glucose up to 4.5 g/ml, 1x L-glutamine and 3 % FCS. For C2C12 and 3T3-L1 cells transfection media were used according to the Thermo Scientific/Dharmacon protocol.

4.1.6   EUKARYOTIC CELL LINES

Cell-Line	Description	Reference
3T3-L1	Mouse pre-adipocytes	ATCC, Denmark
Beta-TC6	Mouse insulinoma	ATCC, Denmark
C2C12	Mouse myoblasts	ATCC, Denmark
RIN-5AH-T2B	Rat insulinoma	ATCC, Denmark

ATCC, American Type Culture Collection, Manassas, USA

4.1.7   PRIMARY ANTIBODIES

The following antibodies were used for immune-precipitation or as primary antibodies in immuneblot or immunofluorescence analysis.

Antibody Description	Immunogen Origin	Reference
pTyr (4G10)	tyrosine residues	UBI, USA / Homemade
α-Tubulin	mouse, monoclonal	Sigma, Taufkirchen
Actin	rabbit, polyclonal	Cell Signaling Tech., USA
pERK	rabbit, polyclonal	Cell Signaling Tech., USA
ERK	rabbit, polyclonal	Cell Signaling Tech., USA
Insulin receptor (IRα)	rabbit, polyclonal	Santa Cruz Corp., USA
IRS-1	rabbit, polyclonal	Santa Cruz Corp., USA
pAkt (Ser 473)	rabbit, polyclonal	Cell Signaling Tech., USA
Akt	rabbit, polyclonal	Santa Cruz Corp., USA
pSTAT3 (Tyr 705)	rabbit, polyclonal	Cell Signaling Tech., USA
PPARγ	rabbit, polyclonal	Santa Cruz Corp., USA
PI3K	rabbit, polyclonal	Santa Cruz Corp., USA

IRS-2	rabbit, polyclonal	Ubi, USA
p-P38	rabbit, polyclonal	Cell Signaling Tech., USA
p38	rabbit, polyclonal	Santa Cruz Corp., USA
p-JNK (Thr183/Tyr185)	rabbit, polyclonal	Cell Signaling Tech., USA
JNK	rabbit, polyclonal	Santa Cruz Corp., USA
p-ERK (Thr202/204)	rabbit, polyclonal	Cell Signaling Tech., USA
ERK	rabbit, polyclonal	Santa Cruz Corp., USA
MEK 1/2 (Ser217/221)	rabbit, polyclonal	Cell Signaling Tech., USA

4.1.8 SECONDARY ANTIBODIES

For immunoblot analysis corresponding secondary antibodies conjugated with horseradish peroxidase (HRP) were utilized.

Antibody Description	Dilution	Reference
Goat anti-mouse-HRP	1 : 10.000	Sigma, Taufkirchen
Goat anti-rabbit-HRP	1 : 50.000	BioRad, München

4.1.9 IMMUNOPRECIPITATION OF PROTEINS

Cell lysates, which were adjusted to an equal protein concentration were precleared with 20 µl of protein A- or G-Sepharose for one hour. In the meantime, appropriate antibodies were pre-coupled to 40 µl Sepharose beads in lysis buffer for one hour and washed twice with lysis buffer. After combining, pre-cleared lysates and pre-coupled antibody-beads were incubated at 4 °C for 4 h and the precipitates were then washed three times with 700 µl lysis buffer, suspended in 3x Laemmli buffer, boiled for 10 min and directly subjected to western blot analysis.

4.1.10 STOCK SOLUTIONS AND COMMONLY USED BUFFERS

Collecting gel buffer (4x)	0.5 M	Tris/HCl pH 6.8
	0.4 %	SDS
HBS (2x) pH 7.0	46 mM	HEPES, pH 7.5
	274 mM	NaCl
	1.5 mM	Na_2HPO_4

HNTG-buffer	20.0 mM	HEPES, pH 7.5
	150 mM	NaCl
	0.1 %	TritonX-100
	10.0 %	Glycerol
	10.0 mM	$Na_4P_2O_7$
DNA loading buffer (6x)	0.05 %	Bromphenol blue
	0.05 %	Xylencyanol
	30.0 %	Glycerol
	100.0 mM	EDTA pH 8.0
Laemmli buffer (3x)	100 mM	Tris/HCl pH 6.8
	3.0 %	SDS
	45.0 %	Glycerol
	0.01 %	Bromphenol blue
	7.5 %	ß-Mercaptoethanol
4G10- lysis buffer	50 mM	Tris, pH 7.5
	150 mM	NaCl
	1 mM	EDTA
	1 %	NP40
	1 %	Triton X-100
	10 mM	$Na_4P_2O_7$
	2 mM	Na_3VO_4
	10 mM	NaF
	1 mM	PMSF
	100 µg/l	Aprotinin
NET-gelatine	50.0 mM	Tris/HCl pH 7.4
	5.0 mM	EDTA
	0.05 %	Triton X-100
	150.0 mM	NaCl
PBS (pH 7.4)	137.0 mM	NaCl
	27.0 mM	KCl
	80.9 mM	Na_2HPO_4
	1.5 mM	KH_2PO_4
Propidium-Iodide (PI) buffer	0.1 %	Na-Citrate
	0.1 %	Triton
	20 µM	Propidium Iodide

SD-Transblot-buffer	50.0 mM	Tris/HCl pH 7.5
	40.0 mM	Glycine
	20.0 %	Methanol
	0.004 %	SDS
Separating gel buffer (4x)	0.5 M	Tris/HCl pH 8.8
	0.4 %	SDS
SRB buffer	0.057 %	Sulforhodamine
	1 %	AcCOOH
"Striping" buffer	62.5 mM	Tris/HCl pH 6.8
	2.0 %	SDS
	100.0 mM	β-Mercaptoethanol
Stop-Solution (MTT)	9.5 %	SDS
	5 %	2-Butanol
	0.012 M	HCL
TAE-buffer	40.0 mM	Tris/Acetate pH 8.0
	1.0 mM	EDTA
	TE10/0.1	10.0 mM Tris/HCl pH 8.0
	0.1 mM	EDTA pH 8.0
TE10/0.1- Solution	10 mM	Tris/HCl pH 8.0
	0.1 mM	EDTA pH 8.0
Tris-Glycine-SDS	25.0 mM	Tris/HCl pH 7.5
	200.0 mM	Glycine
	0.1 %	SDS

4.1.11 sIRNA OLIGONUCLEOTIDES

A: sIRNA SEQUENCES OF THE MOST PROMISING CANDIDATES

Gene Symbol	Pool Number	Duplex Number	Gene ID	Gene Accession	Sequence
ADCK1	E-057682-00	A-057682-13	72113	NM_028105	GGUUCAGGCUCAAAGCUCU
ADCK1	E-057682-00	A-057682-14	72113	NM_028105	CCCAGAUUUUGAAUUCAUG
ADCK1	E-057682-00	A-057682-15	72113	NM_028105	GUAUUGUAUAUAUUGUUUA
ADCK1	E-057682-00	A-057682-16	72113	NM_028105	GUAUCACUCCCAAAGUUGU
AKT1	E-040709-00	A-040709-14	11651	NM_009652	GAUUCAUGUAGAAAACUAU
AKT1	E-040709-00	A-040709-15	11651	NM_009652	CGUGUGACCAUGAACGAGU
AKT1	E-040709-00	A-040709-16	11651	NM_009652	GCGUGGUCAUGUACGAGAU
AKT1	E-040709-00	A-040709-17	11651	NM_009652	UUCUUUGCCAACAUCGUGU
CASK	E-048887-00	A-048887-13	12361	NM_009806	UCUGUGUUUUGAAAUCGUA
CASK	E-048887-00	A-048887-14	12361	NM_009806	CCAUGAGGAUGCAAUGUAC
CASK	E-048887-00	A-048887-15	12361	NM_009806	GUAGUCAGCUGAAAUGUUG
CASK	E-048887-00	A-048887-16	12361	NM_009806	GUUCGUUGCUUAAAAGAUG
CERK	E-040107-00	A-040107-13	223753	NM_145475	CGUUGAAGUUUAUCGAGUC
CERK	E-040107-00	A-040107-14	223753	NM_145475	GUAUGAUUUCUCAGGGUUG
CERK	E-040107-00	A-040107-15	223753	NM_145475	CGGUGCUAUUUAAUGAUUG
CERK	E-040107-00	A-040107-16	223753	NM_145475	CAGUUAUGUUGAUAUAUCC
CHKB	E-065344-00	A-065344-13	12651	NM_007692	UGAUUAUACUUAUGAAGAA
CHKB	E-065344-00	A-065344-14	12651	NM_007692	UCAUGUUGGUUGAUUUUGA
CHKB	E-065344-00	A-065344-15	12651	NM_007692	GCUAUGUACUCAAAUAAAU
CHKB	E-065344-00	A-065344-16	12651	NM_007692	CCUUGGUAUUAGAAAGCGU
CSNK2A1	E-058653-00	A-058653-13	12995	NM_007788	CCAGCUUGUUCGAAAAUUA
CSNK2A1	E-058653-00	A-058653-14	12995	NM_007788	CUAUGACAUUCGAUUUUAC
CSNK2A1	E-058653-00	A-058653-15	12995	NM_007788	GGGUUUAGCUGAGUUUUAC
CSNK2A1	E-058653-00	A-058653-16	12995	NM_007788	CAAUUAUGAUCAGUUGGUG
EPHA4	E-055030-00	A-055030-13	13838	NM_007936	GGGUGUACAUUGAAAUUAA
EPHA4	E-055030-00	A-055030-14	13838	NM_007936	CGGUGAACUUGGAAUGGAG
EPHA4	E-055030-00	A-055030-15	13838	NM_007936	CCAUCACGCACCAGAAUAA
EPHA4	E-055030-00	A-055030-16	13838	NM_007936	CGUUCCUUCUGAAUGUUUU
FLT3	E-040111-00	A-040111-13	14255	NM_010229	CAGUCAGGUUUAAAGCGUA
FLT3	E-040111-00	A-040111-14	14255	NM_010229	CUGUGAUCAAGUGUGUUUU
FLT3	E-040111-00	A-040111-15	14255	NM_010229	UCAGGGACUAUGAAUAUGA
FLT3	E-040111-00	A-040111-16	14255	NM_010229	CUGUUCACCAUAGAUCUAA
FUK	E-064057-00	A-064057-13	234730	NM_172283	CGUUGAACCACGGUGUCUA
FUK	E-064057-00	A-064057-14	234730	NM_172283	GCUUGGUUUUGGACAUUUA
FUK	E-064057-00	A-064057-15	234730	NM_172283	GCUUUGUCCAGAAGAUCAA
FUK	E-064057-00	A-064057-16	234730	NM_172283	GGCUACAGCUACAUGACGA
GPRK5	E-040343-00	A-040343-13	14773	NM_018869	GGGGUGGACUAGAAUUUUC
GPRK5	E-040343-00	A-040343-14	14773	NM_018869	GCACGGAUUUUAAUAGCAU
GPRK5	E-040343-00	A-040343-15	14773	NM_018869	GCAUGUAUUUUGACCGUUU
GPRK5	E-040343-00	A-040343-16	14773	NM_018869	GUAUGCUUGUAAACGCUUA

Gene Symbol	Pool Number	Duplex Number	Gene ID	Gene Accession	Sequence
Gsk3a	E-059026-00	A-059026-13	606496	NM_001031667	GGGUGUAAAUAGAUUGUUA
Gsk3a	E-059026-00	A-059026-14	606496	NM_001031667	GGCUCAUUCGGAGUAGUAU
Gsk3a	E-059026-00	A-059026-15	606496	NM_001031667	UUGUGAGGCUGCGGUACUU
Gsk3a	E-059026-00	A-059026-16	606496	NM_001031667	GGAUUUUAACUGUUUGUAG
KCNH2	E-045764-00	A-045764-13	16511	NM_013569	CCUUCAACCUUCGAGAUAC
KCNH2	E-045764-00	A-045764-14	16511	NM_013569	CCAUCAAGGACAAGUAUGU
KCNH2	E-045764-00	A-045764-15	16511	NM_013569	CUGGGGUGUCCAAUAUUUU
KCNH2	E-045764-00	A-045764-16	16511	NM_013569	UGACUAUGAAUAAUAAAUA
LCK	E-043878-00	A-043878-13	16818	NM_010693	GGGCUGUGCACAAAGUUGA
LCK	E-043878-00	A-043878-14	16818	NM_010693	UCAUUCCCUUCAACUUCGU
LCK	E-043878-00	A-043878-15	16818	NM_010693	GGAUGGAGAACAUUGACGU
LCK	E-043878-00	A-043878-16	16818	NM_010693	GCAUGGCGUUCAUCGAAGA
MAP2K3	E-040121-00	A-040121-13	26397	NM_008928	CUUGGAAGCUAAUAGGUUU
MAP2K3	E-040121-00	A-040121-14	26397	NM_008928	GCAGGUUGUAUAUAUAUUU
MAP2K3	E-040121-00	A-040121-15	26397	NM_008928	GCCUUUUGCUUUGUGGGUA
MAP2K3	E-040121-00	A-040121-16	26397	NM_008928	CUUUGAACUAUUAUUCCUG
MET	E-040878-00	A-040878-13	17295	NM_008591	GAAUUUUGCAGGAUUGAUC
MET	E-040878-00	A-040878-14	17295	NM_008591	CCAUAAAGUACAUACAUGC
MET	E-040878-00	A-040878-15	17295	NM_008591	CUGUUAGACGGGAUUCUUU
MET	E-040878-00	A-040878-16	17295	NM_008591	CUGUCAAGGUUGCUGAUUU
NEK1	E-065653-00	A-065653-09	18004	NM_175089	GUGAUUUGUUUAAACGAAU
NEK1	E-065653-00	A-065653-10	18004	NM_175089	GGUUUGUGCAGAUAUGUUU
NEK1	E-065653-00	A-065653-11	18004	NM_175089	CUCGAGUUCUUAAUAGUAC
NEK1	E-065653-00	A-065653-12	18004	NM_175089	GCUGUGUCCUUUAUGAGUU
PIK3C3	E-063416-00	A-063416-13	225326	NM_181414	GCAAGAUCUAUGUACGUUC
PIK3C3	E-063416-00	A-063416-14	225326	NM_181414	CGAAUCAUCUCCAAUUUUA
PIK3C3	E-063416-00	A-063416-15	225326	NM_181414	GCGUCAAGAUCAGCUUAUU
PIK3C3	E-063416-00	A-063416-16	225326	NM_181414	CCUUGAUGGUUGAUGCAAA
PIP5K1C	E-042927-00	A-042927-13	18717	NM_008844	CUUCUAUGCAGAGCGCUUC
PIP5K1C	E-042927-00	A-042927-14	18717	NM_008844	UCAAAAUGCACCUUAAGUU
PIP5K1C	E-042927-00	A-042927-15	18717	NM_008844	CCCACCACUUCCAGGAUUU
PIP5K1C	E-042927-00	A-042927-16	18717	NM_008844	UCUACAGACAUCUAUUUUC
PRKCB	E-048412-00	A-048412-13	18751	NM_008855	CUCCCAACCUUGUAUGGUA
PRKCB	E-048412-00	A-048412-14	18751	NM_008855	GGUGCAUUCUUCAGUAUGA
PRKCB	E-048412-00	A-048412-15	18751	NM_008855	GUUUUAAGGUUCGUAGUUG
PRKCB	E-048412-00	A-048412-16	18751	NM_008855	GCAAGAUGUUUGUGGGAAU
PRKCN	E-040692-00	A-040692-13	75292	NM_029239	CUCGUGUGCUCCAUUGUUU
PRKCN	E-040692-00	A-040692-14	75292	NM_029239	GGAGGAUCCUUAGUUGUCA
PRKCN	E-040692-00	A-040692-15	75292	NM_029239	GGCUGUGGAUUAAAUUAUC
PRKCN	E-040692-00	A-040692-16	75292	NM_029239	UUGGCAUGUAUGAUAAAAU
RIOK2	E-056209-00	A-056209-13	67045	NM_025934	GCAGAAUAUUAAAUCGAGU
RIOK2	E-056209-00	A-056209-14	67045	NM_025934	CCCUGCAGUUUGAUUGCUU
RIOK2	E-056209-00	A-056209-15	67045	NM_025934	UUUUCAGGUAACUAAUUUA

Gene Symbol	Pool Number	Duplex Number	Gene ID	Gene Accession	Sequence
RIOK2	E-056209-00	A-056209-16	67045	NM_025934	CCCAAAUGCUGAAUGGUAU
ROR1	E-053825-00	A-053825-13	26563	NM_013845	GCCUGGACCAUGGUGAUUU
ROR1	E-053825-00	A-053825-14	26563	NM_013845	CCAUCAUGUACGGCAAAUU
ROR1	E-053825-00	A-053825-15	26563	NM_013845	GUGAAAUCGACAAAGGUUC
ROR1	E-053825-00	A-053825-16	26563	NM_013845	GCAACAUUUUAAUUGGAGA
SCYL1	E-047892-00	A-047892-13	78891	NM_023912	GCCUCAUCUGGGAAGUUUU
SCYL1	E-047892-00	A-047892-14	78891	NM_023912	GCUUCCUGUCCAAAUUAGA
SCYL1	E-047892-00	A-047892-15	78891	NM_023912	GCAGUGUCCAUCUUCGUGU
SCYL1	E-047892-00	A-047892-16	78891	NM_023912	CGACUGUGCCCAUAAGAUC
TLK2	E-040154-00	A-040154-13	24086	NM_011903	UCUUCAAACUUAGAUUAGG
TLK2	E-040154-00	A-040154-14	24086	NM_011903	UAGUGAAGCUGUAUGAUUA
TLK2	E-040154-00	A-040154-15	24086	NM_011903	CGAUUAGGCCACUUUACUA
TLK2	E-040154-00	A-040154-16	24086	NM_011903	CGAUUAAAUAGAUGUGUCA

B: SIRNA SEQUENCES USED FOR VALIDATION PROCESS TARGET VALIDATION

Gene Symbol	Gene ID	Gene Accession	Gene Number	Sequence
ADCK1	72113	NM_028105	118130450	GGUUCAGGCUCAAAGCUCU
ADCK1	72113	NM_028105	118130450	CCCAGAUUUUGAAUUCAUG
ADCK1	72113	NM_028105	118130450	GUAUUGUAUAUAUUGUUUA
ADCK1	72113	NM_028105	118130450	GUAUCACUCCCAAAGUUGU
CSNK2A1	12995	NM_007788	31542426	CCAGCUUGUUCGAAAAUUA
CSNK2A1	12995	NM_007788	31542426	CUAUGACAUUCGAUUUUAC
CSNK2A1	12995	NM_007788	31542426	GGGUUUAGCUGAGUUUUAC
CSNK2A1	12995	NM_007788	31542426	CAAUUAUGAUCAGUUGGUG
EPHA4	13838	NM_007936	86788142	GGGUGUACAUUGAAAUUAA
EPHA4	13838	NM_007936	86788142	CGGUGAACUUGGAAUGGAG
EPHA4	13838	NM_007936	86788142	CCAUCACGCACCAGAAUAA
EPHA4	13838	NM_007936	86788142	CGUUCCUUCUGAAUGUUUU
GPRK5	14773	NM_018869	31980924	GGGGUGGACUAGAAUUUUC
GPRK5	14773	NM_018869	31980924	GCACGGAUUUUAAUAGCAU
GPRK5	14773	NM_018869	31980924	GCAUGUAUUUUGACCGUUU
GPRK5	14773	NM_018869	31980924	GUAUGCUUGUAAACGCUUA
SCYL1	78891	NM_023912	118130697	GCCUCAUCUGGGAAGUUUU
SCYL1	78891	NM_023912	118130697	GCUUCCUGUCCAAAUUAGA
SCYL1	78891	NM_023912	118130697	GCAGUGUCCAUCUUCGUGU
SCYL1	78891	NM_023912	118130697	CGACUGUGCCCAUAAGAUC

C: PRIMER SEQUENCES

ADCK1
R 5′- GCGCCCTGATACAACACCGAGAC-3′
F 5′- CTGACACGGGCAAGGCTGAGA-3′

CSNK2A1
R 5′-TGCGGCCACATCACCCATTAG-3′
F 5′- GGCTGGCCACTTCATCTCTTCTCT-3′

EPHA4
R 5′- AAGCCCCATGGTTTCAGCAATCTC-3′
F 5′- GCCGCCGGGTACACGACACTA-3′

GPRK5
R 5′-TGGCGGTTCTGGAGGCTGACTTCT-3′
F 5′- GCCGGGTGCTGGAGACTGAGGA-3′

SCYL1
R 5′-CGGCGGCGACGATGTGGTTCTTT-3′
F 5′- CGCCGTTGCCCTGTGCCGAGTA-3′

4.1.12 CUSTOMER COMPOUND LIBRARY

The MPI costumer compound library is a kinase focused library to inhibit kinase activity. It has been assembled by several sub-libraries called 1863_SF_MPK, 2121_SF_MPK, 2145_SF_MPK and 2217_SF_MPK with in total 8827 compounds (Cpds), kindly provided by Prof. Dr. Axel Ullrich.

4.2 METHODS

4.2.1 GENERAL CELL CULTURE TECHNIQUES

Cell lines were routinely assayed for mycoplasma contamination and cultured at 95 % air, 5 % CO_2 and 37 °C in a Hera-Cell-150 incubator. Before seeding, the cell amount was determined using a Coulter Counter system (Coulter Electronics) and the corresponding cell amount for seeding was calculated. All cells were cultured according to the appropriate recommendations of ATCC protocols.

4.2.2 ASSAY PROCEDURE FOR BIOLOGICAL ASSAYS

For analysis of protein expression and phosphorylation of secreted or intracellular proteins, cells were seeded at different plate size and suitable cell-density. After 24 h the cells were washed with PBS and fresh media containing DMSO respectively the appropriate treatment with TKIs, peptides or chemicals, was replaced. Starving for insulin dependent examinations was performed in glucose- and FCS-free DMEM media for 4 h.

Cell line	Culture media	Initial cell amount 96- / 12- / 6- well
3T3-L1	DMEM 1.0 g/L glucose, 10 % (v/v) NCS, 2 mM L-glutamine, 1x Pen/Strep	5×10^3 / 5×10^4 / 1×10^5
Beta TC-6	DMEM 4.5 g/L glucose, 15 % (v/v) FCS, 2 mM L-glutamine, 1x Pen/Strep	3×10^4 / 3×10^5 / 6×10^5
C2C12	DMEM 4.5 g/L glucose, 10 % (v/v) FCS, 2 mM L-glutamine, 1x Pen/Strep	3×10^3 / 3×10^4 / 6×10^4
RIN-5AH-T2B	RPMI-1640 4.5 g/L glucose, 10 % (v/v) FCS, 2 mM L-glutamine, 1x Pen/Strep	3×10^4 / 3×10^5 / 6×10^5

4.2.3 SRB ASSAY

The assay was performed as described by Vichai and Kirtikara *et al.* [250]. After treatment, cells were fixed with ice-cold 10 % TCA for 1 h at 4°C, then washed with dH_2O and incubated with sulforhodamine B (0.057 % in 1 % AcCOOH) for 30 min at room temperature. Incorporated dye was dissolved in 10 mM Tris-buffer (pH = 10.5) and the optical density (OD) measured using a multiwell spectrophotometer at a wavelength of 510 nm.

4.2.4   MTT-Assay

For MTT transformation, 1/5 of total volume of a 5 mg/mL MTT stock solution was added to the cells as well as control wells and incubated at 37 °C, 5 % CO_2 (v/v) for 1 h. Then 1/2 of total volume of MTT-stop solution was added and plates were incubated overnight in the dark at 25 °C. The optical density (OD) was measured using a multiwell spectrophotometer at a wavelength of 570 nm.

4.2.5   Lysis of Cells with Phospho- (4G10) and RipA- Lysis Buffer

For protein analysis, cells were washed with cold PBS and lysed by adding ice cold the 4G10-/RIPA- lysis buffer supplied with 10 mM $Na_4P_2O_7$, 2 mM Na_3VO_4, 10 mM   NaF,   1   mM PMSF and 100 µg/L Aprotinin for 5 min on ice. Afterwards, cell lysate was transferred to 1.5 mL pre-cooled aliquots and pre-cleared by centrifugation at 1.3×10^4 rpm for 10 min at 4 °C. The supernatant was then transferred to new 1.5 mL pre-cooled aliquots and directly subjected to protein determination and SDS-gel approach. All lysates were permanently preserved on ice. For long term storage, lysates were frozen down with liquid nitrogen and stored at -80 °C.

4.2.6   Determination of Total Protein Concentration in Cell Lysates

The overall protein concentration was determined using the Micro-BCA Protein Assay Kit (Pierce, Sankt Augustin) according to the supplied standard protocol.

4.2.7   Immune-Precipitation of Proteins

For immune-precipitation, cell lysates were adjusted to an equal protein concentration and pre-incubated at 25 °C with 20 µL of protein A-/G-Sepharose beads in a 1:1 ratio with the previously used lyses buffer on a turning wheel for 1 h. In parallel, used antibodies were pre–coupled to 40 µL A-/G-Sepharose for 1 h and washed three times with 700 µL lysis buffer by softly centrifuging at 1.2×10^3 rpm on 4 °C. Afterwards, both suspensions were pooled and incubated at 4 °C for 4 h. The precipitates were then washed three times with 700 µL of cold lysis buffer, suspended in 3x Laemmli buffer, boiled for 5 min on 95 °C, and directly subjected to SDS-PAGE and western blot analysis.

4.2.8   SDS-PAGE Analysis

SDS-PAGE was conducted as described previously by Sambrook *et al.* [251]. For marking the protein size, a pre-stained protein marker was used.

4.2.9 WESTERN BLOT ANALYSIS

For western blot analysis, total protein was transferred from a SDS-Gel to a nitrocellulose membrane by using a semi-dry blot technique based on the protocol of Gershoni and Palade [252]. The proteins were transferred for 3 h at 0.8 mA/cm^2 using transblot-SD buffer. Afterwards, the membrane was stained with Ponceau S (2 g/L in 2 % TCA) in order to display protein bands. Then, the membrane was de-stained in dH$_2$O and blocked with either NET-gelantine or TBST-buffer, depending on the protocol for the primary antibody. The antibody was diluted according to the manufacturer's instruction and added to the membrane overnight at 4 °C. Next day, the membrane was washed three times in the previously used blocking-buffer and incubated with the appropriate horseradish peroxidase-conjugated secondary antibody diluted in NET-gelatin or TBST-buffer for 1 h at room temperature. Afterwards, the membrane was washed again for at least three times for 20 min each, before the signal was detected by using enhanced chemiluminescence on X-ray films. For detection of the reference proteins, the membrane was incubated at 54 °C in 50 mL stripping buffer containing 433 µL of β-mercaptoethanol and then frequently washed for 3 h until repeating the procedure of protein detection.

4.2.10 BASIC SIRNA RESUSPENSION

Accell siRNA was re-suspended and stored as described in the basic siRNA resuspension protocol of Dharmacon / Thermo Fisher Scientific (USA).

4.2.11 RNA INTERFERENCE

For reduction of gene expression, the Accell technology was used. Cells were seeded 24 h prior and cultured in 96 well plates, 12 well plates or 6 well plates, respectively. Depending on the cell line, different amounts of cells were seeded (see below). After 24 h, cells were washed with PBS-buffer and Accell delivery media containing 1 µM siRNA was replaced according the Accell delivery protocol. Cells were cultured for 72 h for mRNA analysis or 96 h for protein detection, respectively.

Cell line	Supplements for delivery media	Initial cell amount 96- /12- /6- well
3T3-L1	--	5×10^3 / 3×10^4 / 6×10^4
Beta TC-6	Add 3.5 g/L glucose to final concentration of 4.5 g/L, 0.5x L-glutamine, 3 % FCS	1.5×10^4 / 1×10^5 / 2×10^5
C2C12	--	2×10^3 / 1.5×10^4 / 3×10^4

4.2.12 RNA EXTRACTION, cDNA SYNTHESIS, PCR

Total RNA extraction was performed using the RNeasy Protect Mini-Kit (Qiagen) according to the manufacturer's instruction. The resulting pellet was dissolved in nuclease-free water. RNA concentrations were determined using a spectrophotometer at wavelength 260 nm and 280 nm, respectively. Afterwards, 0.5 - 5 µg total RNA was subjected to 1 µL of random primers (K_1 & K_2) in a volume of 10 µl and incubated for 2 min at 68 °C, followed by 10 min incubation at room temperature and heating at 65 °C for 5 min to denature RNA and to inactivate RNases. Then, 1 µl RNase inhibitor, 4 µl of 5x AMV RT buffer, 4 µl dNTPs (2.5 mM each) and 1 µl AMV RT were added and the volume was adjusted to 20 µl. The reaction mix was incubated at 42 °C for 1 h and terminated by heating up to 65 °C for 10 min. For each PCR, 5 µL cDNA (diluted 1:10 in nuclease-free water), 5 µL RedTaq PCR Master Mix, 125 pmol forward and reverse primer and nuclease-free water were added to a final volume of 20 µL. Amplification was performed using an Eppendorf Cycler. The amount of cycles and temperature for annealing depends on the primer-properties and was optimized for each primer-pair. For cDNA denaturation a 5 min cycle at 94 °C was used and 1 min elongation at 72 °C respectively, followed by a final elongation step for 10 min at 72 °C. Detection of the PCR-products was done on a 1 - 3 % agarose-gel and DNA was visualized by ethidium bromide staining. Analysis and quantification was performed with the AIDA Image Reader.

4.2.13 FLOW CYTOMETRY

In order to measure the propidium iodide staining or uptake of the glucose analogue 2-NBDG, transfected or compound-treated cells were washed, trypsinized and harvested in ice-cold PBS before centrifuged at 1.6×10^3 rpm at 4 °C. For propidium iodide detection, the supernatant was collected and used to stop the trypsin reaction. Pooled cells were then incubated with 0.01 % Triton, 0.1 % sodium citrate, 0.02 mM propidium iodide in the dark for 2 h at 4 °C. For 2-NBDG detection, cells were cultured 1 h in glucose free media supplied with 100 µM 2-NBDG at 37 °C before collecting. Cells were analyzed by flow cytometry (FACS Calibur, BD Bioscience, respectively a BD Accuri® C6 Flow Cytometer). For evaluation, cells were gated using the side- and forward scatter SSC/FSC and quantified by excited at 488 nm and the appropriate detection wavelength (FL1 533 nm).

4.2.14 RAT/MOUSE INSULIN ELISA

In order to measure the insulin released upon compound treatment or reduction of gene expression, insulinoma cells were washed and incubated for 2 h in high (4.5 g/L) or low (1.125 g/L) glucose media at 37 °C. After incubation, the supernatant of the beta-TC6 insulinoma cells was diluted 1:20, whereas the supernatants of the RIN-T2B-5AH were diluted 1:10. The insulin release was measured with rat/mouse insulin ELISA by following the

manufacture´s protocol. The enzyme activity of the horseradish peroxidase of the immobilized biotinylated antibodies was monitored spectrophotometric by the increased absorbency at 490 nm, corrected by the absorbency at 610 nm.

4.2.15   ADIPOGENISIS OF 3T3-L1 PRE-ADIPOCYTES

Adipogenesis was performed according to the manual of the Cayman Chemicals adipogenesis kit. For 3T3-L1 differentiation 5 x10^4 pre-adipocytes were cultured in a 12-well for 48 h. Two days post confluence (day 0), media was changed to either induction media (DMEM 1.0 g/L, 10 % FCS, 0.5 mM IBMX, 1 µM dexamethasone and 1 µg/mL insulin with or without sunitinib) or fresh DMEM containing 10 % NCS. Two days after induction, media was changed to progression media (DMEM 1.0 g/L, 10 % FCS, 0.5 mM IBMX, 0.5 µM dexamethasone and 10 µg/mL insulin with or without sunitinib). After two further days, media was replaced with freshly maintained media (DMEM 4.5 g/L, 10 % FCS, insulin) and cultured for at least 2 more days, monitoring the accumulation of lipid droplets under a microscope. Lipid droplets were stained using Oil Red O for 20 min before washed several times with distilled water and extracting the dye using the provided extraction solution, respectively isopropanol. Staining was monitored spectrophotometric by the increased absorbency at 492 nm.

4.2.16   TREATMENT WITH CYCLOHEXIMID

Cycloheximid (CHX) was used to block the insulin production based on protein biosynthesis. Cells were cultured for 24 h before treated with 25 µg/mL, 50 µg/mL and 100 µg/mL for 8 h. Every hour, the appropriate wells were washed with PBS and replaced with fresh media supplied with the suitable concentration of CHX and compound respectively. For follow up experiments 100 µg/mL CHX for 4 h was used.

4.2.17   PHOTOMETRIC DETECTION OF FLUORESCENCE BY A TECAN EVOLUTION READER

In order to detect glucose uptake, we used a fluorescent d-glucose analog 2-[N-(7-nitrobenz-2-oxa-1,3-diazol-4-yl)-amino]-2-deoxy-d-glucose (2-NBDG) [250]. Cells were cultured for 24 h before treated with glucose free media supplied with 100 µM 2-NBDG, respectively inhibitor compounds for 1 h at 37 °C. Fluorescence was collected by a Tecan Evolution Reader at wavelength 535 nm (excitation wavelength 485 nm).

4.2.18   KINOME SCANTM

The KINOME*scan*™ technology was provided by DiscoverX. Compounds that bind the kinase active site and directly (sterically) or indirectly (allosterically) prevent kinase binding to the immobilized ligand reduced the amount of kinase captured on the solid support. Conversely, test molecules that did not bind the kinase displayed no effect on the amount of kinase captured on the solid support. Screening hits were identified by measuring the amount of kinase captured in test versus control samples by using a quantitative qPCR method that detects the associated DNA label.

4.2.19   CLONING OF GENE-PRODUCTS

Gene constructs were designed according to Proteros' internal construct design process. A selection of 4 different constructs per target using several lengths and a GST-Tag appropriate for assay development were produced in vectors suitable for intracellular expression in insect cells. The DNA sequences of all resulting expression vectors were verified by sequencing (GATC). Recombinant high titer virus stocks (HTVS) for all constructs were generated and amplified by standard procedures. Intracellular expression was performed by infecting Sf9 cells grown in Grace´s medium supplemented with 10 % FCS and 0.1 % Pluronic with recombinant virus. After expression, cells were harvested by centrifugation and the cell pellet was stored frozen (-80 °C) until used for purification.

4.2.20   SCYL1 PROBE DISPLACEMENT ASSAY AND HIGH THROUGHPUT SCREEN

For the Scyl1 displacement assay, the following protocol was used:

Target enzyme: full length Scyl1 (1-808), human
Assay plates: 384 well U bottom, PP, black, low volume (Corning, 3676)
Reaction temperature: 25°C
Reaction buffer: 20mM Mops, pH 7.5, 1mM DTT, 0.01 % Tween20
Final assay concentrations: 20 nM Scyl1, reporter porbePRO16 = 607 nM (= K_D-probe)
Pipetting sequence: 1) Add 10 Al 15/10 fold concentrated target enzyme in reaction buffer 2) Add 5 Al 15/5 fold concentrated reporter probe in reaction buffer 3) Incubate for 30 min 4) Add 62.4 nl inhibitor in 100 % DMSO using pin tool 5) Measure time dependency of reporter displacement

4.2.21   IC$_{50}$ DETERMINATION FOR SCYL1

To determine the IC$_{50}$ values for all compounds ≥ 75 % inhibition, triplicates at 12 different concentrations with a dilution factor of three were used. The maximal compound assay

concentration was set to 58 μM, exceeding the compound assay concentration used in the primary screen. For all assay plates, z-prime values were found to be significantly larger than 0.5, proving statistical relevance of the data.

4.2.22 GRK5 ENZYMATIC ASSAY AND HIGH THROUGHPUT SCREEN

For Grk5 kinase activity assay, the following protocol was used:

Target enzyme: full length Grk5 (Millipore, #14-714).

Assay plates: 384 well U bottom, PP, white, low volume (Corning, 3674)

Reaction Volume: 6 μl

Reaction Time: 60 min

IMAP Incubation Time: 60 min

ADP Glo™ Kinase Assay Kit: Promega, V9101

Reaction temperature: 25 °C

Reaction buffer: 20 mM MES pH 6.0, 1 mM DTT, 10 mM MgCl$_2$, 0.01 % Tween20

Kinase: 20 nM full length GRK5 (Millipore, # 14-714)

ATP: 18.7 μM, adjusted to Km$_{(ATP)}$

Substrate: 10 μM casein

Pipetting Sequence: 1) Add 4 μl 6/4 fold concentrated substrate + 6/4 fold concentrated ATP in 1 fold concentrated Reaction Buffer to each well of Assay Plate 2) Add 6 nl 1000 fold concentrated compound in 100 % DMSO to each well except to C- and C+ wells using pintool 3) Add 6 nl 100 % DMSO to C- and C+ wells using pin-tool 4) Add 2 μl Reaction Buffer to C- wells 5) Add 2 μl 6/2 fold concentrated Kinase in Reaction Buffer to each well except C- wells 6) Incubate 120 min at room temperature 7) Add 6 μl ADP-Glo™ Reagent to each well to stop the kinase reaction and deplete the unconsumed ATP 8) Incubate 40 min at room temperature 9) Add 12 μl of Kinase Detection Reagent to convert ADP to ATP and start luciferase / luciferin reaction to detect ATP 10) Incubate 40 min at room temperature 11) Measure luminescence intensity

4.2.23 IC$_{50}$ DETERMINATION FOR GRK5/GPRK5

In order to determine the IC$_{50}$ values for all compounds ≥ 35 % inhibition, triplicates at 12 different concentrations with a dilution factor of three were used. The maximal compound assay concentration was set to 100 μM, representing the compound assay concentration used in the primary screen. For all assay plates, z-prime values were found to be significantly larger than 0.5, proving statistical relevance of the data.

5 RESULTS

5.1 INFLUENCE OF SUNITINIB ON PERIPHERAL TISSUES *IN VITRO*

5.1.1 DIFFERENTIATION OF 3T3-L1 CELLS

The 3T3-L1 cell line is a frequently used model system for adipose tissue and diabetes research. Regularly, 3T3-L1 cells have a fibroblast-like morphology, which can be differentiated by IBMX, dexamethasone and insulin into an adipocyte-like phenotype [253]. As one of the main consumer tissue of glucose and because of its impaired response to insulin in diabetes [254], we examined the effect of sunitinib on 3T3-L1 differentiation to investigate if sunitinib can substitute or enhance insulin in adipocyte formation. An adipogenesis assay kit (Cayman Chemicals) was used for differentiation, according to manufacturer`s instructions. 3T3-L1 pre-adipocytes were treated with either an adipogenesis initiation media with sunitinib and with (AIM+) or without (AIM-) insulin, respectively adipogenesis progression media with sunitinib (APM+) with and without insulin (APM-), for two days each. Further differentiation was maintained according to the assay instructions.
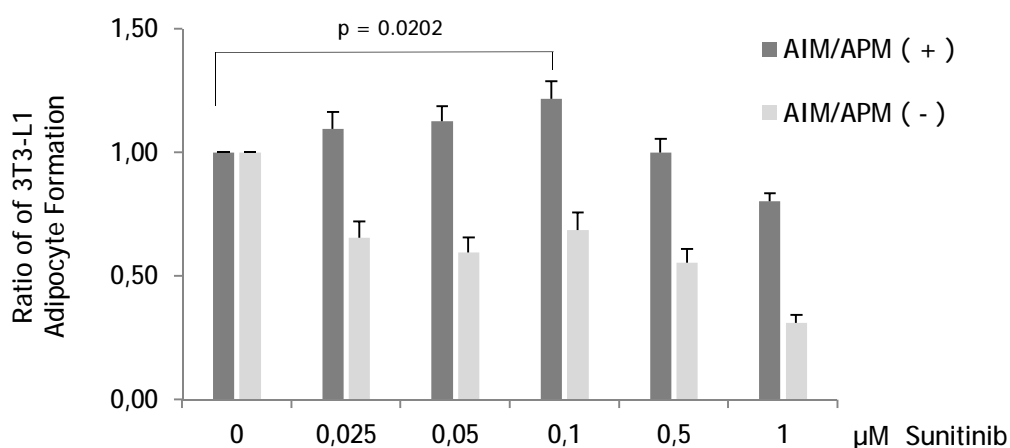
Figure R1 | *3T3-L1 differentiation upon sunitinib treatment. Sunitinib, in addition to insulin, increases the differentiation of 3T3-L1 adipocytes but cannot substitute for insulin. AIM/APM+ (dark grey) adipogenesis initiation/progression media supplemented with sunitinib/insulin; AIM/APM– (light grey) adipogenesis initiation/progression media with sunitinib/without insulin.*

Pre-adipocytes differentiation over 8 days upon sunitinib treatment improved the formation of matured 3T3-L1 adipocytes within a narrow concentration window ranging from 0.025 µM to 0.1 µM but could not substitute for insulin (Figure R1). Moreover, treatment without insulin but sunitinib as well as higher sunitinib concentrations in combination with insulin seemed to impair adipocyte formation (Figure R1). A similar observation of increased differentiation and growth arrest during sunitinib treatment has been published for monocyte differentiation of acute myelogenous leukemia [255]. A comparable observation in C2C12 cells was not monitored.

5.1.2   EFFECTS OF SUNITINIB ON DIFFERENTIATION-RELATED PROTEINS

The previously described increased differentiation of 3T3-L1 adipocytes by sunitinib should also be reflected by important differentiation related candidate proteins like the signal transducer and activator of transcription 3 (STAT3), the serine/threonine kinase Akt/PKB and the peroxisome proliferator activated receptor gamma (PPARγ). STAT3, which is a mitogenic signaling protein activated during the formation of adipocytes, plays an important role in mitotic clonal expansion and differentiation [256]. Another indicator of differentiation is the Akt/PKB, which becomes active by PI3K mediated phosphorylation. Akt/PKB induces the differentiation into adipocytes in 3T3-L1 [27, 257] and activates GLUT4 translocation, which subsequently increases glucose uptake [27]. Also important is PPARγ, which is pre-dominantly expressed in adipose tissue and regulates fatty acid metabolism as well as induction of adipocyte differentiation. Already available drugs like e.g. thiazolidinedione affect the peroxisome proliferator-activated receptors (PPARs), specifically PPARγ, resulting in an increased amount of insulin-sensitive adipocytes as well as a significant decrease in serum-free fatty acid levels (FFA) and tumor-necrosis-factor alpha (TNFα) expression [103, 105]. However, Akt/PKB, STAT3 and PPARγ were investigated for phosphorylation or

expression, respectively, during adipocyte formation by comparing the sunitinib treated cells to the DMSO control. For each concentration and each point of time the cells were lysed using RIPA lysis buffer.
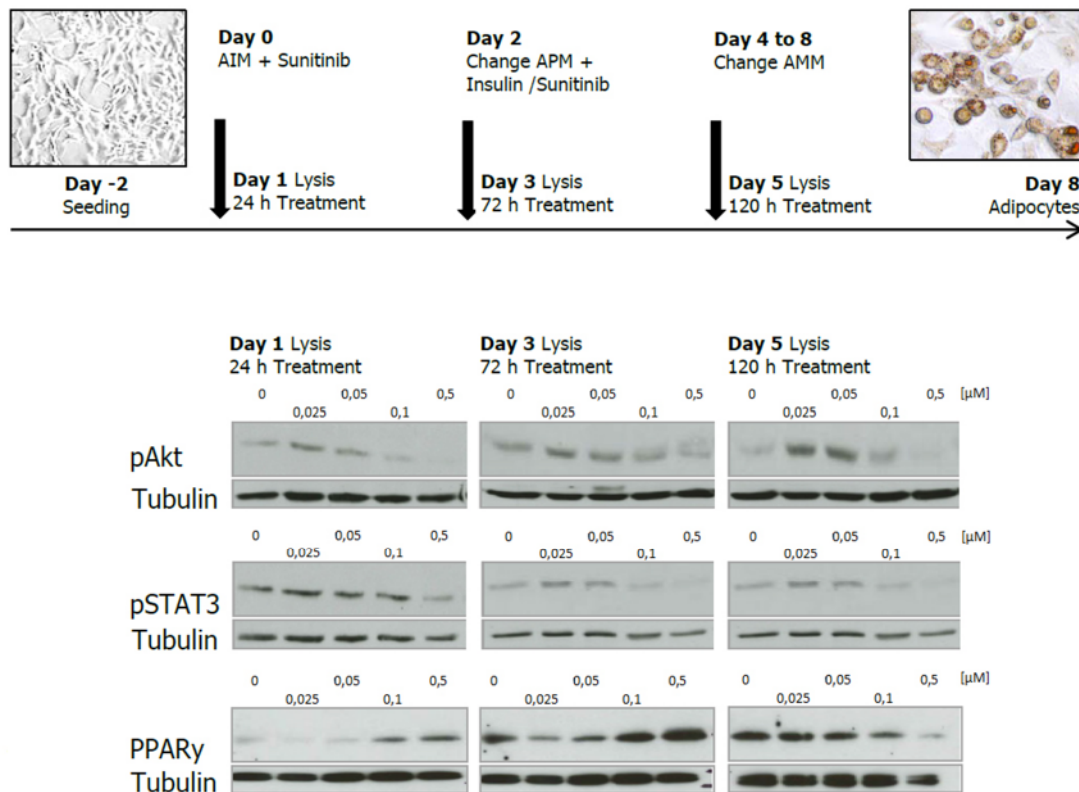

Figure R2 | *3T3-L1 differentiation markers after additional sunitinib treatment at day 0 and day 2. Cells were treated with sunitinib concentrations ranging from 0.025 to 0.5 µM and lysed after 24 h of treatment. AIM = adipogenesis initiation media, APM = adipogenesis progression media, AMM = adipogenesis maintaince media. Blots depicted the phosphorylation levels after sunitinib treatment for Akt/PKB and STAT3 as well as protein levels of PPARγ, respectively.*

Akt/PKB and STAT3 displayed increased phosphorylation and PPARγ increased protein levels after sunitinib treatment (Figure R2). Akt/PKB depicted increased phosphorylation of nearly 2-fold after 24 h and 72 h and almost 4-fold after 120 h by sunitinib concentrations ranging between 0.025 – 0.05 µM. In parallel, STAT3 was just slightly regulated in an equal concentration window of 0.025 µM to 0.05 µM. Here, the increase of phosphorylation was nearly 1.5-fold for 0.025 µM and 1.15-fold for 0.05 µM over the period of time (Figure R2).

In contrast, PPARγ seemed to be regulated by sunitinib at higher concentrations. The expression of PPARγ inclined with increasing concentration of sunitinib, ranging between the 1.5-fold (0.05 µM) to the 12-fold (0.5 µM) after 24 h during initiating of adipocyte formation and the 1.25-fold (0.1 µM) to the 1.7-fold (0.5 µM) during the progression of adipocyte formation (Table R1).

Table R1 | *Densitometry analysis of 3T3-L1 differentiation markers after sunitinib treatment. All data displayed as ratio to DMSO control.*

Treatment	Sunitinib [µM]	pAkt	pSTAT3	PPARγ
24 h	0	1	1	1
24 h	0.025	1.80	1.25	0.76
24 h	0.05	1.28	1.01	1.51
24 h	0.1	0.69	1.14	6.98
24 h	0.5	0.21	0.57	12.05
72 h	0	1	1	1
72 h	0.025	1.98	1.48	0.45
72 h	0.05	1.81	1.14	0.32
72 h	0.1	0.96	0.55	1.25
72 h	0.5	0.82	0.37	1.77
120 h	0	1	1	1
120 h	0.025	4.32	1.50	1.24
120 h	0.05	3.89	1.17	1.0
120 h	0.1	1.20	0.59	0.64
120 h	0.5	0.27	0.34	0.22

5.1.3 INSULIN SIGNALING IN 3T3-L1 AND C2C12 CELLS AFTER SUNITINIB TREATMENT

In order to investigate key regulators of insulin signaling in peripheral tissue, we used C2C12 myoblast and 3T3-L1 pre-adipocytes to detect phosphorylation levels of the insulin receptor (InsR) as well as protein kinases and substrates like the insulin receptor substrate 1 (IRS-1), phosphoinositide-3-kinase (PI3K), AKT/PKB and the mitogen-activated protein kinase 14 (p38/MAPK14). Cells were cultured with 5 µM, and 10 µM sunitinib, respectively, in the presence or absence of 10 µg/mL insulin for 2 h.
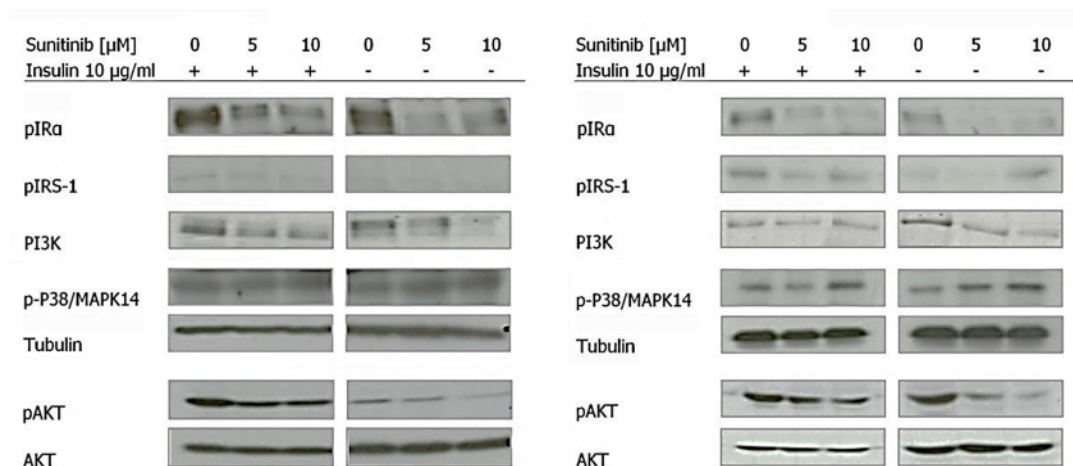
Figure R3 | *Phosphorylation in C2C12 (left) and 3T3-L1 (right) after sunitinib treatment (5µM and 10µM) in absence and presence of insulin, monitored by western blot. IRα, IRS-1 and PI3K are precipitated using an anti-Tyr(P) 4G10, respectively Phospho-Ser/Thr antibody. For p38/MAPK14 and Akt, phosphor-specific antibodies were used.*

Treatment of C2C12 and 3T3-L1 with sunitinib in the presence or absence of insulin displayed a clear decrease of IRα, IRS-1, PI3K and AKT1 in both cell lines used. In contrast, p38/MAPK14, which has already been connected to GLUT4 translocation after phosphorylation [146, 258], was increased along with increasing concentrations of sunitinib. 3T3-L1 cells displayed the strongest effect of increased p38/MAPK14 phosphorylation, ranging from the 2.43-fold (10 µM sunitinib, without insulin) to 1.86-fold (10 µM sunitinib,

with 10 µg/mL insulin) (Figure R3). C2C12 myoblasts depicted an equal tendency, ranging from 1.84-fold (10 µM sunitinib, without insulin) to 1.42-fold (10 µM Sunitinib, with 10 µg/mL insulin) (Figure R3). However, due to the controversial picture of the phosphorylation pattern and the multitude of possible sunitinib targets, an obvious mode of action for the effect of sunitinib in peripheral tissues remains obscure.

5.2 EFFECTS OF SUNITINIB ON INSULIN SECRETING INSULINOMA CELL LINES

5.2.1 RELEASE OF INSULIN AFTER SUNITINIB TREATMENT

The observation that sunitinib led to a remission of diabetes and an improvement of glucose-levels in patients with metastatic renal cell carcinoma [122, 128] could either depend on the previously described results of the peripheral tissue or is based on an improved insulin release by pancreatic beta cells. To investigate if sunitinib has an anti-diabetic effect due to increased insulin release, we treated the insulinoma beta-TC6 cells (mouse) and RIN-5AH-T2B (rat), which are able to secrete insulin, with sunitinib and imatinib. The cells were treated for 2 h with concentrations ranging from 0 to 10 µM in a high glucose (4.5 g/L) DMEM media. Afterwards, the supernatant was analyzed using a rat/mouse insulin ELISA.
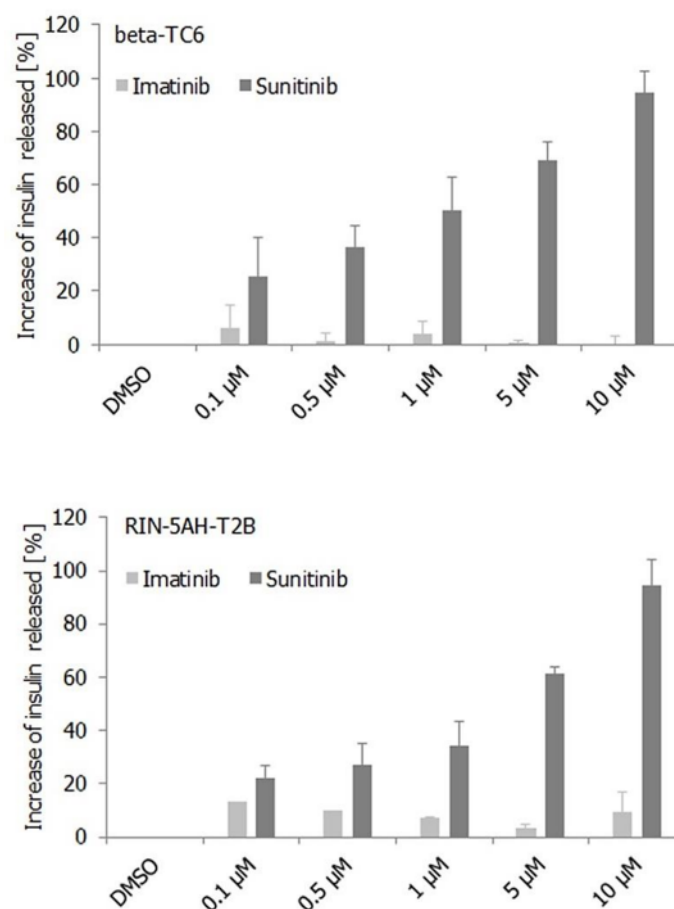
Figure R4 | *Insulin released by insulinoma cell lines after sunitinib and imatinib treatment. Cells were treated for 2 h with concentrations ranging from 0 to 10 µM. Insulin was detected using a rat/mouse insulin ELISA. Sunitinib improved the insulin release ranging from 21.87 ±*

13.16 % (0.1 µM) to 94.23 ± 9.3 % (10 µM) for beta-TC6 cells (upper bar chart) as well as form 30.78 ± 12.04 % (0.1 µM) to 96.26 ± 8.8 % (10 µM) in RIN-5AH-T2B cells (lower bar chart). Imatinib displayed no significant effect on insulin release.

Sunitinib, but not imatinib, displayed a concentration dependent increase of insulin released by beta-TC6 and RIN-5AH-T2B cells. Sunitinib concentrations between 0 and 10 µM increased the insulin release up to 13.16 % (0.1 µM) to 94.23 ± 9.3 % (10 µM) in beta-TC6 and 12.04 % (0.1 µM) to 96.26 ± 8.8 % (10 µM) in RIN-5AH-T2B, respectively (Figure R4). This observation provided a possible link to the previously described observation of lowered blood glucose levels in patients [122]. Furthermore, the treatment of insulinoma cell lines, which mimic the effect of insulin secreting beta-islets, revealed an effect similar to already used drugs, e.g. sulfonylureas.

5.2.2 INSULIN RELEASE IN BETA-TC6 CELLS AFTER SUNITINIB TREATMENT AND BLOCKING OF PROTEIN-BIOSYNTHESIS BY CYCLOHEXIMID

Cycloheximid (CHX) is produced by the bacterium *Streptomyces griseus* and is known as an inhibitor of protein-biosynthesis in eukaryotic organism. It is interfering within the translational elongation of the mRNA in the cytosol, respectively the endoplasmatic reticulum (ER) and thus blocking the production of proteins by the ribosome. In this case, we used CHX to determine if the previously described effect is based on increased translation of insulin mRNA or on an improved insulin release. Furthermore, we defined the half-life of insulin stored in the beta-TC6 cells upon CHX treatment by using 25 µg/mL, 50 µg/mL and 100 µg/mL of CHX over 8 h.
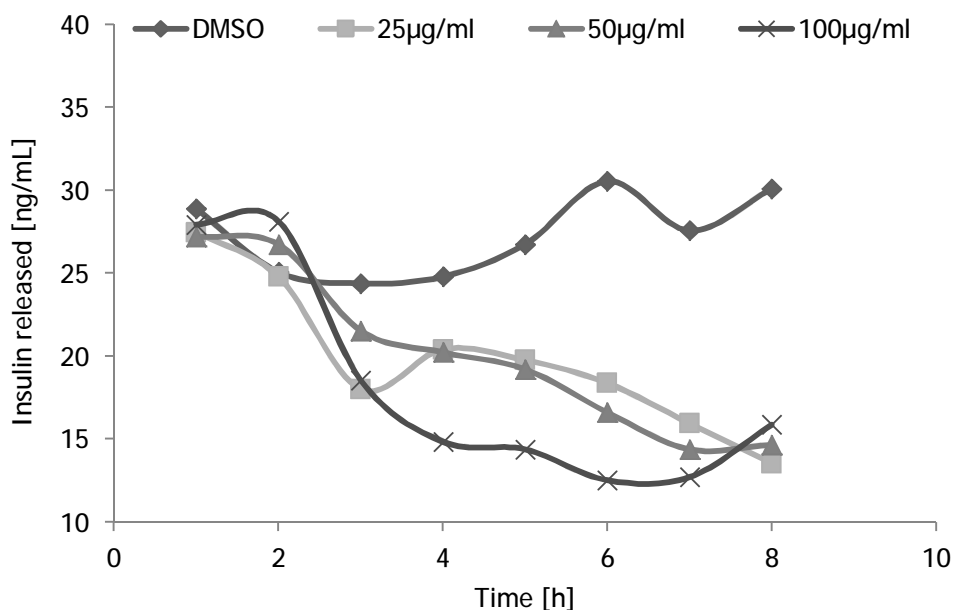
Figure R5 | *Insulin released by beta-TC6 cells after cycloheximid (CHX) treatment over 8 h in high glucose (4.5 g/L) DMEM. Cells were exposed to various concentrations of CHX to determine the amount of insulin that was still available without renewing due to protein biosynthesis.*

After 3 h of CHX treatment, cells reduced the amount of insulin released down to nearly 70 % (~ 20 ng/mL) compared to the DMSO control for all three concentrations used. Exposure to 100 µg/mL CHX directed into a continuous decrease of insulin released to almost 43 % (~12 ng/mL), whereas the treatment with 50 µg/mL and 25 µg/mL did not display a comparably decrease until an 8 h treatment (Figure R5). Thus, for further investigations a 4 h treatment at 100 µg/mL CHX was used.
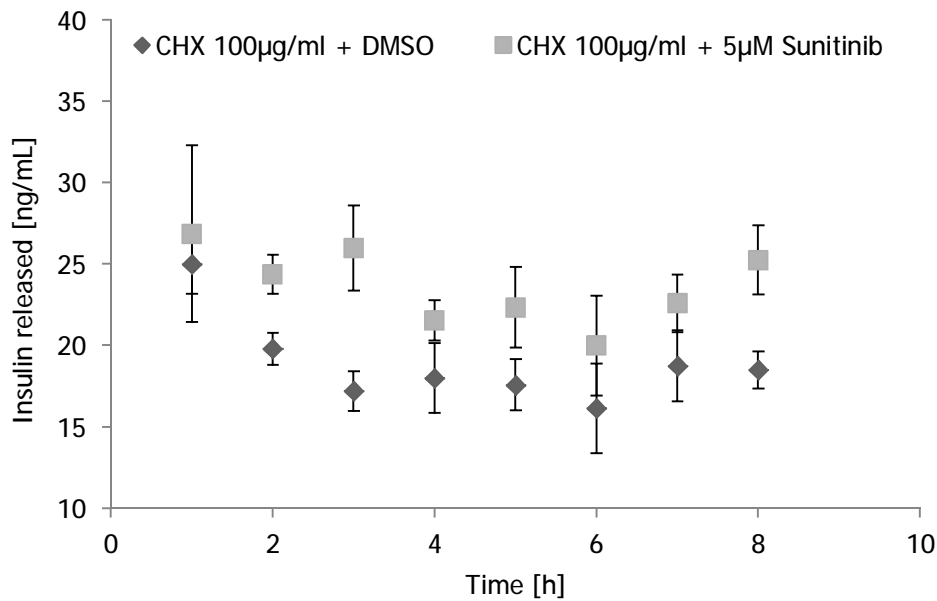
Figure R6 | *Insulin released by beta-TC6 cells after a combined cycloheximid (CHX) and sunitinib treatment. Cells were exposed to 100 µg/mL CHX over 8 h and treated with 5 µM sunitinib for 1 h each in high glucose (4.5 g/L) DMEM.*

In general, the reduced amount of insulin released after a 100 µg/mL CHX treatment was similar to the previously described experiment. The reduction of insulin accounted for nearly 60 % (~ 16 ng/mL) after 6 h compared to the DMSO control output (Figure R5). However, in spite blocking the gene transcription, sunitinib increased the amount of insulin released by the beta-TC6 cells ranging between 51.1 ± 3.82 % after 3 h and 20.49 ± 3.94 % after 6 h of treatment (Figure R6). Hence, sunitinib improved the insulin release in beta-TC6 cells by inhibiting negatively regulating kinases that play a role in triggering metabolic effects for insulin release and do not work by regulating the insulin turn-over.

5.2.3 INTRINSIC INSULIN SIGNALING IN BETA-TC6 CELLS AFTER SUNITINIB TREATMENT

Beside the insulin receptor (InsR) or the insulin like growth factor receptor (IGFR), which both possibly mediate insulin feedback signaling for pancreatic beta cells [139, 140], protein kinases and substrates are crucial factors in triggering insulin release. Thus, we investigated prominent candidates like IRS-1, PI3K, AKT/PKB, the protein kinase C (PKC), p38 as well as the JUN N-terminal kinase (JNK) and mitogen-activated protein kinase 1 and 2 (ERK1/2) regarding their phosphorylation after a sunitinib treatment in absence and presence of 10 µg/mL insulin for 2 h in high glucose (4.5 g/L) media.
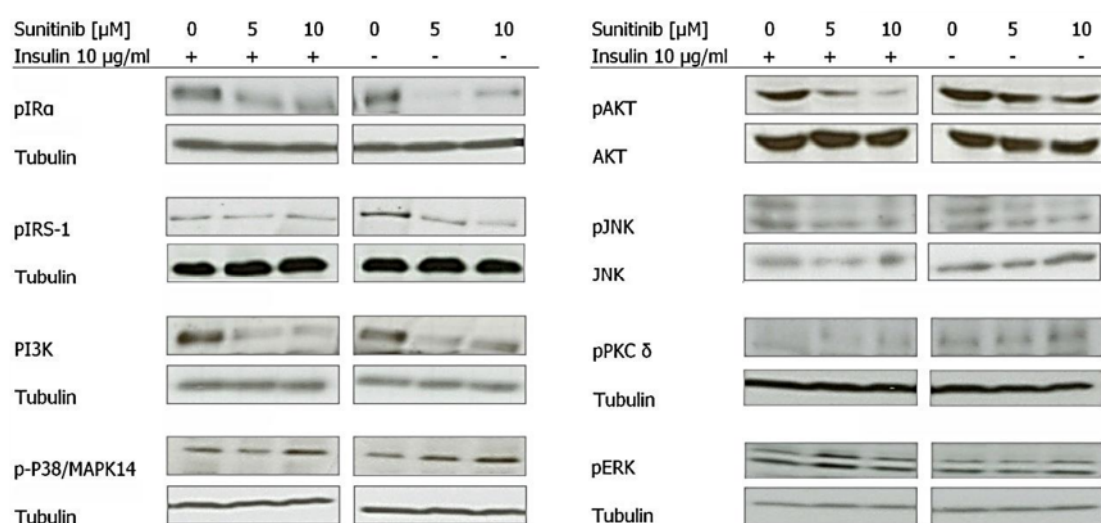
Figure R7 | *Phosphorylation of prominent candidates for insulin release after sunitinib treatment with 5 µM and 10 µM in present or absence of 10 µg/mL insulin in beta-TC6 cells. Western blot analysis was used to determine the phosphorylation level after a 2 h treatment.*

The beta-TC6 intrinsic insulin receptor (IR) displayed a strong reduction of phosphorylation after sunitinib treatment as well as the whole IR mediated signal cascade. Subsequently, phosphorylation of PI3K and Akt/PKB decreased significantly, whereas IRS-1 seemed just to be regulated slightly after sunitinib treatment. However, the reduced inhibition of IRS-1 could possibly be based on JNK activation, which is known as a negative regulator of IRS-1

(Figure R7). Interestingly, p38, which is known as trigger for insulin release was up-regulated with increasing sunitinib concentrations. Suggested to be active and effective in the maintenance of the phosphorylation state of the voltage-gated L-type calcium-channels and thereby enabling an appropriate function of this channel in insulin secretion [259, 260], PKCδ displayed an increased phosphorylation and therefore indicated a further possible mode of action of increased insulin release after sunitinib treatment (Figure R7). However, thinking of the core character of sunitinib as multiple kinase inhibitor, which inhibits more than 300 putative kinase targets [138], manifold mechanisms to trigger insulin release - by negatively regulating known and unknown kinases - become possible. Therefore, we performed a kinome wide siRNA based screen in beta-TC6 cells.

5.3 Kinome Screen

Insulin secretion is mainly based on the oxidative metabolism of glucose and the subsequent voltage mediated release of insulin. However, today more and more triggers of insulin secretion like GLP-1, NEFAs, acetylcholine and several kinases e.g. AMPK, CK2, SGK1 and p38 have been revealed. Recently, tyrosine kinase inhibitors (TKIs) have been connected to the remission of type 2 diabetes [127, 128], suggesting a previously unnoticed impact of kinases in this disease. Furthermore, our *in vitro* experiments revealed a significant and concentration dependent increase of insulin release in beta-TC6 and RIN-5AH-T2B cells after sunitinib treatment as well as promising phosphorylation patterns in intrinsic insulin signaling. Assuming the presence of more than the already known kinases, which are responsible for initiating insulin release, we investigated a siRNA based kinome screen in beta-TC6 cells. Cells were treated with Accell siRNA technology for 96 h and then the supernatant was replaced with fresh high glucose (4.5 g/L) DMEM for 2 h. Afterwards, the supernatant was collected and the amount of insulin measured using a rat/mouse insulin ELISA. The cell viability after siRNA treatment was detected using either a SRB- or a MTT-

assay. The whole kinome panel (652 kinases and pseudo-kinases) was repeated twice to generate a heat map to display the most important regulators of insulin release upon reduction of gene expression. To get the most comprehensive data for n = 2, we compared the raw data of insulin release for each biological independent experiment as well as the insulin release to the performed SRB-assay (Figure R8).
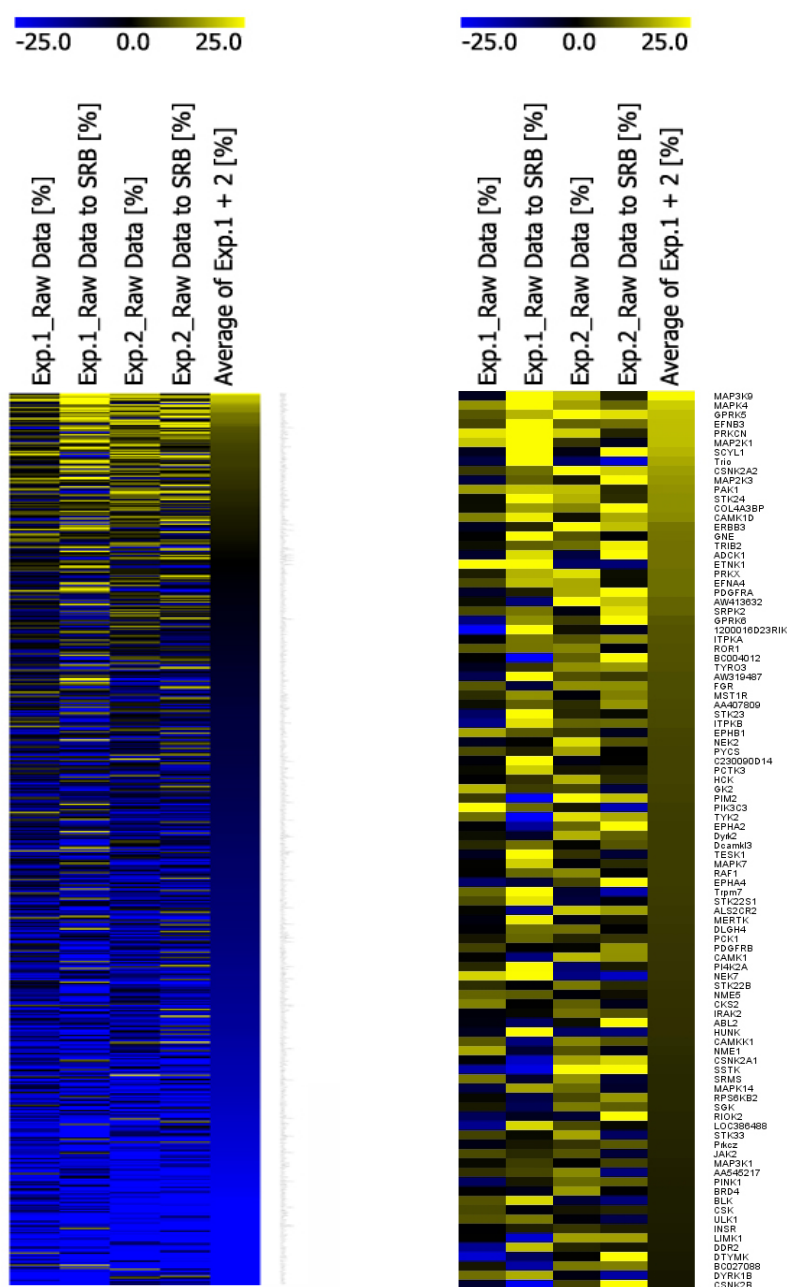

Figure R8 | *Insulin released by beta-TC6 cells after reduction of gene expression using a kinome siRNA library. Heat map of the first two biologically independent experiments. Data depicted the increase or decrease of insulin release in percentage to average release of the*

approach (raw data) as well as the ratio to the performed SRB-assay, ranged between -25 % (blue) and 25 % (yellow). Heat map for all 652 depleted kinases (left) and enlargement of most promising kinases, which were ranging between 0 % and 25 % for insulin released (right). Heat map was generated by using multiple experiment viewer (MeV 4.8.1).

The first two biologically independent experiments revealed interesting candidate genes of several groups and canonical pathways, that seem to increase insulin release upon reduction of gene expression. For example, various MAP/ERK-kinases like MAP2K1, MAP2K3, MAP3K1, MAP3K9, MAPK14 (p38), MAPK4 and MAPK7, which are partly known to play an important role in glucose homeostasis and insulin release have been detected [261]. Furthermore, calcium dependent kinases like CAMK1, CAMK1D and CAMKK1 as well as CSNK2A1, CSNK2A2 and CSNK2B, which have already been connected to insulin release [165, 172, 262], displayed an improved release of insulin upon reduction of gene expression. Kinases in the inositol-phosphate metabolism (e.g. ITPKA, ITPKB, GPRK5 and GPRK6) and PDGF signaling (e.g. CSNK2A1, JAK2 of MAP-Kinases) were also detected. Some kinases like EFNB3, SCYL1, TRIB2 and ADCK1 were not linked to the pathway of insulin release but seemed to be novel interesting negative regulators. In contrast, there were also positively regulating kinases which decrease the insulin released by beta-TC6 cells upon reduction of gene expression. Representatives of this group were, for example, the Janus kinase 1 JAK1 (- 53.4 ± 4.2 %), the hepatocyte growth factor receptor (HGFR/MET – 39.9 ± 2.4 %), the fucokinase (FUK; - 34.3 ± 6.0 %) and the Akt1/PKB (Akt/PKB – 29.3 ± 2.7 %). All but the fucokinase have already been linked to impaired insulin release upon inhibition, knock-out or reduction of gene expression [263-265], respectively, and thus were excellent internal assay controls. However, the evaluation revealed 72 promising negatively regulating candidates which were further investigated in a third biological experiment and hence narrowed down to 40 candidates (Figure R9). The following experiments 4 – 6 were treated likewise and exposed new negatively regulating kinases for triggering insulin release. The viability of the cells in experiments 3 – 6 was detected using a MTT-assay.
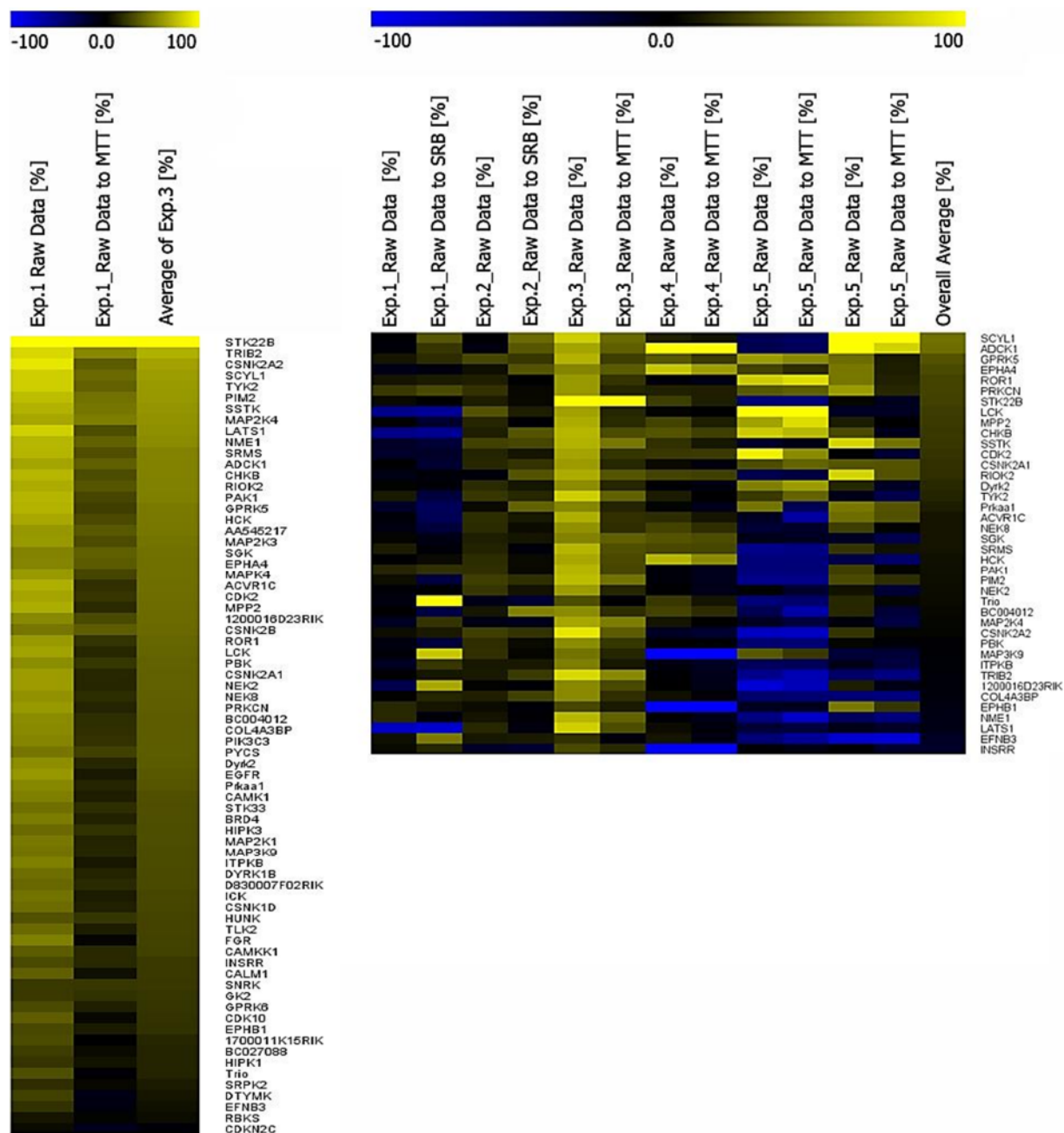
Figure R9 | *Insulin released by beta-TC6 cells after reduction of gene expression using a pre-selected kinase panel. Heat map for the third biologically independent experiment, containing 72 pre-selected kinases (left) and heat map of all experiments for the selected 40 candidate kinases (right). Data depicted the increase or decrease of insulin release in percentage to average release of the approach (raw data) as well as the ratio to the performed MTT-assay, ranging from -100 % (blue) to 100 % (yellow). Heat map was generated by using multiple experiment viewer (MeV 4.8.1).*
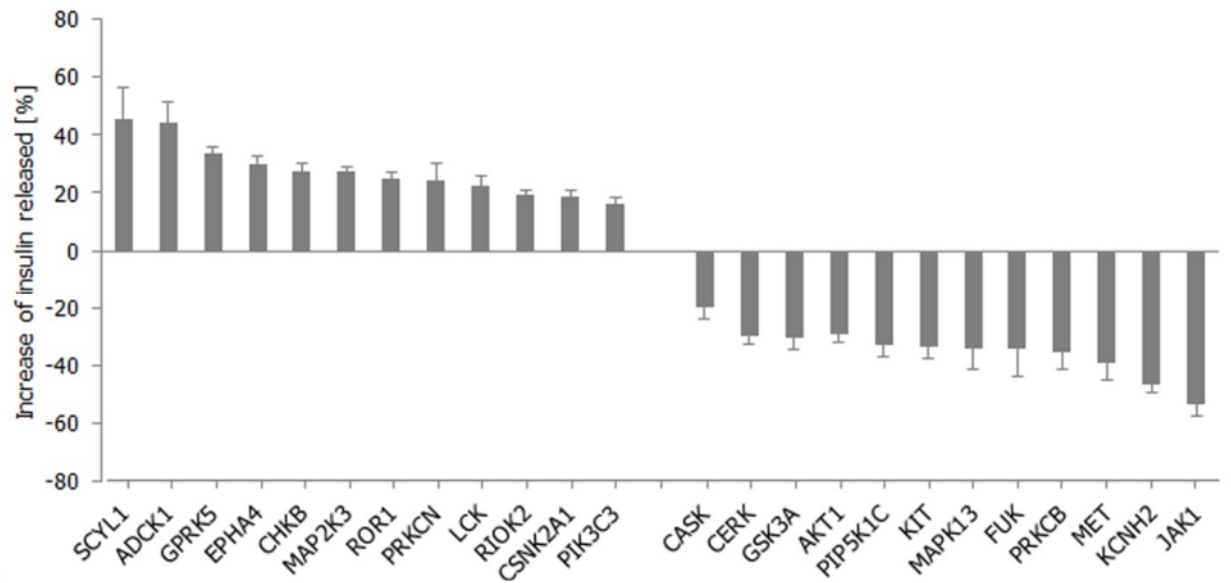
Figure R10 | *Insulin release of negatively and positively regulating kinases upon reduction of gene expression. Candidate genes were limited by using heat map analysis and by proposing an in-/decrease of insulin of at least 15 %.*

Promising candidate kinases of the siRNA screen were limited by heat map analysis and by postulating a significant in-/decrease of the insulin release of at least 15 % (Figure R10). Reduction of gene expression for SCY1-like kinase 1 (SCYL1), aarF-containing kinase 1 (ADCK1), G protein-coupled receptor kinase 5 (GRK5), Eph receptor A4 (EPHA4), choline kinase beta (CHKB), mitogen-activated protein kinase kinase 3 (MAP2K3), receptor tyrosine kinase-like orphan receptor 1 (ROR1), protein kinase D3 (PRKCN), lymphocyte-specific protein tyrosine kinase (LCK), RIO kinase 2 (RIOK2) as well as casein kinase 2, alpha 1 (CSNK2A1) and phosphoinositide-3-kinase, class 3 (PIK3C3) displayed an increase of the insulin release in beta-TC6 cells upon siRNA treatment, rendering those kinases as potential negative modulators of insulin release. The increased insulin release was target dependent and ranged from 45.29 ± 10.90 % (SCYL1) to 16.37 ± 1.97 % (PIK3C3). Despite the fact that in general just a few negatively regulating kinases are known, representatives of PKCs (PRKCN), PI3Ks (PIK3C3) and MAP-Kinases (MAP2K3), which have not been published yet, but their corresponding family members playing important roles in insulin secretion [145,

260, 266] have been monitored. Moreover, CSNK2A1 was depicted as a negative regulator for insulin release [172, 267] and thus could be announced as a positive screening control.

In contrast, the screen also displayed kinases that decreased the amount of insulin released after reduction of target gene expression. Here, we were highlighting the Janus kinase 1 (JAK1), the potassium voltage-gated channel, subfamily H, member 2 (KCNH2), the met proto-oncogene kinase (MET), the protein kinase C beta (PRKCB), the kinase fucokinase (FUK), mitogen-activated protein kinase 13 (MAPK13/p38δ), the proto-oncogene tyrosine-protein kinase (KIT), the phosphatidylinositol-4-phosphate 5-kinase, type I, gamma (PIP5K1C), the thymoma viral proto-oncogene 1 (AKT1), the glycogen synthase kinase 3 alpha (GSK3A) as well as the ceramide kinase (CERK) and the calcium/calmodulin-dependent serine protein kinase (CASK) as positive regulators of insulin release. The decreased insulin release was target dependent and ranged from -19.90 ± 4.2 % (CASK) to -53.4 ± 4.2 % (JAK1). Highlighting JAK1, Akt/PKB and MAPK13 as already published kinases which have been connected to an impaired insulin secretion due to inhibition, knock-out or reduction of gene expression, respectively, thus we rendered those kinases as positive controls for the expressiveness of the screening performance. However, due to the character of sunitinib as a multiple kinase inhibitor, we focused on negatively regulating kinases that increased the insulin release after reduction of gene expression. We selected the most promising candidates SCYL1 (45.29 ± 10.90 %), ADCK1 (44.21 ± 7.40 %), GPRK5 (33.65 ± 2.04 %), EPHA4 (27.9 ± 2.55 %) as well as CSNK2A1 (18.89 ± 2.31 %) as a positive control for further investigation.

5.3.1 CONFIRMATION OF THE MOST PROMISING TARGET CANDIDATES

For target confirmation of the negatively modulating kinases SCYL1, ADCK1, GPRK5, EPHA4 and CSNK2A1, four different Accell siRNA-sequences for each revealed target kinase were used for reduction of gene expression. Cells were cultured for 24 h in a 12 well plate,

washed with PBS and then treated with Accell siRNA for 72 h. Then, cells were washed with PBS and high glucose media (4.5 g/L) was replaced for 2 h. Afterwards, the supernatant was taken to detect the amount of insulin released in a rat/mouse insulin ELISA. In parallel, RNA was extracted according the manual of the QIAGEN RNeasy Mini Kit. The mRNA expression levels were detected using PCR analysis and densitometry evaluation.
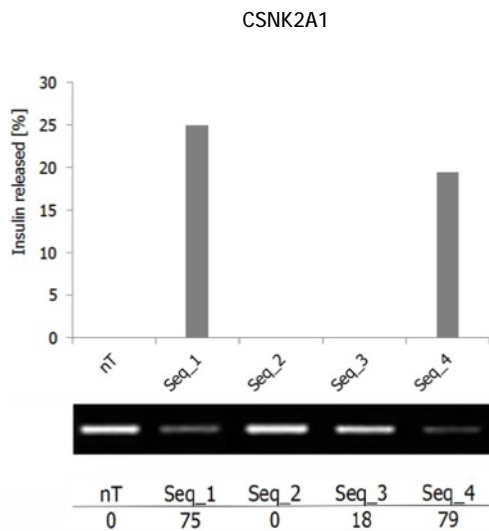

SCYL1

nT	Seq_1	Seq_2	Seq_3	Seq_4
0	66	34	65	51

GPRK5

nT	Seq_1	Seq_2	Seq_3	Seq_4
0	63	72	65	53

ADCK1

nT	Seq_1	Seq_2	Seq_3	Seq_4
0	99	70	53	15

EPHA4

nT	Seq_1	Seq_2	Seq_3	Seq_4
0	65	73	67	56
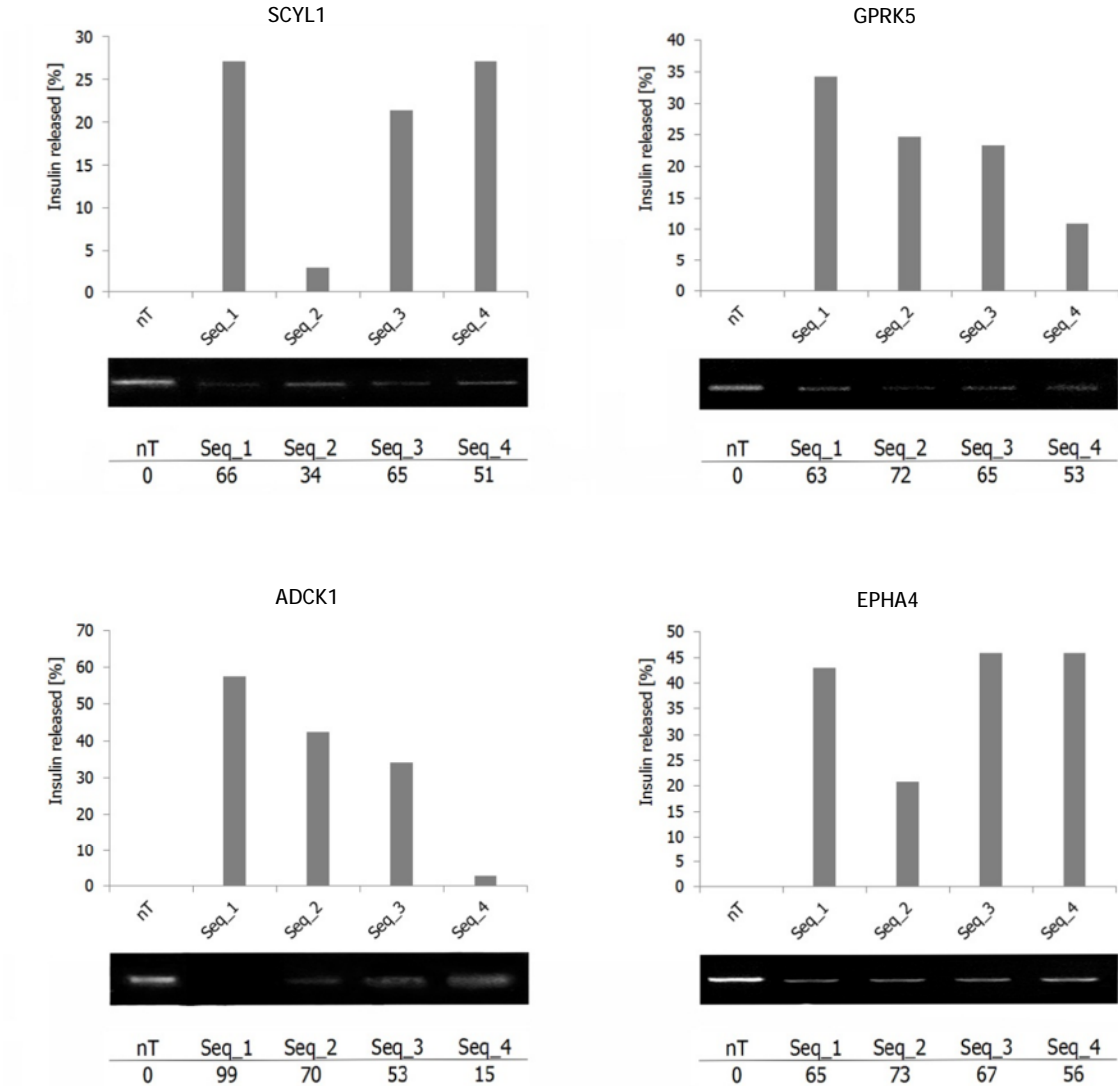
Figure R11 | *Comparison of increased insulin release and reduction of gene expression using 4 different sequences for each target candidate. Targets from left to right, respectively up to down: SCYL1, GPRK5, ADCK1, EPHA4 and CSNK2A1. The insulin released by kinase knock-down (bar chart) correlated with their knock-down efficiency (middle panel and lower table), except for GPRK5 and EPHA4, where all sequences lead to nearly equal knock-down efficiency. The knock-down displayed as knock-down efficiency in percentage. Seq = sequence, nT = non targeting control.*

The reduction of gene expression of the target kinases SCYL1, GPRK5, ADCK1, EPHA4 and CSNK2A1 led to an increased insulin release. Comparison of insulin released upon reduction of gene expression and the knock-down efficiency itself displayed a noteworthy inverse correlation (Figure R11). In contrast, impaired reduction of gene expression did not result in an increased release of insulin (SCYL1, ADCK1, CSNK2A1) whereas the knock-downs with higher efficiency did. For GPRK5 and EPHA4, where all sequences lead to nearly equal reduction of gene expression, insulin was released in a similar amount for each target sequence. Repeating the previously described procedure confirmed the revealed negatively regulating kinase candidates which led to an increased insulin release after reduction of gene expression in beta-TC6 cells.
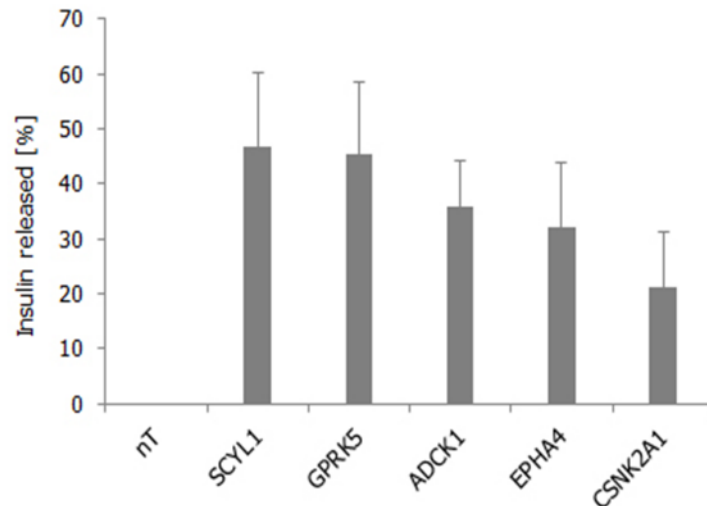
Figure R12 | *Confirmation of improved insulin release after reduction of gene expression for revealed kinase candidates. Data based on previously described experiments using 4 different siRNA sequences for each target candidate. nT = non-targeting control.*

At this point, we presented four new negatively regulating kinases, which had led to increased insulin release after reduction of target gene expression, highlighting SCYL1 (46.74 ± 13.58 %) and GPRK5 (45.38 ± 13.02 %) as most potent new target kinases, followed by ADCK1 (35.97 ± 8.29 %) and EPHA4 (31.97 ± 12.00 %). CSNK2A1, as already published positive control, led to an increase of 21.06 ± 10.30 % (Figure R12).

5.3.2 PARALLEL REDUCTION OF TARGET GENE EXPRESSION FOR THE IDENTIFIED KINASES

The candidate kinases SCYL1, GPRK5, ADCK1, EPHA4 and CSNK2A1 are involved in various signaling and metabolic pathways. To investigate whether the kinases have a redundant or additive effect on insulin release, we performed parallel reductions of gene expression for each possible kinase pair. Cells were cultured for 24 h in a 12-well and 96 -well plate respectively, washed with PBS and afterwards treated with 1 µM Accell siRNA each for 96 h. Then cells were washed with PBS and high glucose media (4.5 g/L) was replaced for 2 h.

Afterwards, the amount of insulin released was monitored in a rat/mouse insulin ELISA. The insulin increase due to the double knock-down was correlated to the single knock-downs as well as to the non-targeting siRNA.
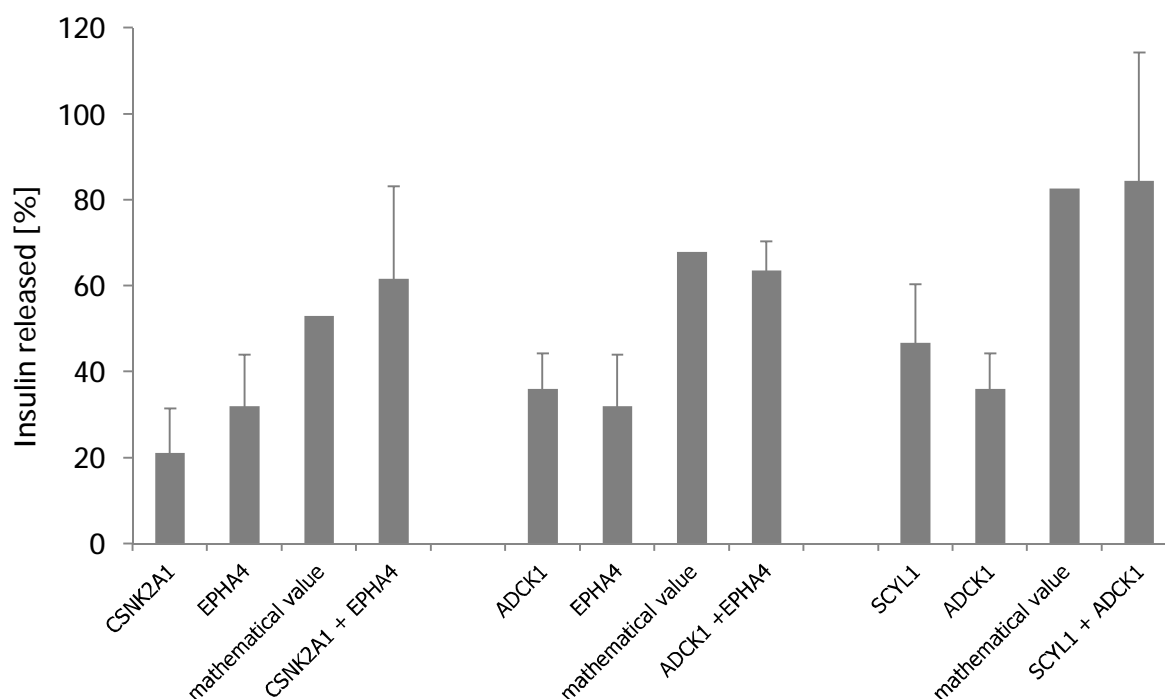
Figure R13 | *Additional increase of insulin release due to a double knock-down for the kinase pairs SCYL1 and EPHA4; SCYL1 and ADCK1; ADCK1 and EPHA4; EPHA4 and CSNK2A1. Values of the single knock-down are based on the confirmation results; the expected mathematical value was calculated of those. Displayed are just kinases pairs with additional effects.*

After investigating 10 possible kinase pairs in a parallel reduction of gene expression approach, three double knock-downs positively affected the insulin release. Here, SCYL1 and ADCK1; ADCK1 and EPHA4 and CSNK2A1 and EPHA4 displayed an additive insulin release compared to the single knock-downs, rendering the kinases of those kinase pairs as pathway independent targets. SCYL1 and ADCK1 depletion resulted in the highest insulin release (84.41 ± 29.82 %) which equaled the 5 µM sunitinib induced insulin release. Furthermore, CSNK2A1 and EPHA4 (61.71 ± 20.43 %) as well as ADCK1 and EPHA4 (63.58 ± 6.80 %)

depicted a remarkable increase of insulin (Figure R11). For the other kinase pairs, no increased insulin release was observed (data not shown).

5.4 GLUCOSE-MEDIATED EFFECT ON INSULIN RELEASE IN BETA TC6 CELLS AFTER REDUCTION OF TARGET GENE EXPRESSION

Metabolism of glucose and subsequently secretion of insulin is based on available blood glucose. The mean blood glucose level in humans is about 4 mM (72 mg/dl) but can be increased up to approx. 7.2 mM (130 mg/dl) due to food ingestion [268]. Blood sugar levels outside the normal range may be an indicator of a therapeutic condition. A persistent high level is referred to hyperglycemia and low levels are referred to hypoglycemia, both damaging the body [269]. However, as hyperglycemia is treated with the previously described anti-diabetic drugs, it can also be caused by them. Highlighting for example impaired cognitive function, motor control and consciousness as most harmful events of hypoglycemia. For safety reasons, it is important that the revealed candidate kinases are glucose dependent and not causing hypoglycemia upon inhibition or reduction of gene expression. We verified the glucose dependent insulin release in beta-TC6 cells using concentrations ranging between 1.125 mM (20 mg/dL) and 4.5 mM (81 mg/dL) glucose, published by Poitout V. and colleagues [270]. Cells were cultured for 24 h in a 96-well plate, washed with PBS and then media was replaced for 2 h. Afterwards, the supernatant was taken to detect the amount of insulin released with a rat/mouse insulin ELISA.
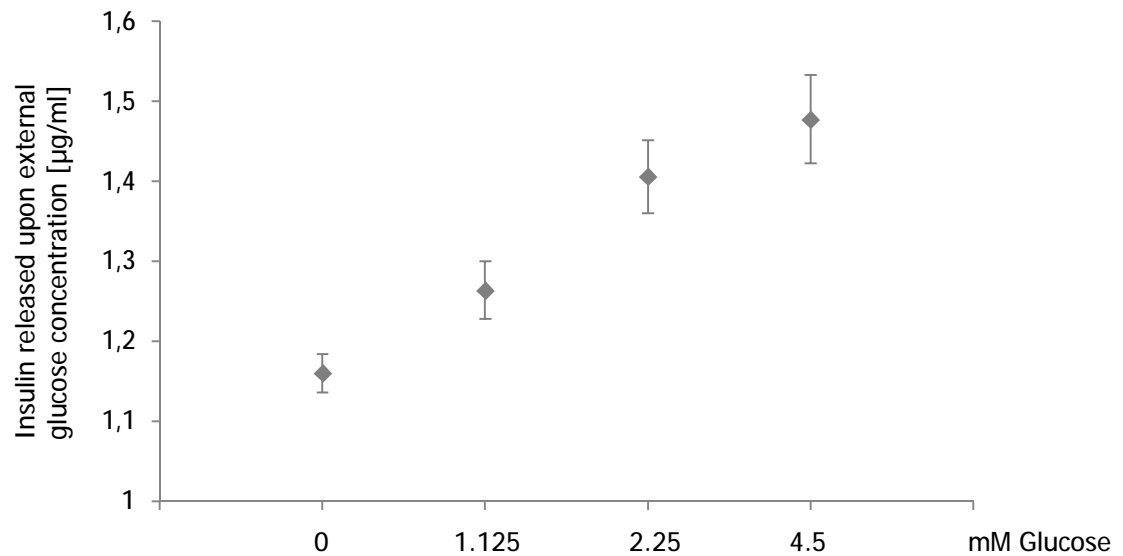
Figure R14 | *Insulin secretion mediated by external glucose ranging from 1.125 mM (20 mg/dL) to 4.5 mM (81 mg/dL).*

We detected a glucose dependent insulin release in the beta-TC6 cell line (Figure R14); for further experiments in low glucose media, we chose a glucose concentration of 1.125 mM (20 mg/dL). For detection of insulin release upon reduction of target gene expression, cells were cultured for 24 h in a 96-well plate, washed with PBS and then treated with 1 µM Accell siRNA each for 96 h. After that, cells were washed with PBS and low glucose media was replaced for 2 h. The supernatant was used to detect the amount of insulin released with a rat/mouse insulin ELISA.
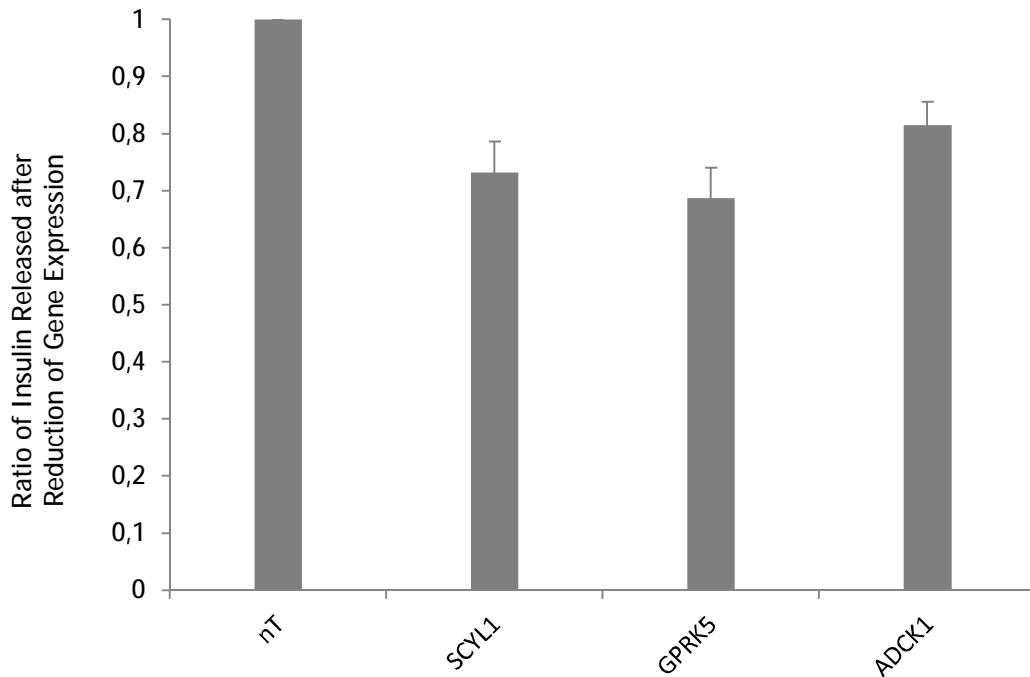
Figure R15 | *Insulin release after reduction of gene expression for SCYL1, GPRK5 and ADCK1 in low glucose media 0.2 g/L (1.125 mM).*

Reduction of target gene expression of SCYL1, GPRK5 and ADCK1 decreased the amount of insulin released in a low glucose media, ranging between 0.687 ± 0.053 (GPRK5) and 0.815 ± 0.04 (ADCK1) (Figure R15). Hence, all three target kinases regulated the insulin release in dependence of external glucose concentrations and therefore appear to be good anti-diabetic targets.

5.5 GLUCOSE UPTAKE IN C2C12 AND 3T3-L1 CELLS AFTER REDUCTION OF TARGET GENE EXPRESSION

Impaired glucose uptake by peripheral tissues in response to insulin is the key problem in type 2 diabetes and leads to chronically elevated blood glucose levels. To investigate if the revealed kinase candidates SCYL1, GPRK5 and ADCK1 have an impact on glucose uptake and possibly mediate the increased insulin release, we used a fluorescent d-glucose analog 2-[*N*-(7-nitrobenz-2-oxa-1,3-diazol-4-yl)-amino]-2-deoxy-d-glucose (2-NBDG) [250]. Cells were

cultured overnight in a 96 well plate, washed with PBS and then treated with 1 µM Accell

siRNA each for 96 h. For 2-NBDG detection, cells were washed and cultured 1 h in glucose

free media supplied with 100 µM 2-NBDG at 37 °C before collecting the fluorescence by a

Tecan Evolution Reader at wavelength 535 nm (excitation wavelength 485 nm).
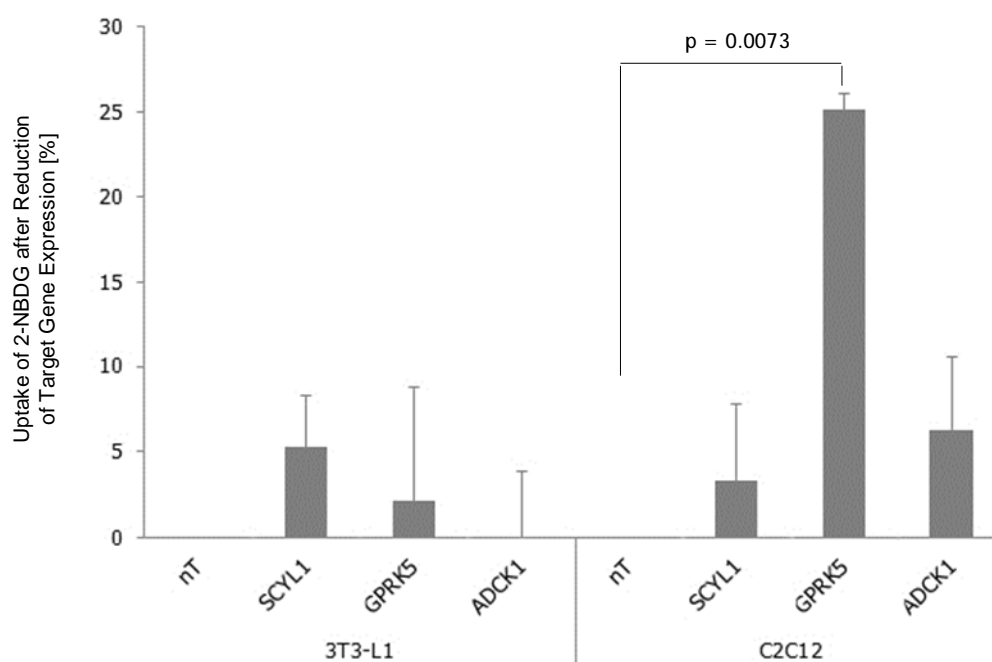
Figure R16 | *Levels of glucose uptake using 2-NBDG after reduction of candidate gene expression. Down-regulation of GPRK5 significantly affected uptake of 2-NBDG in C2C12 (25.1 ± 6.61 %). Fluorescence of 2-NBDG was collected by a Tecan Evolution Reader 535 nm wavelength (excitationwavelength 485 nm).*

Remarkably, reduction of candidate gene expression of SCYL1, GPRK5 and ADCK1 in 3T3-L1

and C2C12 cells respectively, displayed a significantly increased uptake of 2-NBDG for GPRK5

in C2C12 cells (25.1 ± 6.61 %) but not in 3T3-L1 cells (Figure R14), possibly also indicating

a mode of action for the negatively regulating kinase GPRK5 in beta-TC6 cells. Furthermore,

Scyl1 as well as Adck1 seemed to be slightly, but not significantly, involved in glucose

uptake.

5.6 PHOSPHORYLATION OF AKT/PKB UPON REDUCTION OF TARGET GENE EXPRESSION

Based on the increased 2-NBDG uptake and the previously mentioned connection of Akt/PKB to GLUT4 translocation [27], we examined the pAKT levels after reduction of SCYL1, GPRK5 and ADCK1 gene expression in beta-TC6, C2C12 and 3T3-L1 cells. Cells were cultured for 24 h in a 12 well plate, washed with PBS and then treated with 1 µM Accell siRNA each for 96 h. Afterwards, media was replaced for 2 h and then the cells were lysed using 4G10 lysis buffer. Phosphorylation levels were detected by western blot analysis. Proteins were visualized using a chemiluminescence detection kit and densitometry evaluated with a UV trans-illuminator.
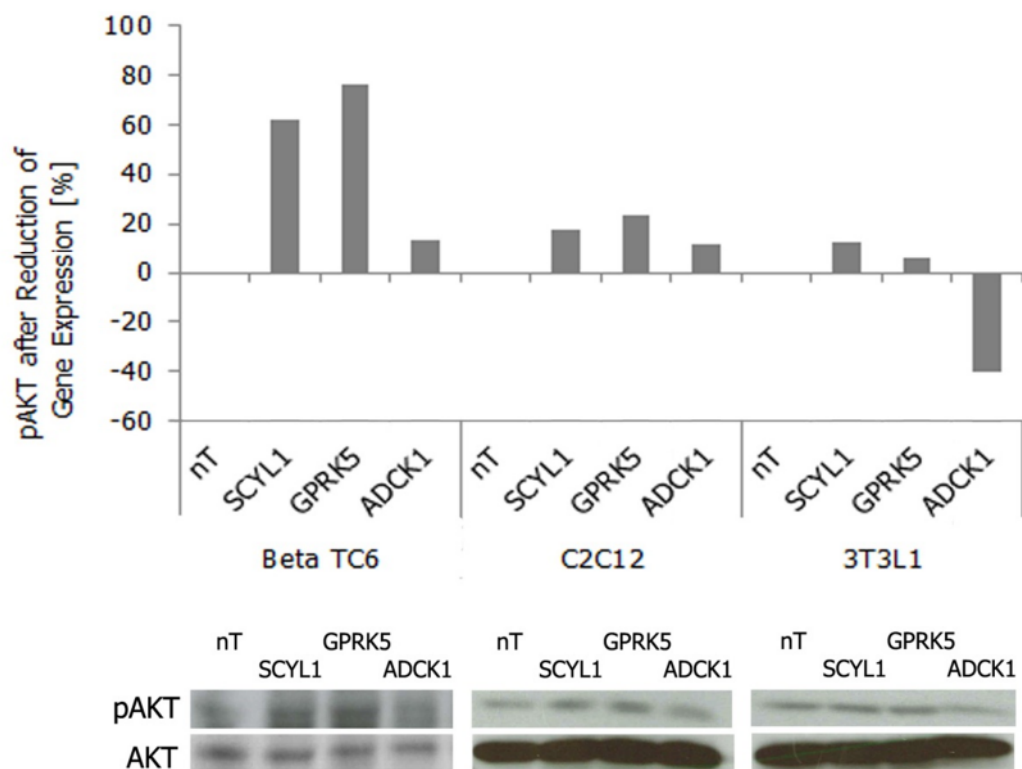
Figure R17 | *Phosphorylation of AKT/PKB after reduction of candidate gene expression. Upper bar chart depicts the activation of AKT derived from the performed western blot analysis (lower panel). nT = non targeting control.*

The siRNA mediated reduction of SCYL1 and GPRK5 displayed a clear increase of pAKT in beta-TC6 cells, whereas in C2C12 cells and undifferentiated 3T3-L1 cells just a slight increase

of phosphorylation was detected. However, in C2C12 the Akt/PKB phosphorylation was up to 16 % for SCYL1 and 24 % for GPRK5 (Figure R17), which confirmed the previously monitored increase of 2-NBDG uptake after reduction of gene expression (Figure R14). Furthermore, a similar activation pattern but higher increased phosphorylation for SCYL1 (62 %) and GPRK5 (76 %) was monitored in beta-TC6 cells (Figure R17), suggesting both targets as negative regulators that are positively connected to glucose uptake and subsequently induce Akt/PKB phosphorylation.

5.7 SCYL1, GPRK5, ADCK1, EPHA4 AND CSNK2A1 AS SUNITINIB TARGETS

In order to detect a possible effect of sunitinib on the identified target candidates, we checked sunitinib in a KINOME*scan*™ screening platform. Here, compounds that bind the kinase active site and directly (sterically) or indirectly (allosterically) prevent kinase binding to the immobilized ligand reduced the amount of kinase captured on the solid support (Figure R18 A & B). In contrast, test molecules that did not bind the kinase had no effect on the amount of kinase captured on the solid support (Figure R18 C). Screening hits were identified by measuring the amount of kinase captured in test versus control samples by using a quantitative qPCR method that detects the associated DNA label (Figure R18 D).
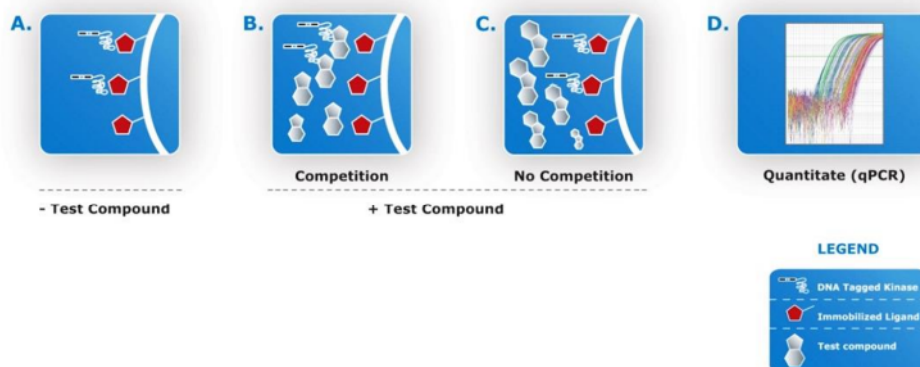
Figure R18 | *Compound that bind the kinase active site and directly (sterically) or indirectly (allosterically) prevent kinase binding to the immobilized ligand reduced the amount of kinase captured on the solid support (A & B). Conversely, test molecules that did not bind the kinase had no effect on the amount of kinase captured on the solid support (C). Screening hits were identified by measuring the amount of kinase captured in test versus control samples by using a quantitative qPCR method that detects the associated DNA label (D). Source of figure: DiscoveRX.*

Sunitinib was screened at a concentration of 5 µM and inhibition was reported as "%Ctrl", where lower numbers indicate stronger hits in the matrix.

$$\% \ Ctrl = \frac{Sunitinib - Positive \ Control}{Negative \ Control - Positive \ Control}$$

negative control = DMSO (100 %Ctrl)
positive control = control compound (0 %Ctrl)

With the KINOME*scan*™ technology, sunitinib was revealed to be less selective, targeting 219 non-mutant kinases (out of 392 available) with %Ctrl <35, 164 with %Ctrl <10 and 85 with %Ctrl <1. Focusing on the kinase candidates, we detected a low sunitinib binding efficiency for EPHA4 (%Ctrl = 69) and the ADCK1 family members ADCK3 (%Ctrl = 87) and ADCK4 (%Ctrl = 95). A moderate sunitinib binding efficiency was displayed for CSNK2A1 (%Ctrl = 16) whereas the GPRK5 family members GPRK1 (%Ctrl = 7.3), GPRK4 (%Ctrl = 0.95), GPRK7 (%Ctrl = 2.5) depicted a high sunitinib binding efficiency, suggesting similar binding characteristics for GRK5. SCYL1 or corresponding family members, respectively, have not been screened yet.

5.8 MEASUREMENT OF SCYL1, GPRK5, ADCK1, EPHA4 AND CNSK2A1 MRNA LEVELS UPON 24 H SUNITINIB TREATMENT

We investigated the mRNA levels after a 24 h sunitinib treatment to detect effects due to a long term treatment. Beta-TC6 cells were cultured overnight in a 12 well plate and then treated with 1 µM and 5 µM sunitinib for 24 h. RNA was extracted according to the manual of the QIAGEN RNeasy Mini Kit. After reverse-transcription into cDNA, mRNA expression levels were detected using PCR analysis and densitometry evaluation.
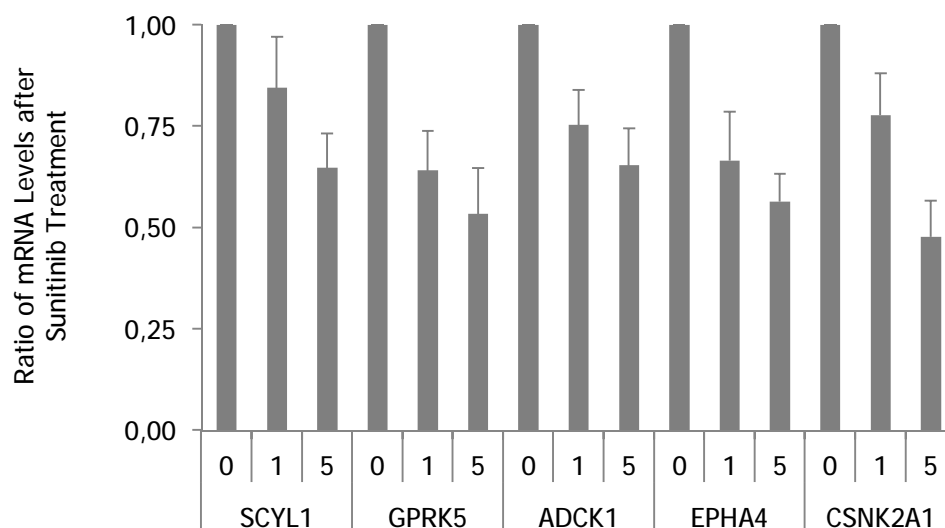
Figure R19 | *Sunitinib treatment decreased mRNA levels of candidate kinases. mRNA levels of SCYL1, GPRK5, ADCK1, EPHA4 and CSNKA1 were measured after a 1 µM as well as a 5 µM 24 h sunitinib treatment period.*

In addition to its direct inhibitory effect on the candidate kinases, sunitinib treatment led to concentration dependent decreases of SCYL1, GPRK5, ADCK1, EPHA4 and CSNK2A1 mRNA levels after 24 h (Figure R19). This might represent a further explanation for the positive anti-diabetic effect of sunitinib in clinics, where it has been applied for a longer period of time.

For further anti-diabetic therapy development, we focused on the two most promising kinases SCYL1 and GPRK5. Both displayed striking characteristics on insulin release, Akt/PKB phosphorylation and glucose uptake after reduction of target gene expression.

5.9 Scyl1 as Anti-Diabetic Target for Drug Development

5.9.1 Cloning, Expression and Purification of the Human Kinase Scyl1

Constructs of the human Scyl1 kinase domain (14 – 328) as well as the full-length protein (1 – 808) were designed according to the internal construct design process of the providing company Proteros. A selection of 4 different constructs of the target using several lengths and a GST-Tag appropriate for assay development were produced in vectors suitable for intracellular expression via insect cells. Recombinant high titer virus stocks (HTVS) were generated for all constructs and amplified by standard procedures. Intracellular expression was performed by infecting Sf9 cells. After expression, cells were harvested by centrifugation and the cell pellet was stored frozen (-80 °C) until used for purification.
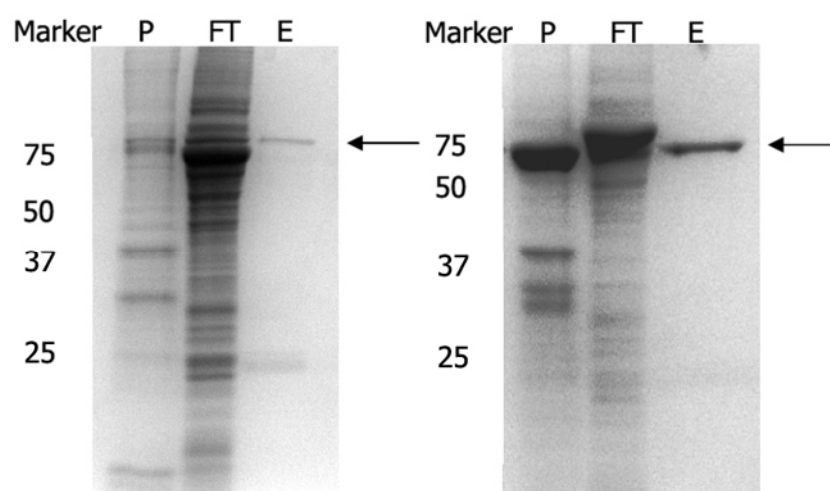
Figure R20 | *Test purification of GST-Scyl1 (left) and GST-Scyl1 kinase domain (right) by affinity chromatography. Lane 1: molecular weight marker; lane 2: P = pellet; lane 2: FT = flow through of the culture medium applied on a GSH column; lane 3: E = eluate fraction of*

GSH column. The arrow indicates the position of recombinant GST-Scyl1 / GST-Scyl1 kinase domain.

Suitable amounts of recombinant protein could be produced with the Baculo virus/insect cell expression system. Protein was accessible for purification by affinity chromatography.

5.9.2 ESTABLISHMENT OF A REPORTER PROBE SYSTEM

To identify a peptide substrate for Scyl1, Proteros used its own collection of potential peptide substrates, which was screened for phosphorylation by using the IMAP technology (Molecular Devices). The fluorescein labeled peptides were incubated with either a full length Scyl1 or the kinase domain of Scyl1, respectively. The background signal was measured in the absence of either full length protein or the kinase domain of Scyl1. Peptide binding to the IMAP beads as an indicator for peptide phosphorylation was quantified by measuring fluorescence polarization (FP) (Figure R21). Unfortunately, no significant difference between the FP signal in the presence and absence of one of the Scyl1 was observed for either the investigated peptides.
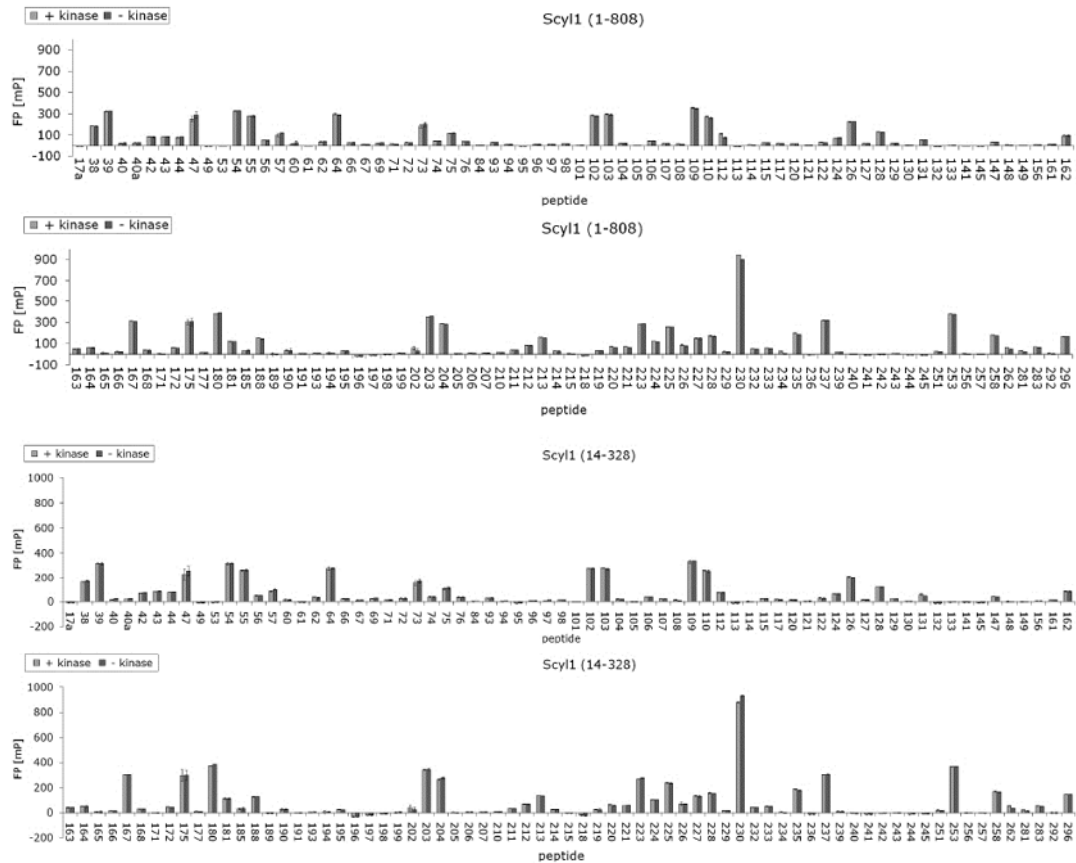
Figure R21 | *Identification of peptide substrate for Scyl1 using IMAP technology. 50 nM of full length Scyl1(1-808), respectively the kinase domain of Scyl1 (Scyl1(14-328) were incubated for 4 h with 400 nM of various fluorescein labeled potential peptide substrates at room temperature with 100 µM ATP. Background signals were determined in the absence of Scyl1. Thereafter, IMAP beads were added and fluorescence polarization (FP) for substrate phosphorylation was quantified. FP signal was compared in the presence and absence of kinase.*

Due to various degrees of non-specific binding, the levels of FP signal for the peptides ranged between the non-phosphorylated peptides and the IMAP beads (Figure R21). Consequently, no peptide substrates were identified for Scyl1 and thereby prevented the development of an IMAP based enzymatic assay. However, in lack of a Scyl1 peptide substrate, histone, myelin basic protein (MBP) and casein were investigated as protein substrates for Scyl1 using the ADP-Glo™ assay technology (Promega). Here, increasing concentrations of full length Scyl1 and the kinase domain of Scyl1 were incubated together with 100 µM ATP in the absence and presence of 10 µM histone mix, MBP or casein in a

standard reaction buffer for 60 min. Unfortunately, none of the investigated potential protein substrates displayed a dose dependency between kinase concentration and ADP levels (Figure R22).
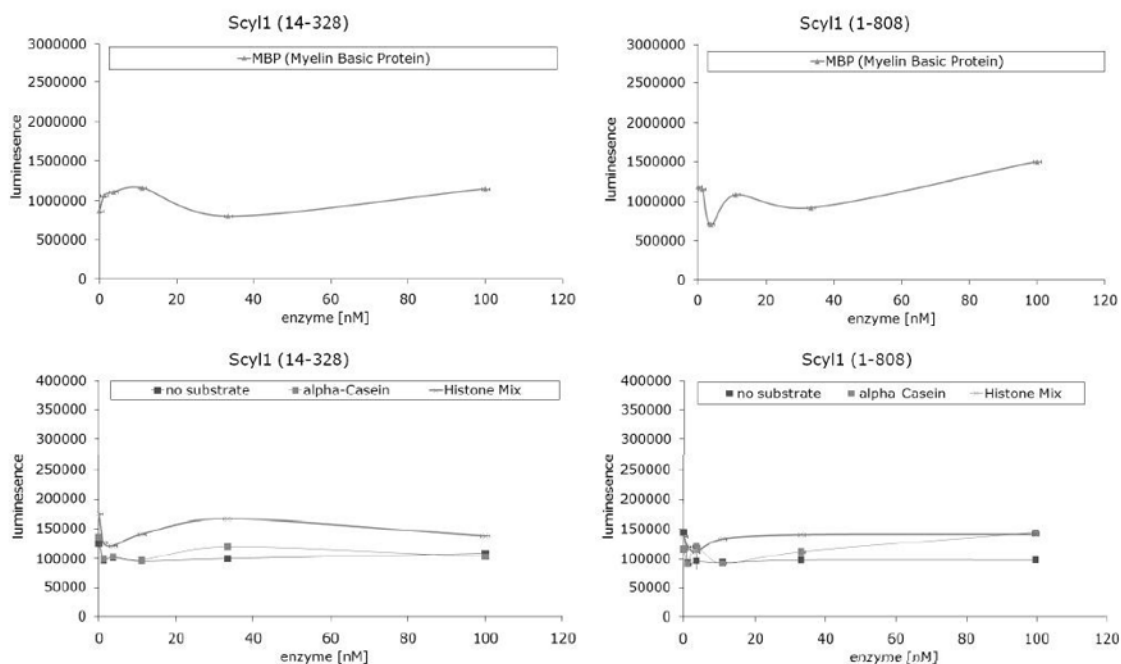

Figure R22 | *Identification of protein substrate for Scyl1 using* ADP-Glo™ *Kinase Assay Technology. Increasing concentrations of full length or kinase domain of Scyl (Scyl1(1-808), Scyl1(14-328)) were incubated with 100 µM ATP in the absence and presence of 10 µM casein, MBP or histone mix for 60 min. Reaction was stopped by adding* ADP-Glo™ *solution. Potential Scyl1 activity was quantified by converting measuring luciferase-mediated luminescence.*

None of the investigated protein substrates served as a suitable substrate for a biochemical enzymatic Scyl1 assay. In addition, also in the absence of substrate, no dose dependency between kinase concentration and ADP levels was observed, indicating that Scyl1 does not undergo auto-phosphorylation *in vitro*. Due to the lack of a peptide substrate, a protein substrate or an auto-phosphorylation activity of both the full length Scyl1 and the kinase domain of Scyl1, an enzymatic assay for Scyl1 could not be developed. However, in order to provide the possibility to identify compounds that bind to the ATP binding site of Scyl1, a binding assay based on the Proteros Reporter Displacement Technology was established.

The Proteros reporter displacement assay is based on reporter probes that are designed to bind to the site of interest of the target protein [271, 272]. Compounds that bind to the same site as the reporter probe displace the probe and cause signal reduction. The rate of reporter displacement was measured over time at various compound concentrations. For K_D-determination, percent probe displacement values were calculated for the last time point at which the system had reached equilibrium. For each compound concentration percent of probe displacement values were calculated and plotted against the compound concentration. IC_{50}-like values (corresponding to 50 % probe displacement) were calculated using standard fitting algorithms. The reporter probe was used at a concentration reflecting its own K_D-(probe) value. Thus, according to the Cheng Prusoff equation [273], the K_D-value was calculated with $K_D = 0.5 \times IC_{50}$. However, small molecule inhibitors that bind to the ATP binding site of kinases were tested for their binding activity to either the full length Scyl1 or its kinase domain (Figure R21). The two Scyl1 constructs were incubated at several concentrations with increasing probe concentrations and probe binding could be detected for either one.
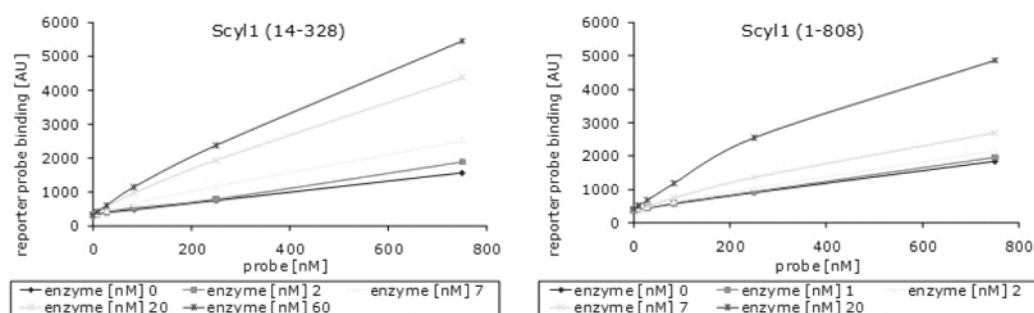

Figure R23 | *Identification of probe binding to Scyl1. Increasing concentrations of full length or kinase domain Scyl1 (Scyl1(1-808), Scyl1(14-328)) were incubated with increasing concentration of a reporter probe in binding buffer and probe binding signal was measured.*

With higher concentration, the probe binding signal increased until it reached saturation, indicating that all binding sites on the target protein were occupied. Since full-length as well

as the kinase domain of Scyl1 bind the reporter probe with similar affinity, further assay development activities were focused on full length Scyl1. Here, 20 nM Scyl1 (1-808) yielded a signal robust enough for further experiments.

To investigate the probe affinity for Scyl1, 20 nM Scyl1 (1-808) were incubated with increasing concentrations of reporter probe (Figure R24). The binding was measured and the K_D-value of the probe was quantified to be 607 nM by fitting to equation 1.

Equation 1:

Probe binding signal = ((Bmax x [probe]) / (K_D + [probe]))
Bmax: maximal probe binding signal at [probe]= ∞
[probe]: probe concentration
K_D: dissociation constant
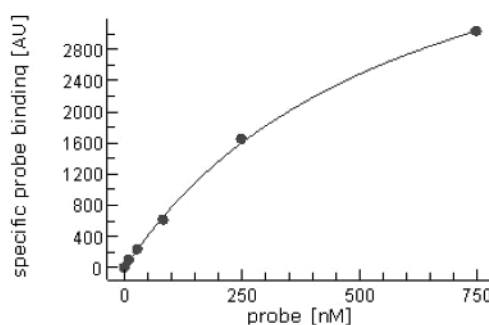
Figure R24 | *K_D-determination for probe binding to Scyl1 (1-808). Increasing concentration of full length Scyl1 were incubated with increasing concentrations of a reporter probe in binding buffer and probe binding signal was measured. K_D was quantified to be 607 nM by applying equation 1.*

To ensure sensitivity for detecting compounds that bind to Scyl1 and thereby compete with the reporter probe, the reporter probe was used at K_D -(probe) = 607 nM for further experiments. Read-out stability was proven by forming the probe-target complex and measuring the probe binding signal over time (Figure R25).
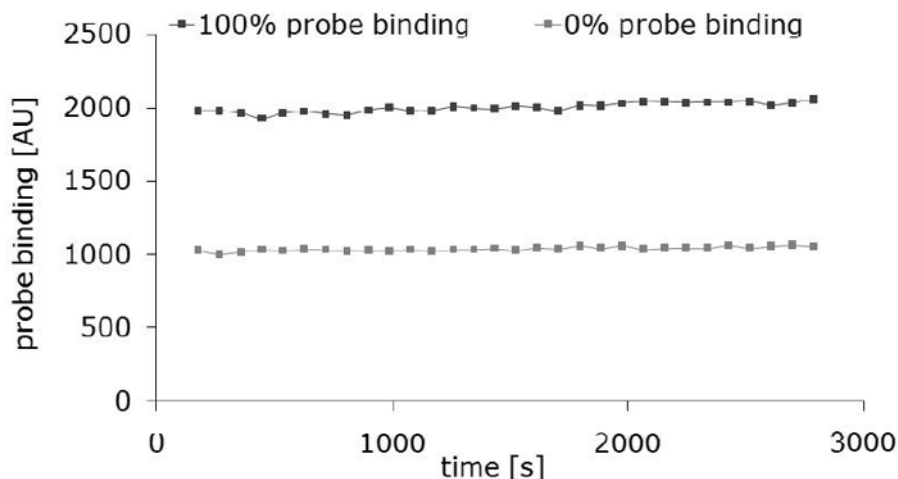
Figure R25 | *Signal stability of probe binding to Scyl1 (1-808). Here, 607 nM reporter probes were incubated in the absence and presence of 20 nM full length Scyl1 in binding buffer. Probe binding signal was measured over time.*

In order to validate the assay and to prove that the assay was suitable to identify compounds that bind to Scyl1, the IC_{50} value of a reference compound was measured (Figure R26). Percent probe displacement was measured in the presence of increasing concentrations of the reference compound. A regular IC_{50} curve could be observed and the IC_{50} value was quantified to be 20 µM by fitting the inhibition data to equation 2.

<u>Equation 2</u>:

probe displacement [%] =
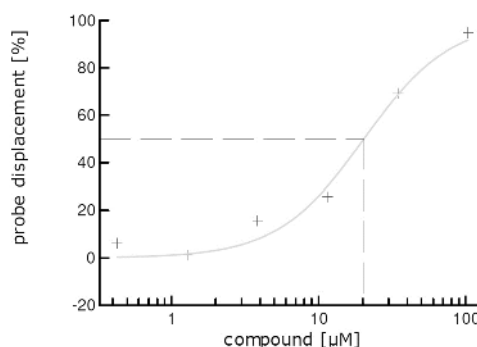$100 / (1 + ((IC_{50}/[\text{reference compound}])^h)$

Figure R26 | *IC_{50} value of reference compound. Increasing reference compound concentration was incubated with 20 nM full length Scyl1 and 607 nM reporter probe in binding buffer. Probe displacement was calculated in relation to the C+ and C- controls. The signal reflecting 0 % probe displacement (C+) was measured in the absence of reference*

compound, while the signal representing 100 % probe displacement (C-) was measured in the absence of Scyl1. The IC$_{50}$ value of 20 µM was quantified by data fitting to equation 2.

Using reporter probe # 16, which showed specific binding to Scyl1, an assay was established that is suitable for HTS and the detection of compounds binding to the active site of Scyl1 was validated.

5.9.3 HIGH THROUGHPUT SCREENING OF INHIBITOR COMPOUNDS FOR SCYL1

Using the previously described Proteros reporter displacement assay, Proteros screened a MPI customer compound library (1863_SF_MPK, 2121_SF_MPK, 2145_SF_MPK, 2217_SF_MPK) with in total 8827 compounds (Cpds) for their ability to bind to the ATP binding site of Scyl1. The compounds were delivered at 10 mM stock concentration and tested at a final assay concentration of 25 µM. In all cases, Z′ ≥ 0.5 was reached and the signal was sufficiently stable over all assay plates. A hit distribution was observed with an average inhibition of 9 % and a standard deviation of 12 % (Figure R27). In consequence, compounds with an inhibition value above 45 % (= inhav + (3 x inhstdev)) were recommended to be considered as hit. As control, sunitinib was added and an inhibition of 23 % was observed at a final concentration of 25 µM.
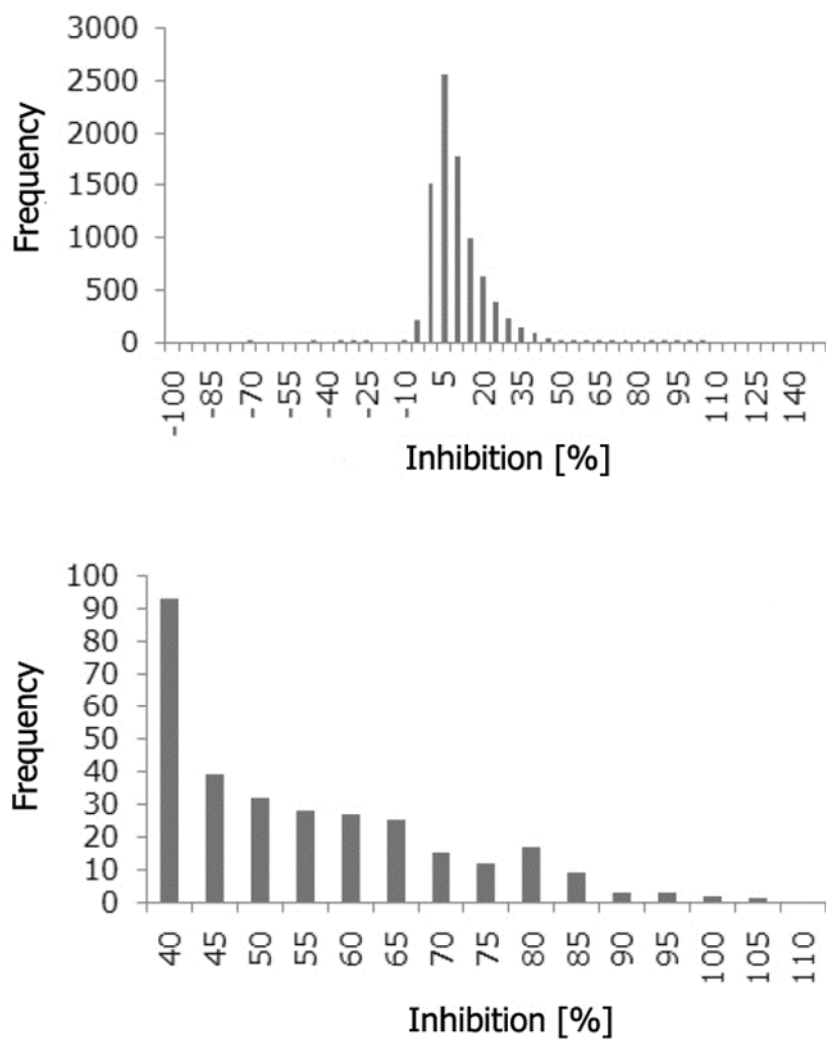
Figure R27 | *Hit distribution for all compounds (upper bar chart) and as a blow up for all compounds with an inhibition value of ≥ 40 % (lower bar chart).*

Table R2 | *Hit rate for the total of 8827 compounds. The average (av) of percentage inhibition was calculated to be 9 % and the standard deviation (stdev) 12 %, which resulted in the threshold of av + 3 x stdev = 45 % for significant probe binding inhibition.*

Inhibition [%]	Compounds [#]	Hit rate [%]
≥90	6	0.1
≥80	19	0.2
≥70	49	0.6
≥60	91	1.0
≥50	148	1.7
≥45	183	2.1

The reporter displacement assay revealed different small-kinase-inhibitor compounds with several kinds of structural groups. For further experiments we choose the five most promising inhibitors (Cpd 10 – 14) with an inhibition over 90 % as well as two compound structures that displayed no inhibition on Scyl1 in the screen as target controls (Cpd 15, 16).

Table R3 | *Representative kinase inhibitors revealed in the Scyl1 displacement assay screen.*

Scyl1 Inhibitor	Plate ID	Well ID	Cpd ID	PROBE DISPLACEMENT [%]
10	2nd BF_22_BFCP_555-558_c_10mM	M07	828_0071_0087	100
11	2nd BF_21_BFCP_551-554_c_10mM	C04	828_0069_0079	98
12	2nd BF_21_BFCP_551-554_c_10mM	A05	828_0081_0081	96
13	2nd BF_21_BFCP_551-554_c_10mM	C19	828_0314_0087	93
14	2nd BF_21_BFCP_551-554_c_10mM	N16	828_0176_6488	92
15	2nd BF_16_BFCP_347-350_c_10mM	N09	033_0114_0085	0
16	2nd BF_16_BFCP_347-350_c_10mM	J10	443_0313	0

Furthermore, Proteros determined the IC_{50} values for all compounds ≥ 75 % inhibition using triplicates at 12 different concentrations with a dilution factor of three (Figure R28). The maximal compound assay concentration was set to 58 µM, exceeding the compound assay concentration used in the primary screen. For all assay plates z-prime values were found to be significantly larger than 0.5, proving statistical relevance of the data. All screening hits

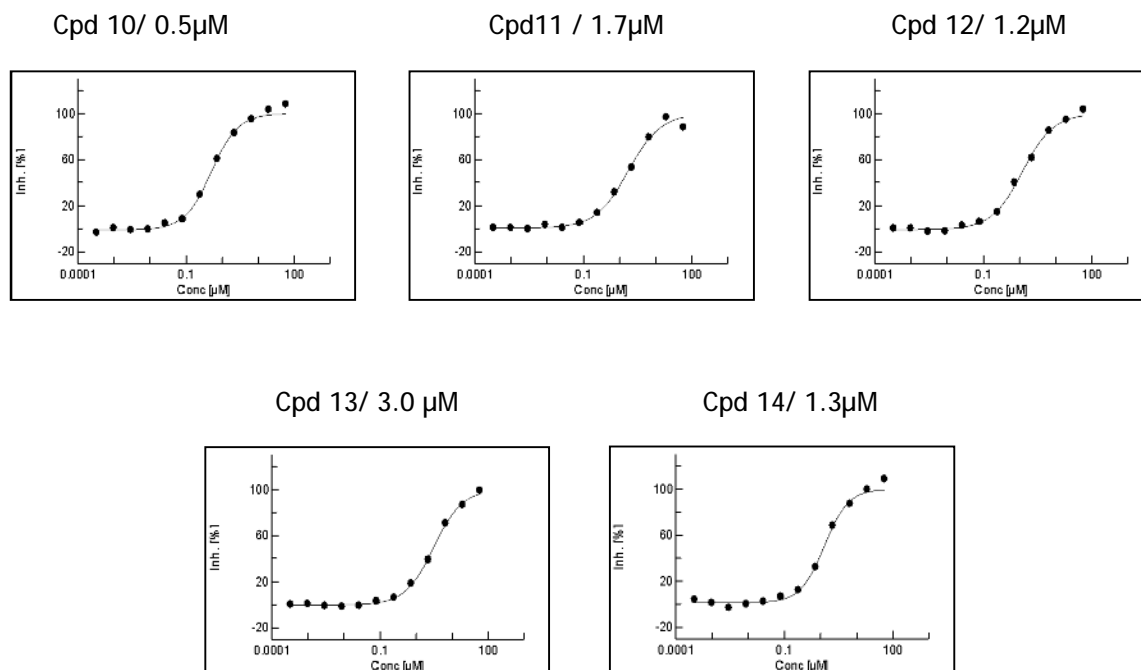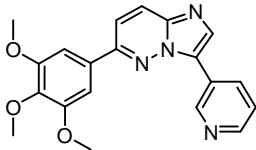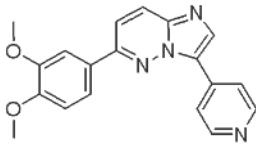could be verified. IC_{50} values were in good correlation with inhibition values from the primary
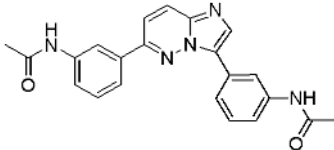
screen.

Cpd 10/ 0.5µM

Cpd11 / 1.7µM

Cpd 12/ 1.2µM

Cpd 13/ 3.0 µM
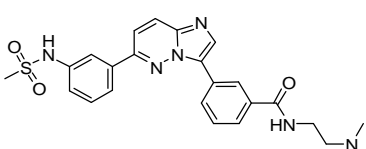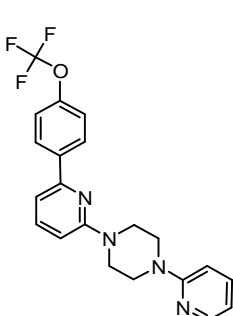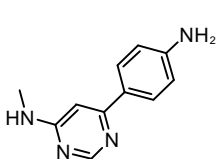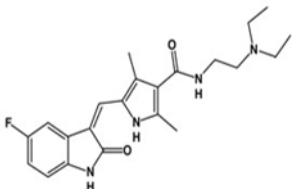
Cpd 14/ 1.3µM
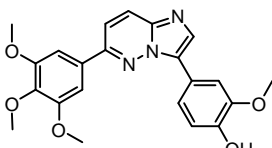
Figure R28 | *Determination of IC$_{50}$ values for the most promising kinase inhibitors Cpd 10 - 14. Maximal compound assay concentration was set to 58 µM.*

Table R4 | *Structures of Scyl1 binding partners.*

Scyl1 Inhibitor	Compound ID	Structure	Purity	Mol_W
10	828_0071_0087		97	362.38
11	828_0069_0079		100	332.36
12	828_0081_0081		98	385.42
13	828_0314_0087		100	407.42
14	828_0176_6488		99	478.57
15	033_0114_0085		96	400.40
16	443_0313		100	203.21
Sunitinib			n.a.	398.48

Compound 10 – 15 share an *imidazo[1,2-b]pyridazine* backbone
Compound 15 has a pyridyl-piperazine backbone
Compound 16 has a pyrimidine amine backbone

5.9.4 RELEASE OF INSULIN AFTER COMPOUND MEDIATED INHIBITION OF SCYL1

After having rendered the most promising Scyl1 inhibitors for probe displacement, we determined the impact on insulin released by beta-TC6 cells. Cells were cultured overnight, washed with PBS and then treated with 5 µM of candidate compounds as well as non-inhibitor controls for 2 h in a high glucose (4.5 g/L) DMEM at 37°C and 5 % (v/v) CO_2. Release of insulin was detected using a rat/mouse insulin ELISA.
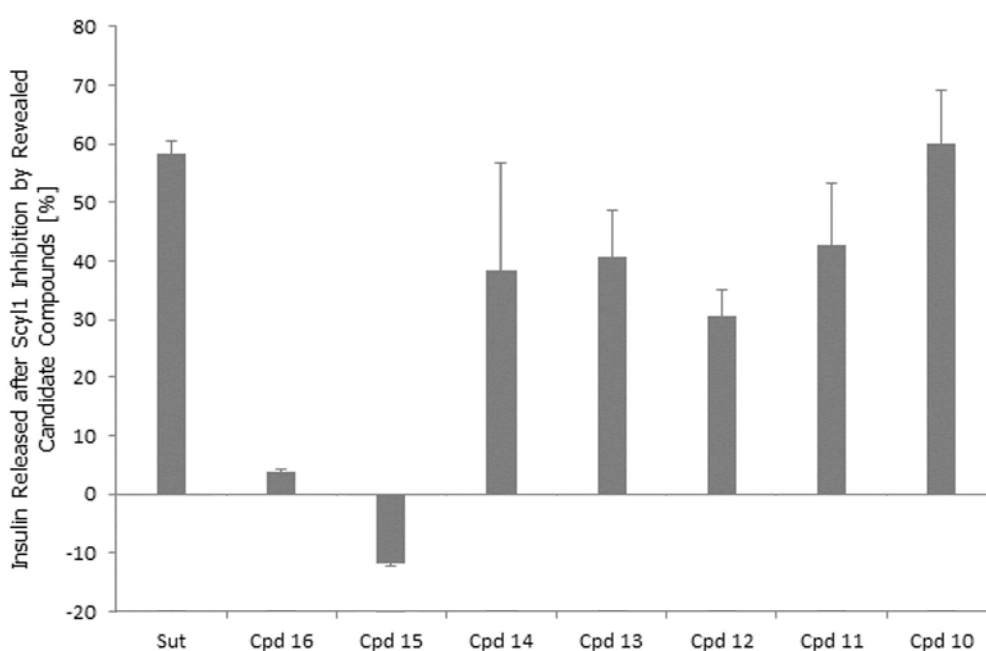

Figure R29 | *5 µM Scyl1 inhibitor treatment increased insulin release in beta-TC6 cells. Scyl1 inhibition by compound 10 to 14 led to a remarkable effect on insulin release, ranging from 60.2 ± 8.9 (Cpd 10) to 30.5 ± 4.5 (Cpd 12). The negative controls – Cpds without inhibition efficacy – displayed no effect -11.7 ± 0.35 (Cpd 15) and 3.69 ± 0.43 (Cpd 16) while the sunitinib control did (Sut: 58.2 ± 2.2).*

Inhibition of Scyl1 by the revealed compounds as well as sunitinib treatment displayed a significant increase of insulin release (Figure R29). Here, Cpd 10 (Inh. 100 % / IC_{50} = 0.5 µM) depicted the strongest effect with an increase of 60.2 ± 8.9 %. The other Cpds 11 – 14 also displayed an increased level of insulin release, ranging from 30.5 ± 4.5 % (Cpd12) to C_{11}: 42.7 ± 10.45 % (Cpd 11). The negative controls – Cpds without Scyl1 inhibition –

displayed no effect on insulin release (C_{15}: -11.7 ± 0.35 %; C_{16}: 3.69 ± 0.43 %) while the sunitinib control did (58.2 ± 2.2 %). The insulin release correlated with the previously monitored percentage of probe displacement as well as the detected IC_{50} values.

To expose if the compounds also have a concentration dependent impact on insulin released by beta-TC6 cells, we treated the cells with compound concentrations ranging from 2 µM to 10 µM for 2 h in a high glucose (4.5 g/L) DMEM. Insulin release was analyzed using a rat/mouse insulin ELISA.
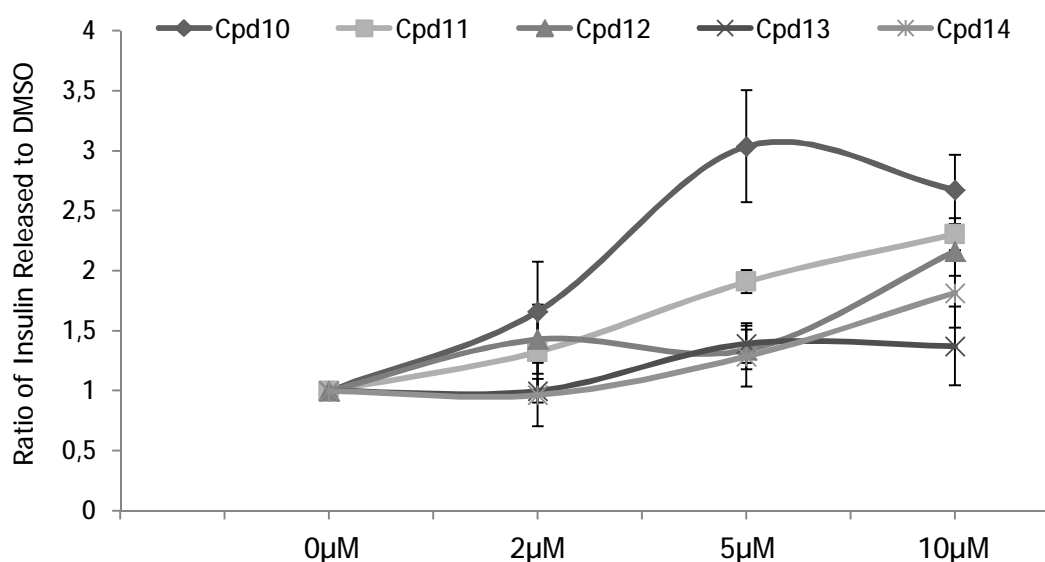
Figure R30 | *Scyl1 inhibitor treatment with various concentrations for each compound in high glucose media (4.5 g/L) ranging from 2 µM to 10 µM.*

Inhibition of Scyl1 by the revealed inhibitors displayed a concentration dependent increase of insulin release for all compounds but Cpd 13 (Figure R30). Highlighting the 5 µM values, which were matching with the previous performed approach for insulin release match for all compounds but Cpd 10, where the induction seemed to be slightly higher as before.

Table R5 | *Release of insulin after inhibition of Scyl1 by compounds 10 – 14 with various concentrations each in a beta-TC6-cell system*

Scyl1 Inhibitor	0 µM	0 µM SD	2 µM	2 µM SD	5 µM	5 µM SD	10 µM	10µM SD
Cpd 10	1	0	1.66	0.41	3.04	0.47	2.68	0.29
Cpd 11	1	0	1.33	0.35	1.91	0.10	2.31	0.13
Cpd 12	1	0	1.43	0.29	1.34	0.17	2.16	0.21
Cpd 13	1	0	1.00	0.10	1.39	0.17	1.37	0.33
Cpd 14	1	0	0.97	0.26	1.29	0.25	1.82	0.29

5.9.5 GLUCOSE MEDIATED EFFECT ON INSULIN RELEASE BY BETA TC6 CELLS AFTER INHIBITION WITH GRK5

Hypoglycemia can cause impairment of cognitive function, motoric control or even consciousness. For safety reasons, it is important that the identified Scyl1 inhibitors are glucose dependent and do not enhance the insulin release in low glucose environment. Therefore, we verified the glucose dependent insulin release in beta-TC6 cells using media with 1.125 mM (20 mg/dL) glucose as described for the reduction of gene expression. Cells were cultured for 24 h in a 96-well plate, washed with PBS and then appropriate media was replaced for 2 h at 37°C and 5 % (v/v) CO_2. Afterwards, the supernatant was used to detect the amount of insulin released in a rat/mouse insulin ELISA.
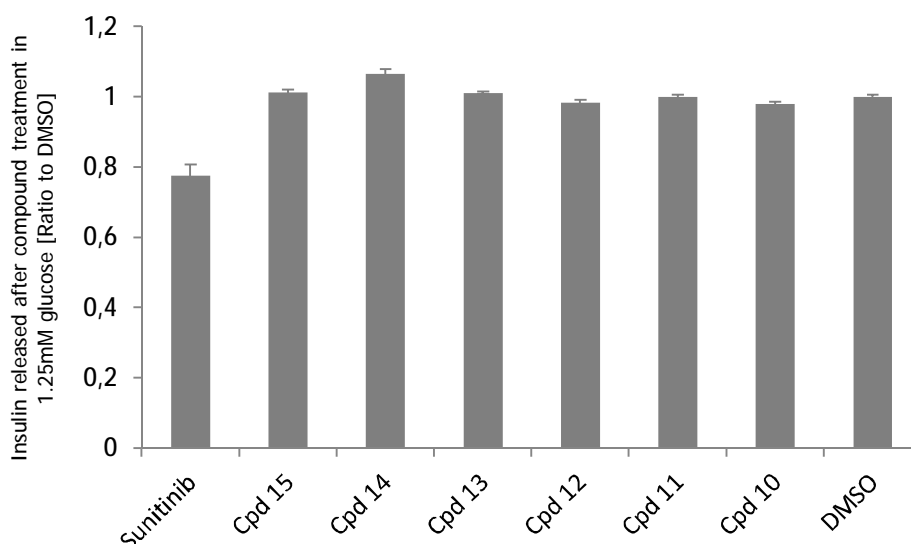
Figure R31 | *Inhibition of Scyl1 in a low glucose environment displayed no increased insulin secretion.*

Treatment of beta-TC6 cells with Scyl1 inhibitor compounds did not lead to increased insulin release like observed in high glucose media. Sunitinib seemed to decrease the insulin release (0.77 ± 0.03), whereas all the Scyl1 inhibitor compounds ranged close to the DMSO control. Thus, we rendered Scyl1 as a negatively regulating kinase which has no effect in low glucose media but increases insulin release in a high glucose environment.

5.9.6 GLUCOSE UPTAKE AFTER SCYL1 COMPOUND TREATMENT IN C2C12 AND BETA-TC6 CELLS

To investigate the impact of the Scyl1 inhibitors on 2-NBDG uptake, we used the fluorescent D-glucose analog 2-[*N*-(7-nitrobenz-2-oxa-1,3-diazol-4-yl)-amino]-2-deoxy-d-glucose (2-NBDG) [250]. For 2-NBDG detection, cells were treated with 5 µM compound for 1 h in glucose free media supplied with 100 µM 2-NBDG at 37 °C. Furthermore, as internal controls, samples of glucose free media, respectively glucose free media with compound were measured. Cells were analyzed by flow cytometry (FACS Calibur, BD Bioscience, respectively a BD Accuri® C6 Flow Cytometer). For evaluation, cells were gated using the

side- and forward scatter SSC/FSC and quantified by excited at 488 nm and collected at 533 nM (FL1).
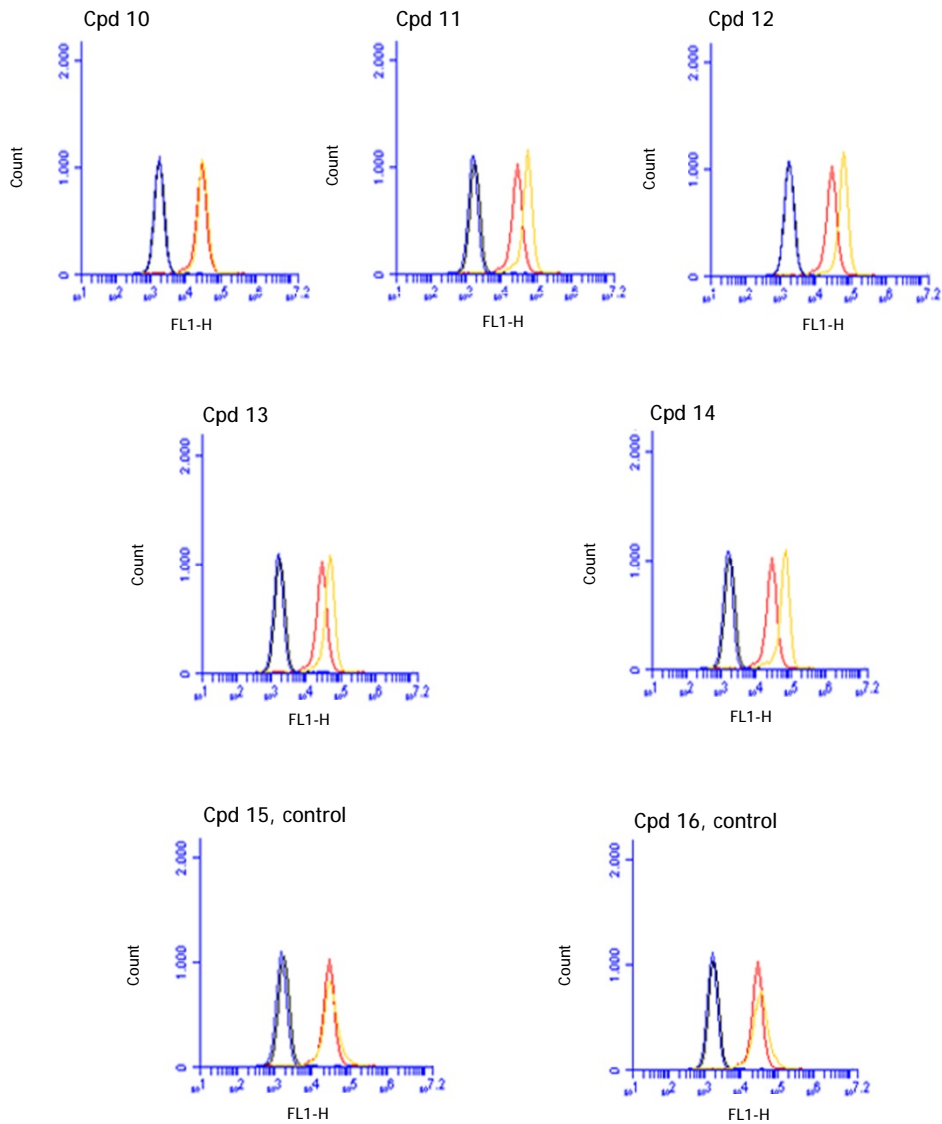

Figure R32 | *Illustration for 2-NBDG uptake after inhibition of Scyl1 in beta-TC6 cells. Upper panel left to right compounds 10 – 12, middle panel left to right compounds 13 – 14, lower panel left to right control compounds 15 – 16; black = glucose free medium; red = glucose free medium + compound; blue = 100µM 2-NBDG, yellow = 100µM 2-NBDG + compound.*
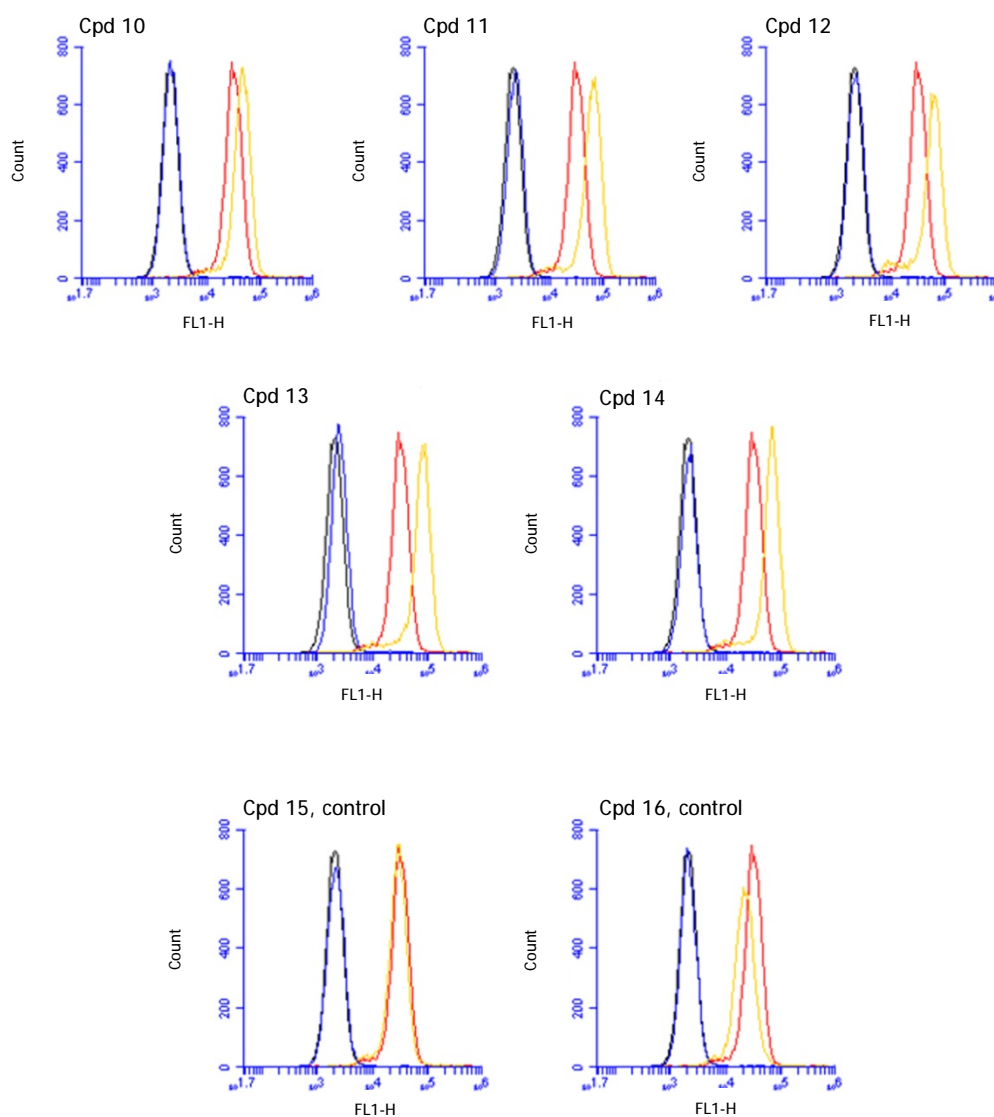
Figure R31 | *Illustration for 2-NBDG uptake after inhibition of Scyl1 in C2C12 cells. Upper panel left to right compounds 10 – 12, middle panel left to right compounds 13 – 14, lower panel left to right control compounds 15 – 16; black = glucose free medium; red = glucose free medium + compound; blue = 100µM 2-NBDG, yellow = 100µM 2-NBDG + compound.*

In contrast to the previously performed knock-down experiments where Scyl1 did not lead to significant 2-NBDG uptake in C2C12 (5.28 ± 3.26 %), respectively 3T3-L1 cells (3.26 ± 4.56 %), the usage of Scyl1 inhibitors displayed a significant increase of 2-NBDG up to 1.55 to 2.4 fold in C2C12 cells as representative for peripheral tissue and 1.14 to 2.6 fold in beta-TC6 cells. Both negative control compounds did not lead to a 2-NBDG uptake (Figure R31).

Table R6 | *Ratio of 2-NBDG uptake after inhibition of Scyl1 by revealed inhibitor compounds.*

Scyl1 Inhibitor	C2C12		beta-TC6	
	Ratio	SE	Ratio	SE
DMSO	1	0	1	n.a.
Cpd 10	1.551	0.024	1.14	n.a.
Cpd 11	2.052	0.039	2.17	n.a.
Cpd 12	2.099	0.099	2.17	n.a.
Cpd 13	2.404	0.150	2.61	n.a.
Cpd 14	2.090	0.099	1.83	n.a.
Cpd 15	0.914	0.040	1.26	n.a.
Cpd 16	0.876	0.049	1.38	n.a.

5.9.7 PROLIFERATION OF C2C12 MYOBLASTS AND BETA-TC6 CELLS AFTER SCYL1 INHIBITOR COMPOUND TREATMENT

Using a MTT approach, we determined the effect on cell viability and proliferation of beta-TC6 and C2C12 cells to display potential cytotoxicity of the revealed Scyl1 inhibitors *in vitro* after a 72 h treatment. The optical density (OD) was measured using a multi-well spectrophotometer at a wavelength of 570 nm.
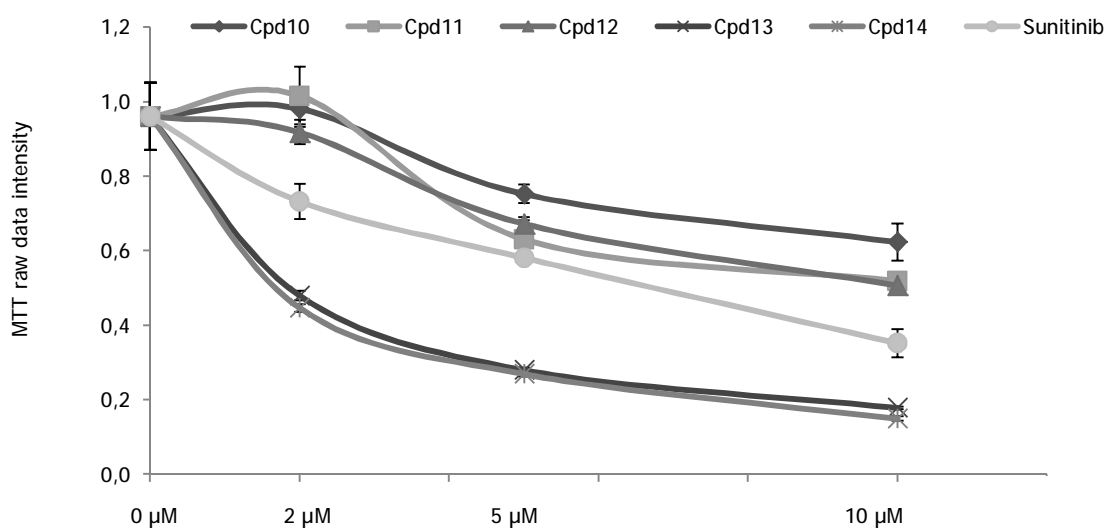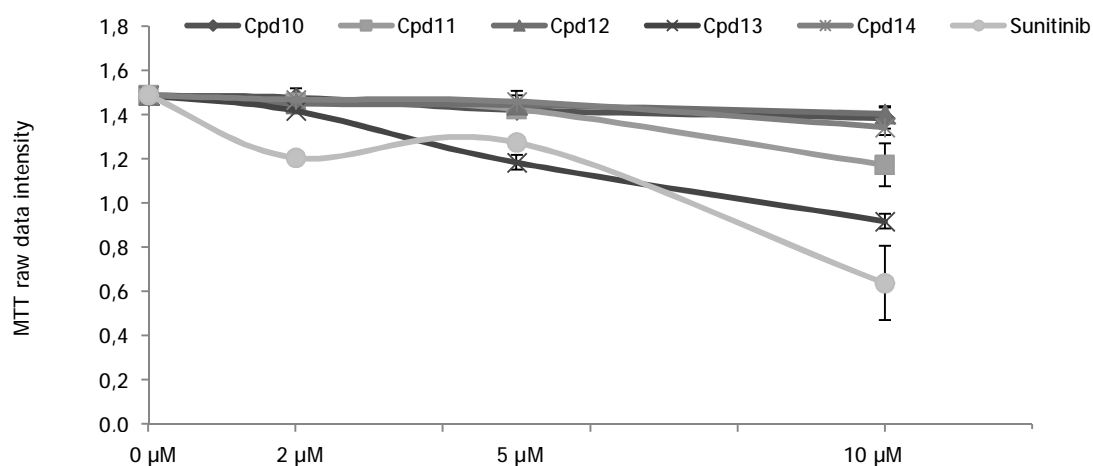
Figure R33 | *Proliferation of C2C12 myoblasts (upper figure) and beta-TC6 (lower figure) after Scyl1 compound treatment for 72h measured by MTT assay.*

Interestingly, beta-TC6 cells seemed to be more robust against the used Scyl1 inhibitors than the C2C12 cell line (Figure R33), suggesting that the metabolic turnover of the compounds inclines with the slow doubling time of approx. 36 - 48 h [274]. Compounds 10 and 12 seemed to have no toxic effect at all, even at concentrations up to 10 µM. Focusing on compounds 11 and 14, we detected only a slight decreased proliferation after a 10 µM treatment; compound 14 with 1.35 ± 0.038 raw data intensity (RDI) and compound 11 with 1.17 ± 0.096 RDI. Compound structure 13 as well as the positive control sunitinib which also appeared to be also toxic in lower concentrations, decreased the proliferation to 0.919 ± 0.034 RDI (Cpd 13, 10 µM) and 0.638 ± 0.167 (sunitinib, 10µM). In contrast, C2C12 cells, which had a doubling time of 13 h [275], displayed impaired proliferation and viability for all used compounds. Only compounds 10 - 12 revealed less toxicity at a 2 µM treatment (Figure R33). However, highlighting these compound structures as hits and not as lead structures, we assumed that structural engineering leads to less toxicity compounds with equal or even better characteristics.

5.10 Grk5 as Anti-Diabetic Target for Drug Development

5.10.1 Development of a Biochemical Enzymatic Grk5 Assay

For Grk5 (h) activity detection, casein was used as Grk5 substrate in combination with the ADP Glo™ Kinase assay technology. Non-phosphorylated casein was converted into phosphorylated casein by Grk5 and in turn ATP was converted into ADP, respectively. Subsequently, the non-converted ATP was digested into AMP by addition of the ADP-Glo™ reagent and in turn ADP produced by Grk5 activity was phosphorylated back to ATP by addition of Promega Kinase Detection Reagent. These ATP levels served as measure for the Grk5 activity and were quantified by a luciferase/luciferin reaction.
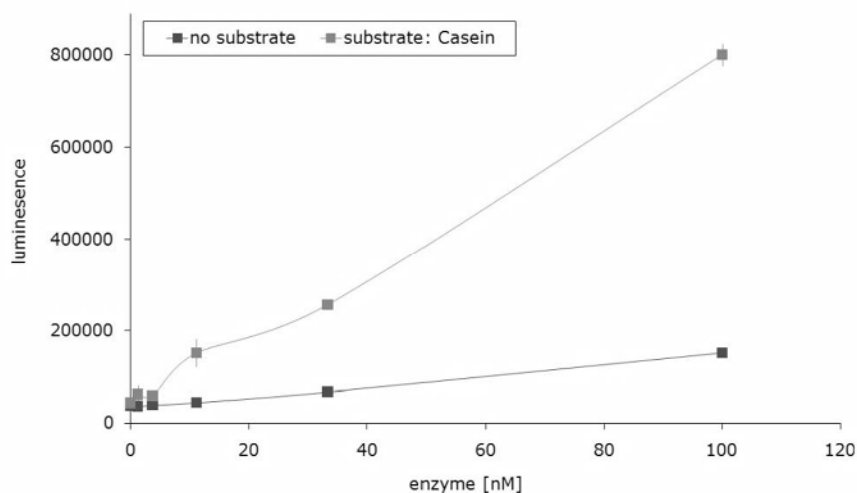
Figure R34 | *ADP Glo Kinase Assay Technology for Grk5 kinase activity measurement. Increasing concentration of Grk5 were incubated with 100 µM ATP in the absence and presence of 10 µM casein. After 60 min reaction was stopped by addition of ADP Glo Reagent. Grk5 activity was quantified by measuring luciferase mediated luminescence.*

In the presence of casein, increasing Grk5 concentration resulted in increasing luminescence activity and consequently in higher substrate turn over (Figure R34). A linear dependence between the Grk5 concentration and the luminescence signal was observed. In contrast, absence of casein in combination with increasing Grk5 concentration resulted in a minor increase of luminescence, demonstrating the specificity of the Grk5 signal and that Grk5

does not convert ATP into ADP by Grk5 auto-phosphorylation. To guarantee that the ADP Glo™ Kinase Assay is sensitive for ATP competitive inhibitors, the Michaelis-Menten constant for ATP ($Km_{(ATP)}$) was determined by measuring the Grk5 activity in combination with increasing ATP concentrations (Figure R35). The Michaelis-Menten constant was determined to be 18.7 µM by fitting the Grk5 activity to equation 3.

Equation 3: (Grk5 activity) = (Vmax x [ATP]) / $Km_{(ATP)}$ + [ATP])

Equation 3:

(Grk5 activity) = (Vmax x [ATP]) / (Km(ATP) + [ATP])])))
Vmax: maximum rate achieved by the system
[probe]: probe concentration
Km: substrate concentration at which the reaction rate is half of Vmax.
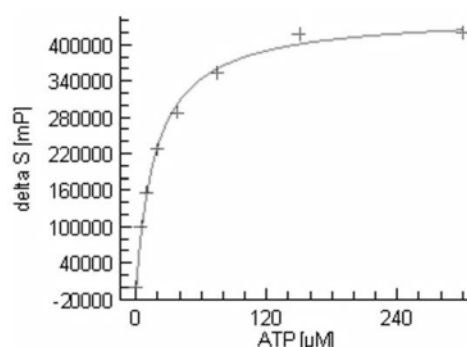
Figure R35 | *Determination of $Km_{(ATP)}$. Increasing concentrations of ATP were incubated with Grk5 and 10 µM casein for 60 min. GRK5 activity was quantified using the ADP Glo™ Kinase Assay technology and $Km_{(ATP)}$ was calculated by fitting the data to equation 3.*

Signal linearity and reaction time was measured by incubating increasing concentrations of Grk5 at 18.7 µM ATP in optimized reaction buffer over time. For all examined reaction times, a linear dependence between the assay signal and Grk5 concentration of up to 20 nM was observed. Moreover, a linear dependence between assay signal and reaction time of up to 120 min was displayed for all examined Grk5 concentrations. Thus, for further assay development and screening steps, a Grk5 concentration of 20 nM and a reaction time of 120 min were used (Figure R36).
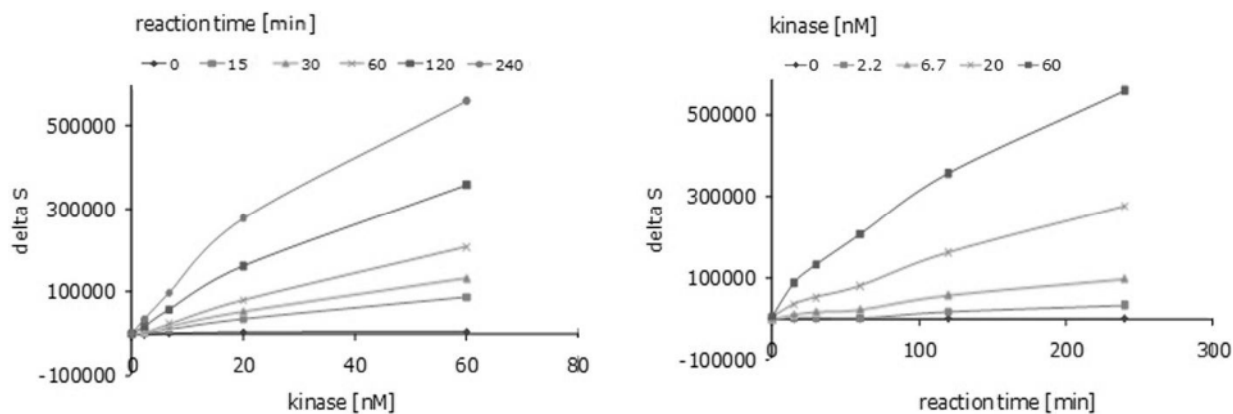
Figure R36 | *Signal linearity with Grk5 concentration and reaction time, increasing Grk5 concentrations were incubated over time before the reactions were stopped.*

In order to validate the assay, the IC_{50} of the reference compound staurosporine was measured in the presence of increasing concentrations (Figure R37). A regular IC_{50} curve was observed, indicating that the assay is suitable to identify Grk5 inhibitors. The IC_{50} value was quantified to be 0.66 µM by fitting the inhibition data to equation 4.

Equation 4:

100 / (1 + ((IC50/[staurosporine])^h)
h: Hill coefficient.
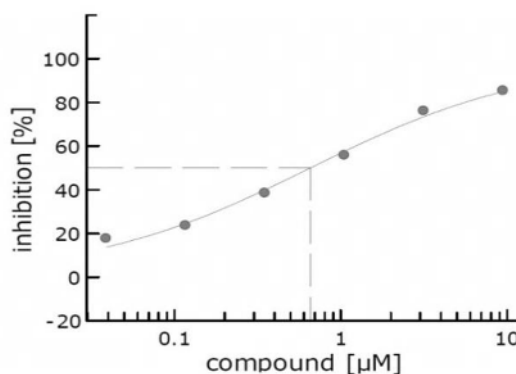
Figure R37 | *IC_{50} of staurosporine. Increasing staurosporine concentrations were incubated with 20 nM GRK5, 10 µM casein and 18.7 µM ATP for 120 min. Grk5 inhibition was calculated in relation to the Cpd + and Cpd - controls. The luminescence signal reflecting 0 % Grk5 inhibition (Cpd +) was measured in the absence of staurosporine, while the luminescence signal representing 100 % inhibition was measured in the absence of Grk5 (Cpd -). The IC_{50} value of 0.66 µM was quantified by data fitting to equation 4.*

For the high throughput screen, the compound library was screend with 20 nM GRK5, 10 µM casein and 18.7 µM ATP for 120 min in an optimized reaction buffer (10 mM MgCl$_2$, 1 mM DTT, 0.01 % Tween20, 20 mM MES, pH 6.0).

5.10.2   HIGH THROUGHPUT SCREENING OF GRK5

Using the established Grk5 activity assay, the company Proteros screened a MPI chemical compound library (1863_SF_MPK, 2121_SF_MPK, 2145_SF_MPK, 2217_SF_MPK) of 8827 compounds (Cpds) for their ability to inhibit Grk5 kinase activity. The Cpds were delivered at 10 mM stock concentration and tested at a final assay concentration of 100 µM. In all cases, Z′ ≥ 0.5 was reached and the signal was sufficiently stable over all assay plates. A hit distribution was observed with an average inhibition of 3.2 % and a standard deviation of 11 % (Figure R38). In consequence, compounds with an inhibition value above 36.1 % (= inhav + (3 x Inhstdev)) were recommended to be considered as hit.
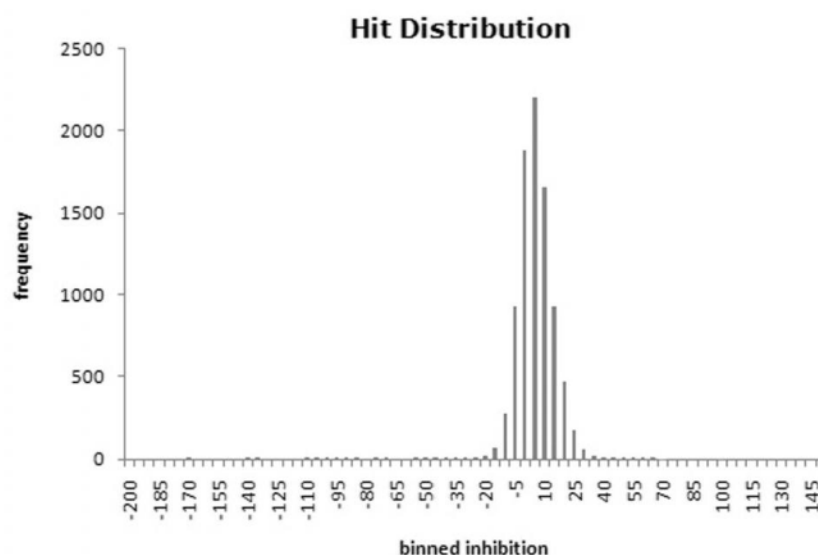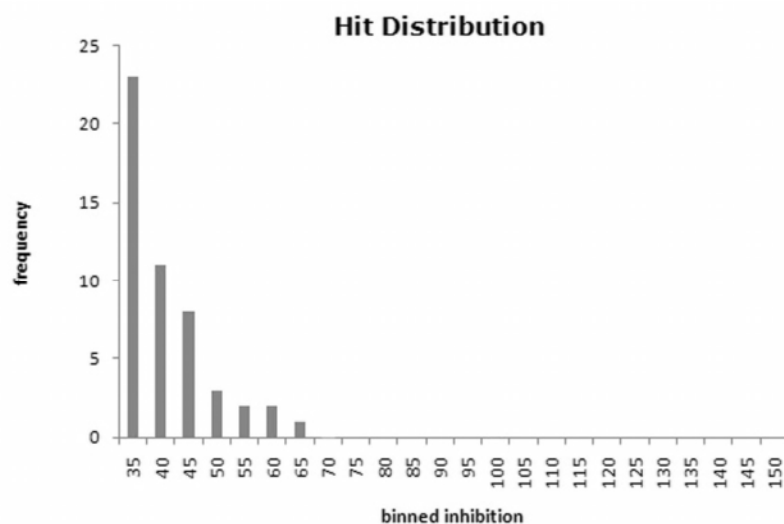
Figure R38 | *Hit distribution for all compounds (upper bar chart) and as a blow up for all compounds with an inhibition value of ≥ 35 % (lower bar chart).*

Table R7 | *Hit rate for the total of 8827 compounds. The average (av) of percentage inhibition was calculated to be 3.2 % and the standard deviation (stdev) 11 %, which resulted in the threshold of 36.1 % (av + 3 x stdev) for significant probe binding inhibition.*

Inhibition [%]	Compounds [#]	Hit rate [%]
≥90	0	0.0
≥80	0	0.0
≥70	0	0.0
≥60	2	0.03
≥50	3	0.04
≥40	17	0.2
≥36	26	0.31

The screen revealed just a few small-kinase-inhibitors with inhibitory impact for Grk5 activity. However, for further experiments we opted for the five most promising inhibitors (Cpd 1 – 5) with an inhibition over 50 % as well as two compound structures which displayed no inhibition on Grk5 in the screen as target controls (Cpd 6, 7).

Table R8 | *Representative kinase inhibitors revealed in the Grk5 inhibitor assay screen.*

Grk5 Inhibitor	Plate ID	Well ID	Cpd ID	Inhibition [%]
1	2nd BF_22_BFCP_555-558_c_10mM	A15	828_0346_6370	68.0
2	2nd BF_21_BFCP_551-554_c_10mM	N19	828_0346_6001	60.0
3	2nd BF_21_BFCP_551-554_c_10mM	C20	828_4147_7468	56.0
4	2nd BF_22_BFCP_555-558_c_10mM	K05	828_0176_0314	52.0
5	2nd BF_10_BFCP_057-060_c_10mM	P02	765_0311	51.0
6	2nd BF_7_BFCP_045-048_c_10mM	F15	802_0339_0192	0
7	2nd BF_7_BFCP_045-048_c_10mM	F16	802_0349_0070	0

Furthermore, Proteros determined the IC_{50} values for all compounds ≥ 50 % inhibition using triplicates at 12 different concentrations with a dilution factor of three (Figure R39). The maximal compound assay concentration was set to 100 µM, matching the assay concentration used in the primary screen.

Cpd1 / 10.5 - 72µM

Cpd2 / 44.5 - 111µM

Cpd3 / 35.9 - 111µM

Cpd4 / 8.35 - 71µM

Cpd5/ >100µM
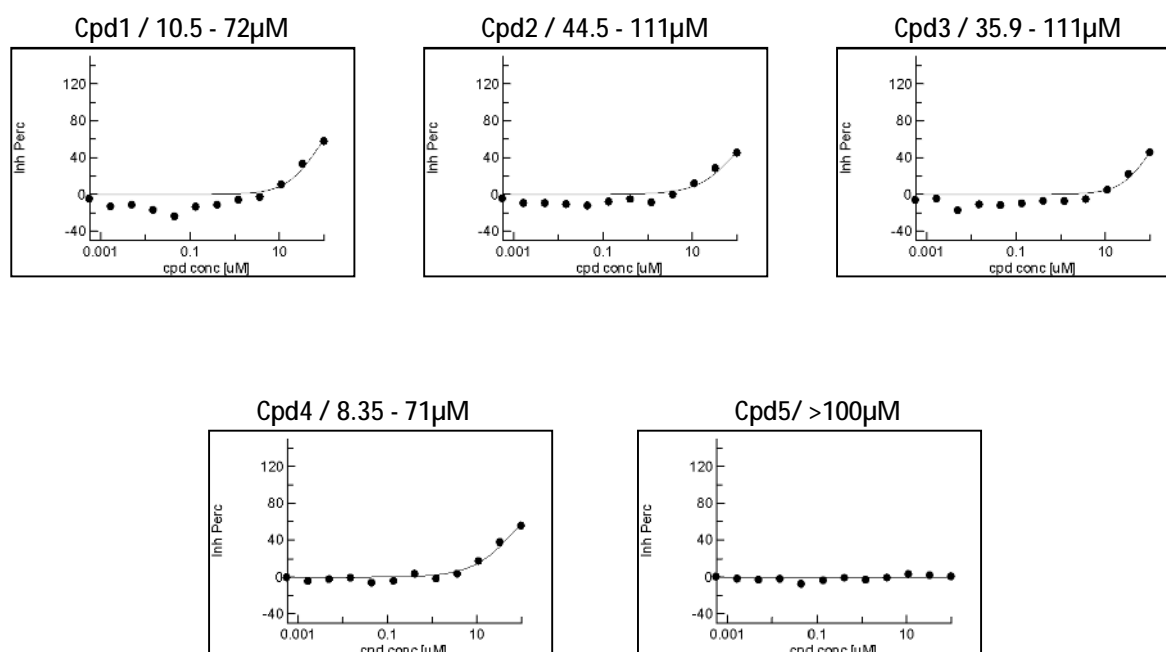
Figure R39 | *Determination of IC_{50} values for the most promising kinase inhibitors Cpd 1 - 5 by Proteros and Millipore.*

Beside the IC_{50} determination by Proteros we investigated the most promising Grk5 inhibitors using the kinase profiling platform of Millipore. The IC_{50}-values were determined within

15 µM of the apparent Km for ATP using 9 different concentrations each (100 µM, 30 µM, 10 µM, 3 µM, 1 µM, 0.3 µM, 0.1 µM, 0.03 µM, 0.01 µM and 0 µM) in a Gold Standard radiometric protein kinase assay.
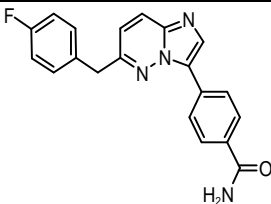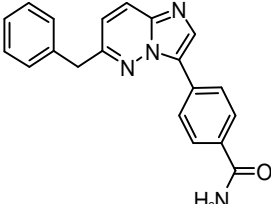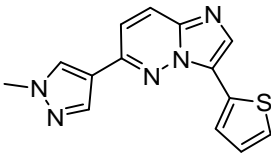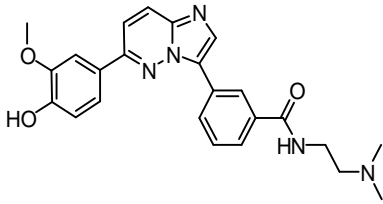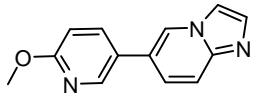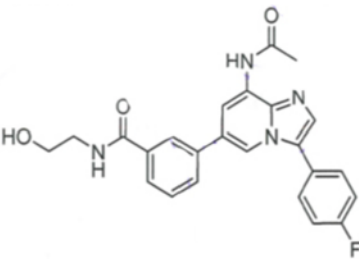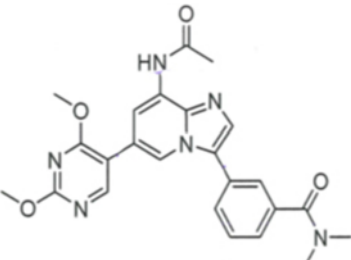
Table R9 | *Comparison of Grk5 IC$_{50}$s derived from Millipore and Proteros.*

Grk5 Inhibitor	IC$_{50}$ by Millipore (µM)*	IC$_{50}$ by Proteros (µM)	InH by Proteros (%)
Cpd1	10.504	72	68.0
Cpd2	44.575	111	60.0
Cpd3	35.925	111	56.0
Cpd4	8.349	71	52.0
Cpd5	>100	>100	51.0
Cpd6 (contr)	>100	n.a.	0.0
Cpd7 (contr)	>100	n.a	0.0
Sut	20.592	169	n.a.
Glev	>100	n.a.	n.a.

* single point data

For every compound tested the IC$_{50}$ value was still in a µM range but varied between 3- and 10-fold when compared to the Proteros screen. The non-inhibitor control did not display any kind of Grk5 affinity.

Table R10 | *Structures of Grk5 inhibitor compounds.*

Grk5 Inhibitor	Compound ID	Structure	Purity	Mol_weight
1	828_0346_6370		98	346.36
2	828_0346_6001		94	328.37
3	828_4147_7468		98	281.34
4	828_0176_0314		98	431.49
5	765_0311		98	225.25
6 Non-Inhibitor	802_0339_0192		95	432.45
7 Non-Inhibitor	802_0349_0070		99	460.49

Compound 1 – 4 share an *imidazo-[1,2-b]pyridazine* backbone
Compound 5 – 7 have an *imidazo-[1,2-a]pyridine* backbone

5.10.3 Release of Insulin after Inhibition of Grk5 in Beta-TC6-cells

After having identified the most promising Grk5 inhibitors and determination of the IC_{50} values, we investigated the impact on insulin release by beta-TC6 cells. Therefore, we used the previously established insulin detection assay, treating the beta-TC6 cells with 5 µM of candidate compounds as well as non-inhibitor controls for 2 h in a high glucose (4.5 g/L) DMEM media at 37 °C and 5 % (v/v) CO_2. Afterwards, the supernatant was analyzed for insulin using a rat/mouse insulin ELISA.
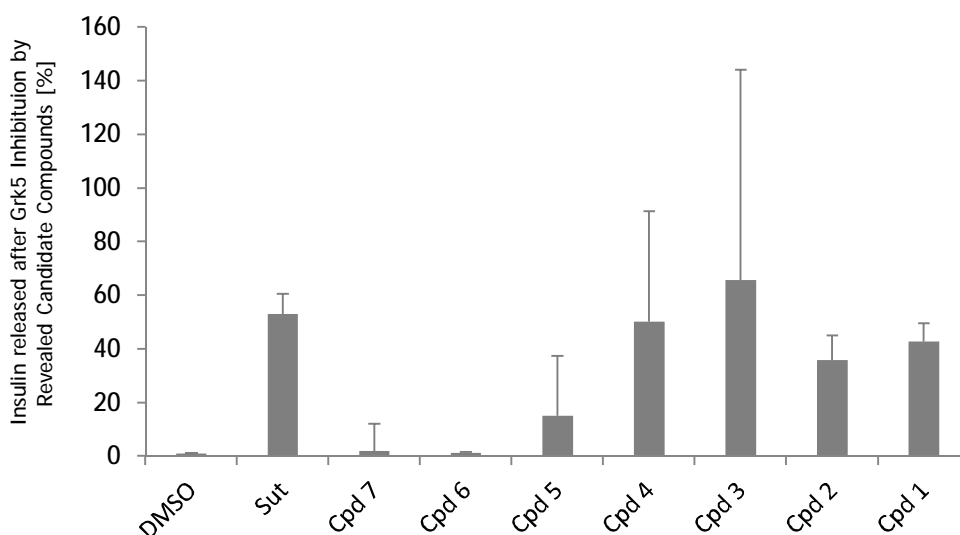
Figure R40 | *5 µM Grk5 inhibitor treatment increases insulin release in beta-TC6 cells. Grk5 inhibition by compound 1 to 4 led to a remarkable effect on insulin release in our system (increase in percent ± SEM: C_1: 42.8 ± 6.8; C_2: 35.9 ± 9.0; C_3: 65.7 ± 78.3; C_4: 50.2 ± 41.2; C_5: 15.1 ± 22.3 at 5µM). The negative control – Cpds without inhibition efficacy – displayed no effect (C_6: 1.3 ± 0.3; C_7: 2.0 ± 10.0) while the sunitinib control did (Sut: 53.2 ± 7.5).*

In spite of the relatively high IC_{50} values, inhibition of Grk5 by the identified compounds as well as sunitinib treatment resulted in a significant increase of insulin release (Figure R40). Here, Cpd 3 (Inh. 56 % / IC_{50} = 111 µM) depicted the strongest effect with an increase of 65.7 ± 78.3 %, whereas Cpds 1, 2 and 4 also had a significant effect on the increase of insulin release ranging from 35.9 ± 9.0 % (Cpd2) to C_4: 50.2 ± 41.2 % (Cpd 11) with lower

standard deviations. The negative controls – Cpds without inhibition efficacy – displayed no effect on insulin release (C_6: 1.3 ± 0.3 %; C_7: 2.0 ± 10.0 %) while the sunitinib control did (53.2 ± 7.5 %). To determine if the identified compounds also have a concentration dependent impact on insulin released by beta-TC6 cells, we treated the cells with compound concentrations ranging from 2 µM to 10 µM. Cells were treated for 2 h in a high glucose (4.5 g/L) DMEM media at 37°C and 5 % (v/v) CO_2. Insulin release was analyzed using a rat/mouse insulin ELISA.
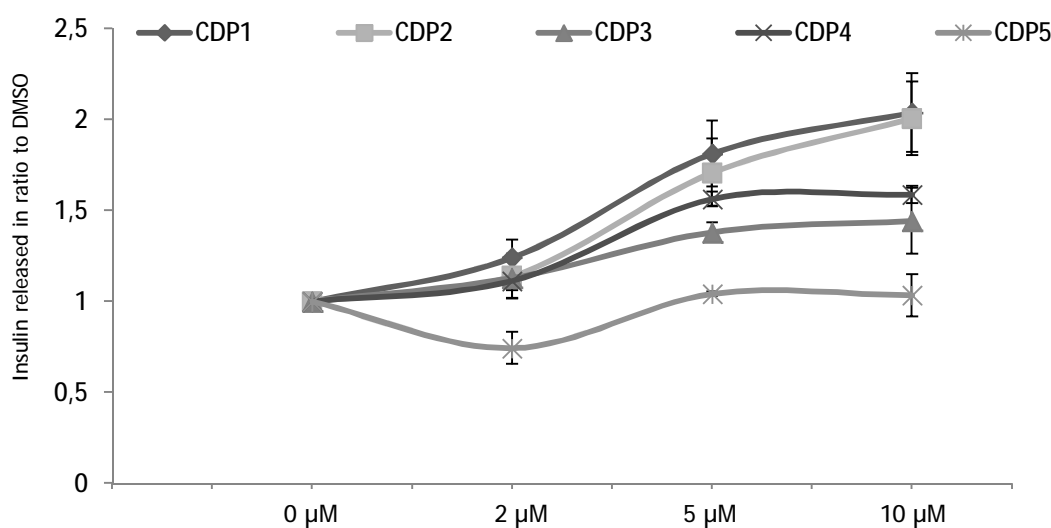
Figure R41 | *Grk5 inhibitor treatment with various concentrations for each compound in high glucose media (4.5 g/L) ranging from 2 µM to 10 µM.*

All Cpds, but Cpd 5, led to a concentration dependent increase of insulin (Figure R41). Interestingly, the insulin release efficiency inclined with the previous inhibitory effect of the compound. Furthermore, the 5 µM values were matching the former insulin release values for all compounds but Cpd 3, where the induction seemed to be lower than before.

Table R11 | *Release of insulin after inhibition of Grk5 by compounds 1 – 5 with various concentrations in a Beta-TC6-Cell System*

GRK5 Inhibitor	0µM	0 µM SD	2µM	2 µM SD	5µM	5 µM SD	10µM	10µM SD
CDP 1	1	0	1.24	0.17	1.81	0.31	2.03	0.37
CDP 2	1	0	1.13	0.21	1.70	0.32	2.00	0.35
CDP 3	1	0	1.12	0.09	1.38	0.06	1.44	0.08
CDP 4	1	0	1.11	0.19	1.56	0.09	1.58	0.31
CDP 5	1	0	0.74	0.12	1.04	0.01	1.03	0.16

5.10.4 THE EFFECT OF GLUCOSE ON INSULIN RELEASE BY BETA TC6 CELLS AFTER GRK5 INHIBITOR TREATMENT

We investigated the glucose dependent insulin release in beta-TC6 cells using media with 1.125 mM (20 mg/dL) glucose as described for Scyl1 and reduction of gene expression (see chapter 3.3). Cells were cultured for 24 h in a 96-well plate, washed with PBS and fresh media was added for 2 h. Afterwards, the supernatant was taken to detect the amount of insulin released with a rat/mouse insulin ELISA.
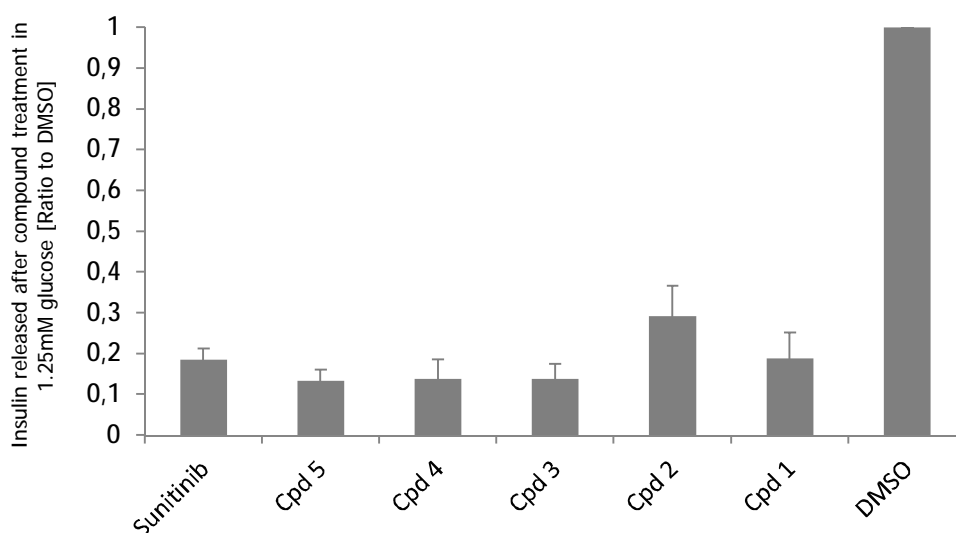
Figure R42 | *Inhibition of Grk5 in a low glucose environment led to a significant decrease of insulin secretion*

Treatment of beta-TC6 cells with Grk5 inhibitor compounds led to a significantly decreased insulin secretion ranging between the 0.14 ± 0.06 (Cpd 2) and 0.094 ± 0.04 (Cpd 4) fold to DMSO control (Figure R42). Thus, we rendered Grk5 as glucose dependent kinase which decreases insulin release at low glucose and increases insulin secretion upon high glucose concentrations.

5.10.5 GLUCOSE UPTAKE AFTER GRK5 COMPOUND TREATMENT IN C2C12 AND TC6 CELLS

To investigate the impact of the Grk5 inhibitors on 2-NBDG uptake, cells were cultured for 1 h in glucose free media supplied with 100 µM 2-NBDG at 37 °C and 5 % (v/v) CO_2. Furthermore, as internal controls, samples of glucose free media, respectively glucose free media with compound, were measured. Fluorescence was analyzed by flow cytometer (FACS Calibur, BD Bioscience, respectively a BD Accuri® C6 Flow Cytometer). For evaluation, cells were gated using the side- and forward scatter SSC/FSC and quantified by excited at 488 and detected at 533 nm (FL1).
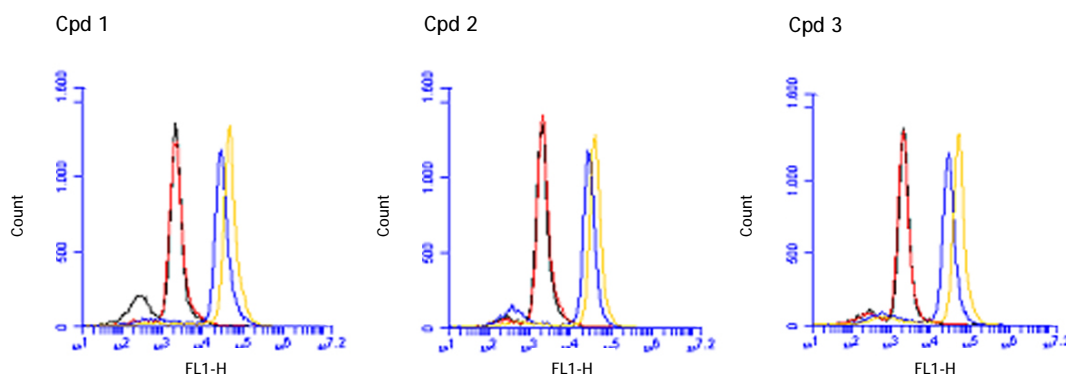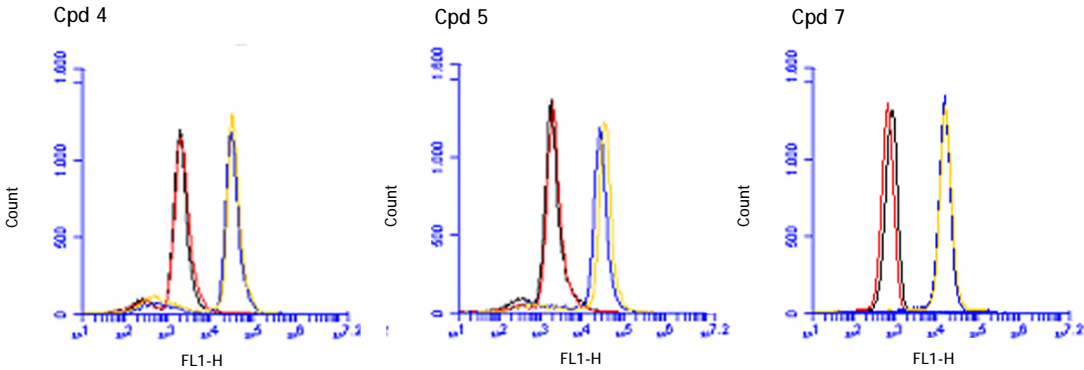
Figure R43 | *Example illustration for 2-NBDG uptake after inhibition of Grk5 in beta-TC6 cells. Upper panel left to right compounds 1 – 3, lower panel left to right compounds 4, 5 and control compound 7; black = glucose free medium; red = glucose free medium + compound; blue = 100µM 2-NBDG, yellow = 100µM 2-NBDG + compound.*
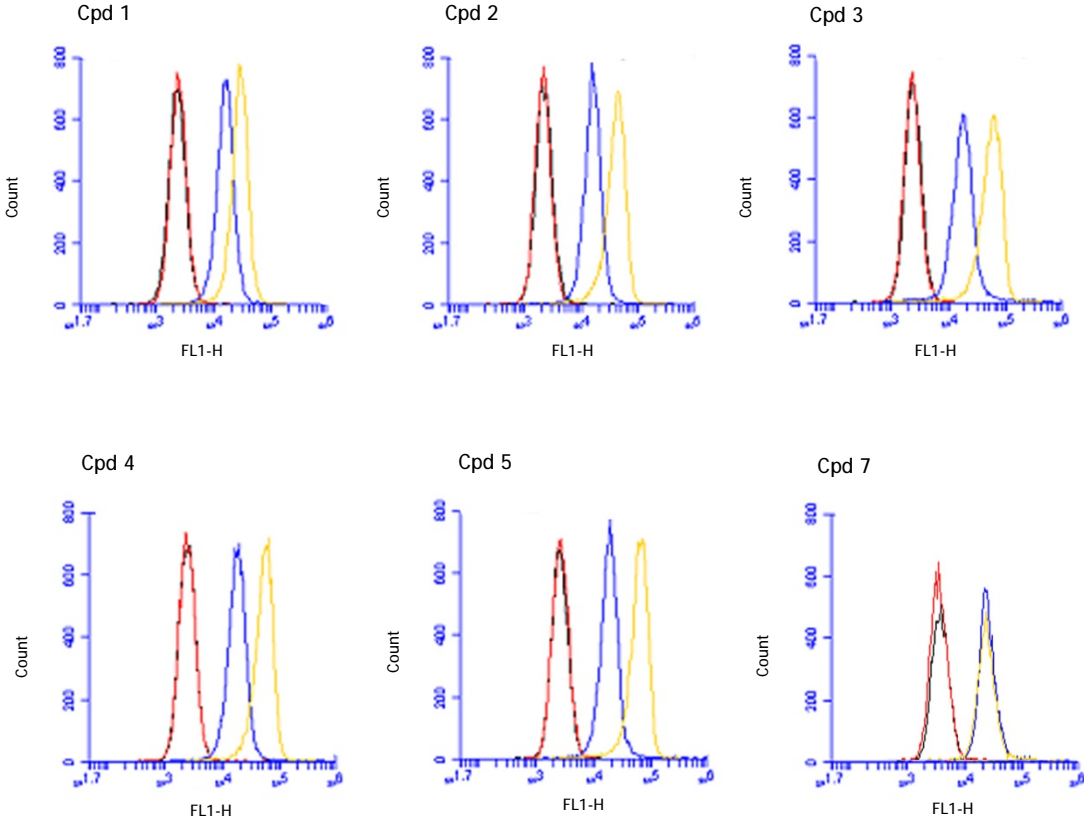
Figure R44 | *Example illustration for 2-NBDG uptake after inhibition of Grk5 in C2C12 myoblast cells. Upper panel left to right compounds 1 – 3, lower panel left to right compounds 4, 5 and control compound 7; black = glucose free medium; red = glucose free medium + compound; blue = 100µM 2-NBDG, yellow = 100µM 2-NBDG + compound.*

Table R12 | *Ratio of 2-NBDG uptake after inhibition of Grk5 by revealed inhibitor compounds.*

Grk5 Inhibitor	C2C12		beta-TC6	
	Ratio	SE	Ratio	SE
DMSO	1	0	1	0
Cpd 1	2.45	0.53	1.57	0.12
Cpd 2	2.12	0.44	1.53	0.07
Cpd 3	2.34	0.46	1.68	0.21
Cpd 4	1.77	0.43	1.29	0.09
Cpd 5	1.47	0.17	1.26	0.02
Cpd 7	1.73	0.11		

As monitored after reduction of target gene expression, inhibition of Grk5 led to an increased uptake of 2-NBDG ranging from 1.47 to 2.45 fold in C2C12 cells (Figure R44), as representatives for peripheral tissue and from 1.28 to 1.68 fold in beta-TC6 cells (Figure R43). Interestingly, the negative control compound displayed a rather high background of 1.74. However, in spite of this high background, the compounds 1 - 3 displayed a significantly higher increase of 2-NBDG uptake upon a 1 h compound treatment.
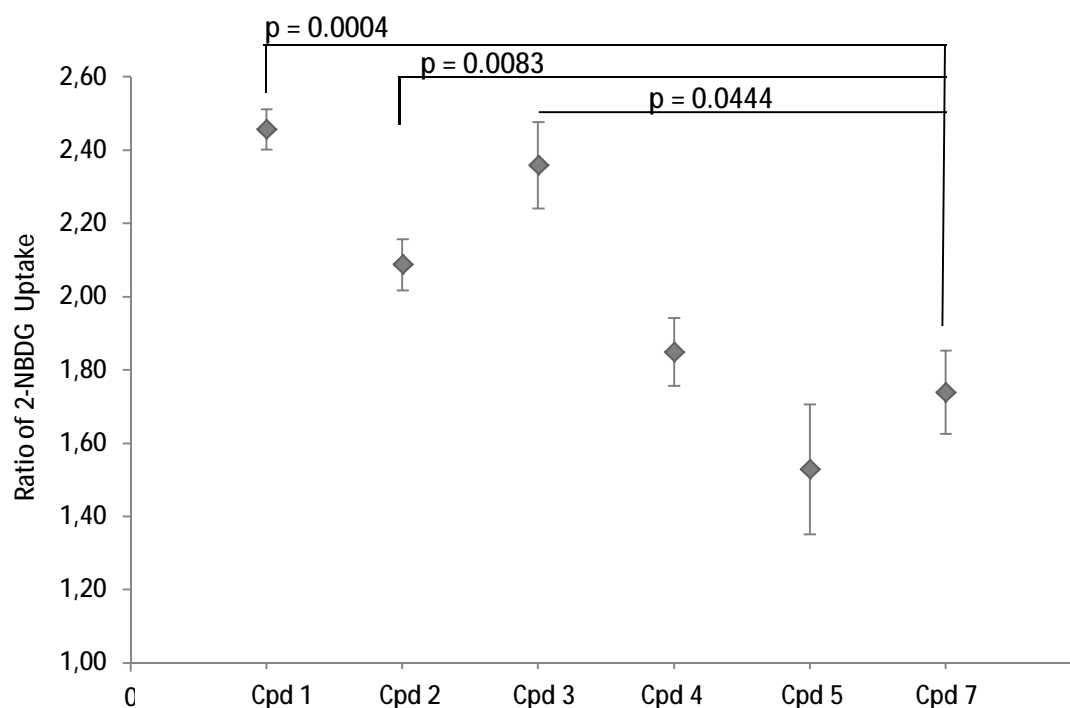
Figure R45 | *Comparison of glucose uptake via 2-NBDG after inhibition of Grk5 in C2C12 mouse myoblasts. Despite a background of 1.7 ± 0.11 (ratio ± SEM) the compounds 1 - 3 displayed a significant higher increase of 2-NBDG uptake upon a 1 h compound treatment.*

Table R13 | *Averages and SEM of Figure R45. Comparison of glucose uptake via 2-NBDG to non-inhibitor compound 7.*

Grk5 Inhibitor	Average Ratio	SEM
Cpd1	2.457	0.055
Cpd2	2.087	0.070
Cpd3	2.359	0.117
Cpd4	1.849	0.092
Cpd5	1.528	0.177
Cpd7	1.739	0.113

Inhibition of Grk5 displayed a significantly increased uptake of 2-NBDG in C2C12 cells for three of the five compounds, namely Cpd 1, Cpd 2 and Cpd 3 (Figure R45). The core structures of Cpds 1 – 4 and 5 – 7 belong to structurally different but related groups, what may be a possible explanation for the high background.

5.10.6   PROLIFERATION OF C2C12 MYOBLASTS AND BETA-TC6 CELLS AFTER GRK5 COMPOUND TREATMENT FOR 72H

Using a MTT approach, we determined the effect on cell viability and proliferation of beta-TC6 and C2C12 cells to display potential cytotoxicity of the Grk5 inhibitors *in vitro* after a 72 h treatment. The optical density (OD) was measured using a multi-well spectrophotometer at a wavelength of 570 nm.
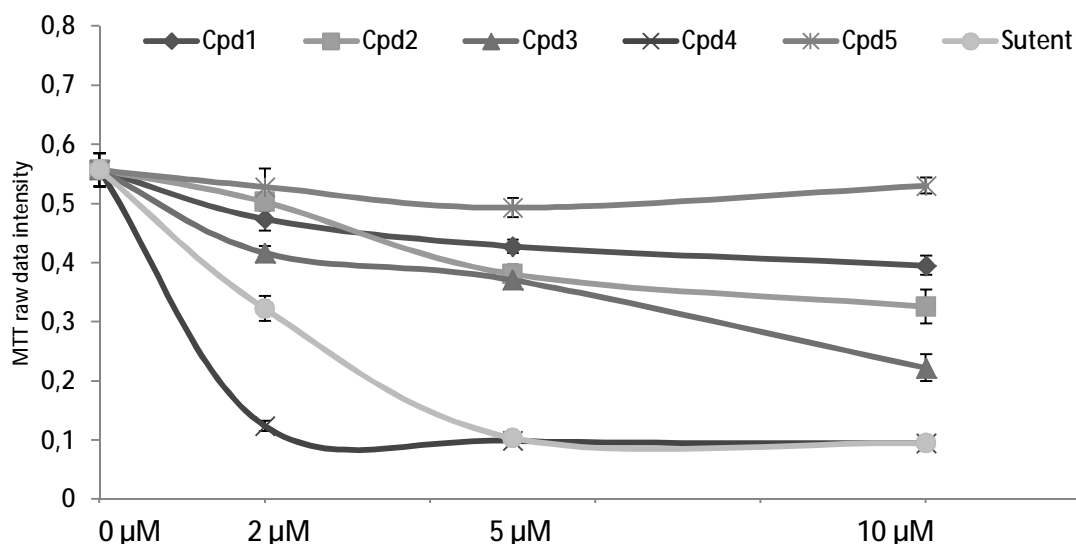
Figure R46 | *Proliferation of C2C12 myoblasts after Grk5 compound treatment for 72 h measured by MTT assay.*

Table R14 | *Averages and SEM of Figure R46*

GRK5 Inhibitor	0µM	0µM SEM	2µM	2µM SEM	5µM	5µM SEM	10µM	10µM SEM
Cpd1	0.557	0.028	0.474	0.020	0.428	0.011	0.396	0.016
Cpd2	0.557	0.028	0.503	0.015	0.381	0.016	0.326	0.028
Cpd3	0.557	0.028	0.416	0.012	0.371	0.010	0.222	0.022
Cpd4	0.557	0.028	0.124	0.009	0.099	0.001	0.095	0.002
Cpd5	0.557	0.028	0.529	0.031	0.493	0.017	0.530	0.013
Sutent	0.557	0.028	0.323	0.021	0.104	0.003	0.095	0.001
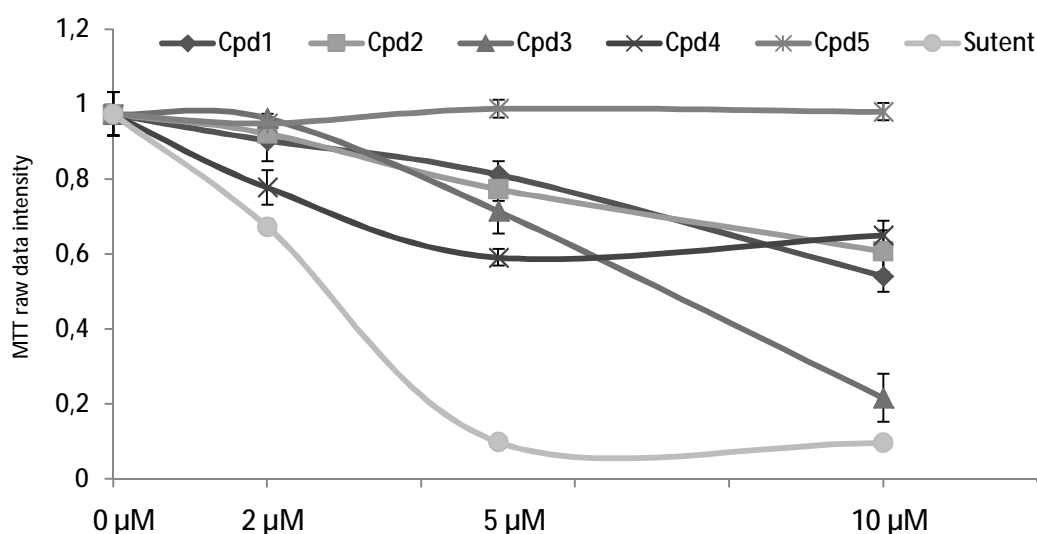
Figure R47 | *Proliferation of beta-TC6 cells after Grk5 compound treatment for 72 h measured by a MTT assay.*

Table R15 | *Averages and SEM of Figure R45*

Grk5 Inhibitor	0µM	0µM SEM	2µM	2µM SEM	5µM	5µM SEM	10µM	10µM SEM
Cpd1	0.973	0.034	0.903	0.032	0.812	0.021	0.541	0.025
Cpd2	0.973	0.034	0.922	0.009	0.773	0.019	0.608	0.032
Cpd3	0.973	0.034	0.962	0.007	0.715	0.034	0.216	0.037
Cpd4	0.973	0.034	0.778	0.026	0.591	0.013	0.651	0.022
Cpd5	0.973	0.034	0.949	0.009	0.988	0.014	0.980	0.013
Sutent	0.973	0.034	0.673	0.012	0.098	0.001	0.096	0.001

The Grk5 inhibitors led to a decreased proliferation over a 72 h treatment. Only Cpd5 seemed to have no impact on C2C12 (Figure R46) or beta-TC6 (Figure R47) proliferation.

5.11 SCYL1 AND GRK5 INHIBITORS COMPARISON

5.11.1 COMPARISON OF SCYL1 AND GRK5 INHIBITOR STRUCTURES

As mentioned before, compounds with an inhibition value above 36.1 % (= inhav + (3 x inhstdev)) (Grk5) and above 45 % (= inhav + (3 x inhstdev)) (Scyl1) were recommended to be considered as hit. To crosscheck the possible influence of each target inhibitor, we compared the compound structures for Scyl1 and Grk5.

Table R16 | *Comparison of target inhibition of the most promising inhibitors from both HTS*

GRK5 Inhibitors

SCYL1 Inhibitors

Cpd	Inh [%] Grk5 / Scyl1	Structure	Cpd	Inh [%] Scyl1 / Grk5	Structure
1	68 / 31		10	100 / 17	
2	60 / 23		11	98 / 5	
3	56 / 41		12	96 / -24	
4	52 / 67		13	93 / -14	
5	51 / 11		14	92 / 10	
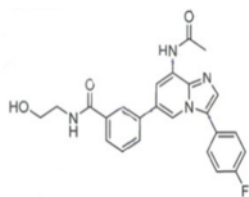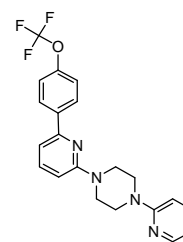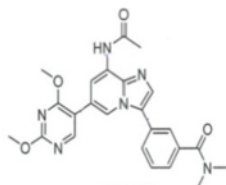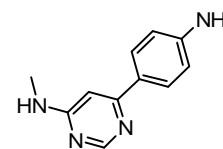
6	0 / 4		15	0 / 32	
7	0 / 7		16	0 / 5	
Sut	20 / 23		Sut	23 / 20	
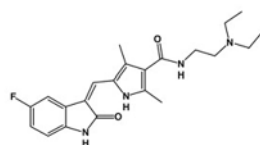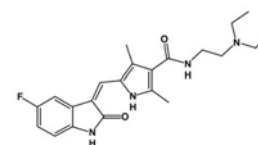
Compound 1 – 4 share an imidazo-[1,2-b]-pyridazine backbone; Compound 5 – 7 have an imidazo-[1,2-a]-pyridine backbone; compound 10 – 15 share an imidazo-[1,2-b]-pyridazine backbone; compound 15 has a pyridyl-piperazine backbone; compound 16 has a pyrimidine amine backbone; Sut = sunitinib.

Comparison of hit structures of Grk5 and Scyl1 exhibited an interesting match. Thus, Grk5 inhibitor structures 3 and 4 seemed to inhibit Scyl1 as well. However, no additive effect of these compound structures regarding insulin release or glucose uptake via 2-NBDG was detected.

5.11.2 INSULIN DEPENDENCE OF SCYL1 AND GRK5 INHIBITOR COMPOUNDS

To investigate if the 2-NBDG uptake of the identified compound inhibitors of Scyl1 and Grk5 are insulin dependent, we differentiated 3T3-L pre-adipocytes to matured adipocytes. Afterwards, cells were starved for 4 h before they were washed and glucose free media supplied with 100 µM 2-NBDG, in the presence and absence of 10 µg/ml insulin and either Cpd 10 (Scyl1) or Cpd 1 (Grk5) inhibitor was replaced for 1 h at 37 °C. Furthermore, as internal controls, samples of glucose free media or glucose free media with compound were

measured (data not shown). Fluorescence was analyzed by flow cytometer (FACS Calibur, BD Bioscience, respectively a BD Accuri® C6 Flow Cytometer). For evaluation, cells were gated using the side- and forward scatter SSC/FSC and quantified by excited at 488 and detected at 533 nm (FL1).
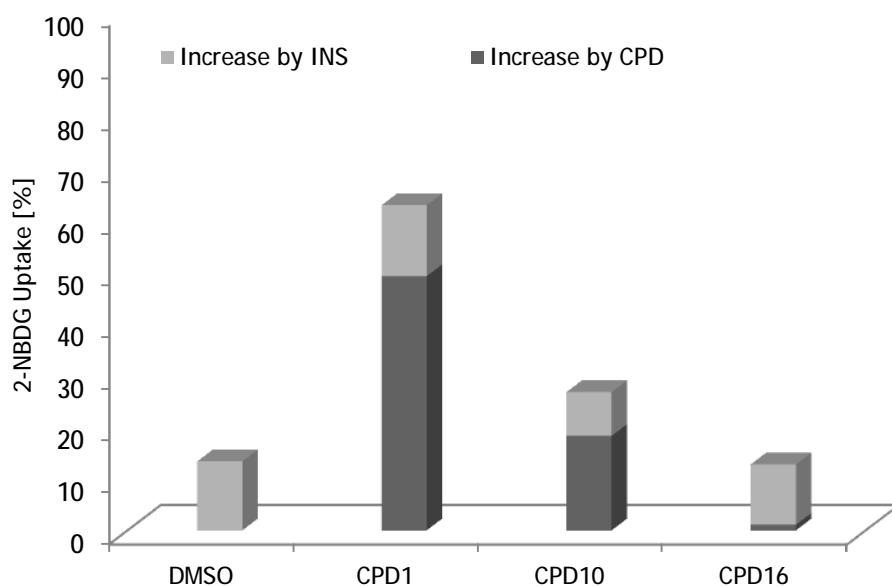
Figure R48 | *Insulin dependency of compound structures Cpd 10 (Scly1) and Cpd 1 (Grk5). Beside the glucose uptake mediated by insulin (average = 11.78 %), the compound structures Cpd 10 and Cpd 1 led to an insulin independent increase of 18.2 ± 3.5 %, respectively 48.9 ± 7.2 %.*

The compounds Cpd 10 (Scyl1 inhibitor) and Cpd 1 (Grk5 inhibitor) led to an insulin independent increase of insulin. Whereas insulin alone led to an increase of 2-NBDG uptake of 11.78 ± 1.22 %, Cpd 10 displayed an additional increase of 18.2 ± 3.5 %, respectively Cpd 1 an additional increase 48.9 ± 7.2 %. Interestingly, Cpd 10 did not show the full additional amount of insulin released after Scyl1 inhibition as without insulin, here an increase of 60.2 ± 8.9 % was determined. For Grk5 inhibitor Cpd 1, in contrast, nearly the same amount of additional insulin release as before (42.8 ± 6.8 %) was monitored.

5.11.3 COMPARISON OF SCYL1 AND GRK5 INHIBITOR STRUCTURES

Based on literature references and on the performed siRNA screen, we decided on several commercially available inhibitors to compare our Scyl1 and Grk5 inhibitors. For comparison we chose the Akt1-Inhibitor II (Calbiochem #124008) [265], which should lead to decreased insulin release, as well as the Map2K3-Inhibitor II (Calbiochem #444938), Exendin-4 (Sigma #E7144) and GLP-1 (Sigma #G8147), which should lead to an increased insulin release [276-278]. Cells were cultured for 24 h before treated with Scyl1, Grk5 and control inhibitors for 2 h at 37 °C and 5 % (v/v) CO_2. Insulin in the supernatant was detected by a mouse/rat insulin ELISA.
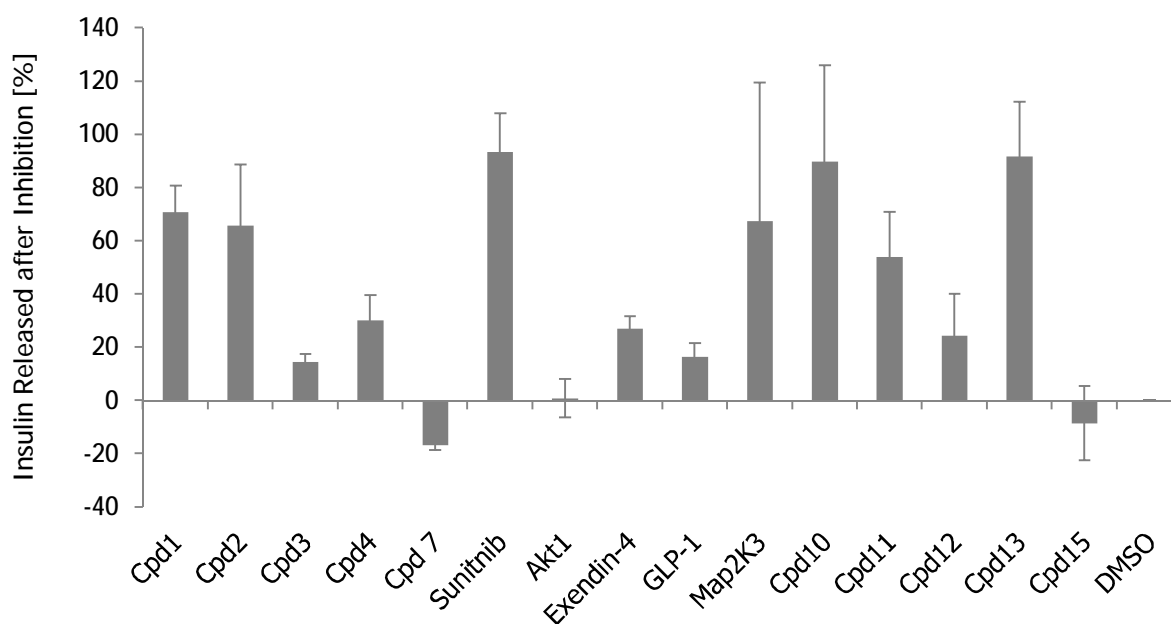
Figure R46 | *Insulin release in beta TC-6 cells upon various treatments. Scyl1 inhibitors (Cpd 10 – 14; 5 µM) as well as Grk5 inhibitors (Cpd 1 – 4; 5 µM) and their negative controls (Cpd 7, Cpd 15; 5 µM) were compared to sunitinib as well as AKT1-, MEKII inhibitors (10 µM each) and GLP-1 and Exendin-4 (20 µg/ml each)*

The revealed inhibitors for Grk5 and Scyl1 stimulated insulin released in the beta-TC6 cell system but their non-inhibiting controls did not. All used internal controls like MEK II, GLP-1 and Exendin-4 that should have displayed an increased insulin release, led to the expected effect while the AKT II inhibitor, which was expected to lead to a decrease of insulin, did not.

The Grk5 inhibitors (Cpd 1, Cpd 2), the Scyl1 inhibitors (Cpd 10, Cpd 11, Cpd 13) as well as sunitinib displayed the highest impact on insulin release, which ranged between 93.35 ± 14.42 % (Sunitinib) and 53.86 ± 17.04 % (Cpd 11). Unfortunatly, Tolbutamide and Glibenclamide displayed no effect.

Table R17 | *Insulin release after target inhibition of Scyl1, Grk5, Akt1, Map2K3 as well as Exendin-4 and GLP-1.*

Name	Inhibitor/Agonist	Conc.	Inulin Release [%]	SE [%]
Cpd 1	Grk5 Inh.	5µM	70.74	9.94
Cpd 2	Grk5 Inh.	5µM	65.67	22.92
Cpd 3	Grk5 Inh.	5µM	14.44	2.85
Cpd 4	Grk5 Inh.	5µM	30.13	9.49
Cpd 7	Grk5 non-Inh.	5µM	-16.75	2.03
Sutent	Pos.-control	5µM	93.35	14.42
Akt1	Akt1 Inh. II	10µM	0.75	7.15
Exendin-4	Glp-1 Agonist	20µg/ml	27.14	4.57
GLP-1	Glp-1 Agonist	20µg/ml	16.46	5.04
MEK	MAP2K3 Inh.	10µM	67.35	51.9
Cpd 10	Scyl1 Inh.	5µM	89.8	36.07
Cpd 11	Scyl1 Inh.	5µM	53.86	17.04
Cpd 12	Scyl1 Inh.	5µM	24.35	15.74
Cpd 13	Scyl1 Inh.	5µM	91.62	20.61
Cpd 15	Scyl1 non-Inh.	5µM	-8.54	13.98
DMSO	Control	5µM	0	0

6 DISCUSSION

6.1 KINASES AS ANTI-DIABETIC TARGET CANDIDATES

Type 2 diabetes is associated with impaired insulin sensitivity of peripheral tissues. Beside inherited factors, it is caused by several influences such as environmental stimuli, lifestyle, metabolic changes like pregnancy and puberty as well as ageing [64-67]. The observation that patients suffering from cancer as well as diabetes who were treated with imatinib or sunitinib became independent of insulin injections led to the hypothesis that diabetes-relevant signaling systems must include negatively regulating kinases, which directed our interest towards such sunitinib-sensitive targets in order to obtain the basis for the development of anti-diabetic drugs with pharmacological properties that are effective and side-effect poor [127, 128]. Thus, we investigated sunitinib, a multi-targeted receptor tyrosine kinase inhibitor approved for the treatment of metastatic renal cell carcinoma (mRCC), imatinib-resistant gastrointestinal stromal tumor (GIST) and pancreatic neuroendocrine tumors (NET) [216, 218], for its anti-diabetic impact *in vitro,* using C2C12 myoblast, 3T3-L1 pre-adipocytes as well as the insulinoma cell lines RIN-5AH-T2B (rat) and beta-TC6 (mouse) cells.

In 3T3-L1 pre-adipocytes, sunitinib led to an enhanced formation of adipocytes within a narrow concentration window, suggesting a first clue for a potential beneficial effect against diabetes. A similar observation of increased differentiation and growth arrest during sunitinib treatment has been reported for monocyte differentiation in acute myelogenous leukemia [255]. In addition to energy storage and enhanced uptake of glucose from the blood, adipose tissue is known to express and secrete a variety of hormones like resistin, leptin, adiponectin as well as visfatin. Furthermore, adipose tissue regulates cytokines and chemokines such as tumor necrosis factor-alpha (TNFa), interleukin-6 (IL6) and monocyte chemoattractant protein-1 (MCP-1) [279] with potential therapeutic roles for some of them [280]. Coming along with the previous results, the signal transducer and activator of transcription 3 (STAT3), the serine/threonine kinase Akt/PKB as well as the peroxisome

proliferator activated receptor gamma (PPARγ) are activated upon sunitinib treatment and support increased differentiation on the protein level. Phosphorylation of Akt/PKB, for example, leads, beside increased differentiation, to a GLUT4 translocation and thus increased glucose uptake [27]. Also of interest is PPARγ which is predominantly expressed in adipose tissue and mediates activation of a number of genes that in turn increase lipid- and glucose uptake as well as oxidation. Furthermore, PPARγ is connected to the decreases of free fatty acid concentration as well as insulin resistance [103, 105]. Already available drugs like thiazolidinediones (TZD) have been in use for the treatment of type 2 diabetes by activating PPARs and subsequently inducing carbohydrate homeostasis by sensitizing the peripheral tissues. However, they have also displayed enormous side effects, which are strongly associated with heart failure [281] as well as induction of cancer [282] and are therefore prescribed with caution. Surprisingly, sunitinib displayed a concentration dependent increase of PPARγ expression and subsequently could be a starting point for further developments of PPAR treatment of type 2 diabetes.

In parallel, sunitinib led to increased insulin release by insulinoma-derived cell lines like beta-TC6 and RIN-5AH-T2B. As several kinases have been already published to play important roles in insulin release such as MAP/ERK-kinases like MAP2K3, MAP3K9 and MAPK14 (p38), MAPK4 and MAPK7 which are involved in glucose homeostasis and insulin release [261] and calcium dependent kinases like CAMKK1 as well as CSNK2A1 [165, 172, 262] several prospects by sunitinib are possible. Furthermore, the effect of enhanced insulin secretion by sunitinib could be an explanation for the previously described observation of lowered blood glucose levels in sunitinib-treated cancer patients [122]. Important triggers of insulin secretion like the intrinsic insulin receptor (InsR), which mediates insulin feedback signaling in pancreatic beta cells in an autocrine way [139, 140], as well as protein kinases and substrates like IRS-1, PI3K, AKT/PKB, PKC, p38, JNK and ERK, which are related to insulin signaling, were investigated upon sunitinib treatment. Focusing on the decreased phosphorylation of the insulin receptor, the self-regulatory role of intrinsic pancreatic

receptors in our model system seems to be obvious [139, 140]. Most publications indicate a negative feedback loop driven by insulin in pancreatic beta cells [283-286], which would increase with the enhanced insulin release upon IGFR and IR inhibition by sunitinib. Though, some recent publications depict a controversial picture [140, 287]. However, following the downstream signaling via IRS-1, PI3K and Akt/PKB, we monitored an inhibition with increasing concentrations of sunitinib. In this case, the roles of IRS-1 and PI3K in pancreatic beta cells are more defined, suggesting that inhibition, reduction of gene expression or knock-out lead to an increased insulin release [288-290]. In line with these findings, Araujo *et al*. revealed that reduction of IRS-1 and IRS-2 protein expression in islets partially restored glucose-induced insulin secretion [291]. Furthermore, wortmannin, a highly selective inhibitor of PI3K, has been reported to enhance insulin secretion [292, 293] thus indicating a possible improvement of insulin release due to sunitinib treatment. In contrast, active Akt/PKB seems to be required for enhanced insulin release [261, 265, 266, 294] but is inhibited by sunitinib in our model system. An additional interesting fact is the increased phosphorylation of p38/MAPK14 and PKCδ. p38, which is known as trigger for insulin release due to activation of PDK1 [276], displayed an increased phosphorylation after sunitinib treatment. Moreover, the protein kinase C (PKC) which has been shown to be active and effective in the maintenance of the phosphorylation state of the voltage-gated L-type calcium-channels enabling an appropriate function of this channel in insulin secretion [259, 260] is slightly increased upon sunitinib treatment.

In summary, the negative feedback loop due to the beta-cell insulin receptor as well as the increase of PKC and p38 phosphorylation possibly explains the increased amount of insulin released by insulinoma cells after TKI treatment. But thinking of the properties of sunitinib as multiple kinase inhibitor which inhibits more than 300 putative kinase targets [138], multiple mechanisms to trigger insulin release by negatively regulating kinases and non-kinases, become possible. In order to reveal new negatively regulated kinases which display increased insulin release after inhibition, we investigated a kinome wide siRNA screen. We

detected various already known kinase family members of MAP/ERK-kinases like MAP2K1, MAP2K3, MAP3K1, MAP3K9, MAPK14 (p38), MAPK4 and MAPK7, which play an important role in glucose homeostasis and insulin release [261], as well as calcium dependent kinases like CAMK1, CAMK1D, CAMKK1, CSNK2A1, CSNK2A2 and CSNK2B, which have also been connected to insulin release [165, 172, 262]. Moreover, kinases involved in the inositol phosphate metabolism (e.g. ITPKA, ITPKB, GRK5 and GRK6), respectively the PDGF signaling (e.g. CSNK2A1, JAK2 of MAP-Kinases), have been detected and revealed some known and some new positively and negatively regulating kinases. Already published kinases e.g. JAK1, AKT1 and MAPK13 were announced as internal assay controls for positively regulating kinases. JAK1 together with STAT activates glucokinase activity as well as up-regulation of insulin genes and beta-cell proliferation [295]. Furthermore, prolactin receptor (PRLR) mediated activation of JAK/STAT activation has been connected to increased insulin release [296] which in turn should lead to a decrease after inhibition. AKT1 and MAPK13, which are key-regulators of glucose induced insulin secretion by positively affecting GLUT4 translocation to the membrane [146, 266], decrease the amount of insulin released by beta-TC6 cells. The connection of PRKCN (PKCs), PIK3C3 (PI3Ks) and MAP2K3 (MAP-Kinases), have not been published yet but corresponding family members play an important role in insulin secretion [145, 260, 266]. Furthermore, CSNK2A1 was already published to be a negatively regulator in insulin release [172, 267]. However, focusing on new negatively regulating kinases which display enhanced insulin release upon inhibition, we present Scyl1, Gprk5, Adck1 and EphA4 as new potential targets for triggering insulin release as well as therapeutic anti-diabetes targets.

Human Scyl1/NTKL is closely related to the mouse NTKL homolog (max. ident. 94 %) and was originally displayed as an Akt/PKB interacting factor in 3T3-L1 adipocytes [297]. Although it was later determined that Scyl1 does not associate with Akt/PKB, the presence of a kinase-like domain which seems to have no kinase activity suggests a possibly negatively regulating kinase by competing with a particular kinase for binding to its upstream kinase

thus interfering with downstream signaling [297]. Mass spectrometry analysis monitored Scyl1/NTK in co-localization to the cis-golgi, the ER-golgi intermediate compartment and where it binds to the Coatomer I (COPI) [298]. Furthermore, it affects ARF, the small GTPase ADP-ribosylation factor 1, which is a key regulator of intracellular membrane traffic due to the KDEL receptor [299]. While SCYL1 appears to have no active kinase domain *in vitro*, it contains HEAT repeats which are involved in intracellular transport [300]. An independent study revealed SCYL1 in a siRNA screen of the human kinome in which it was scored for endocytosis effects [301]. Moreover, the family member Scyl2/CVAK104 has been monitored to act on endocytosis of cell surface proteins by binding clathrin and the plasma membrane adaptor complex, AP2 [302]. Nevertheless, the function and mode of action of Scyl1/NTKL remain elusive.

Grk5 encodes a guanine nucleotide binding protein (G protein)-coupled receptor kinase, which is a member of the protein kinase superfamily, AGC Ser/Thr protein kinase family and GRK subfamily and is acting by specifically phosphorylating agonist-occupied G-protein-coupled receptors on the cytoplasmic loop and C-terminus of the receptors, leading to receptor desensitization [303]. In general, GRK phosphorylated receptors display a high affinity binding of arrestin, which induces receptor internalization and thus feed-back inhibits GPCR responses to extracellular signals [304, 305]. Grk5 has also been connected to IkappaB alpha and NFkappaB signaling [306], here over-expression of Grk5 causes nuclear accumulation of IkappaB alpha, which in turn leads to the inhibition of NFkappaB transcriptional activity. Opposite results are achieved by Grk5 knock-down through siRNA [307]. Both, IkappaB alpha and NFkappaB, are involved in glucose-stimulated insulin secretion of pancreatic beta cells [306, 308]. Interestingly, another family member of GRKs, Grk2, has been connected to GIP-induced insulin release in beta-TC3 cells, where expression of Grk2 attenuated GIP-induced insulin release and cAMP production, whereas glucose-stimulated insulin secretion was not affected [309]. Grk2 can also form a complex with IRS-1 and regulate insulin signaling in skeletal muscle and adipose tissues [310-312]. Additionally,

Grk5 has been associated to single trans membrane low density lipoprotein receptor-related protein 6 (LRP6), where Grk5 directly phosphorylates the PPPSP motifs on LRP6 and thus regulates Wnt/LRP6 signaling [313]. In contrast, reduction of Grk5 gene expression reduces Wnt3A-stimulated LRP6 phosphorylation. Wnt signaling in turn regulates adipogenesis and its activity has been implicated in the pathogenesis of type 2 diabetes and metabolic syndrome [314]. *LRP6* $^{+/-}$ mice which have impaired Wnt signaling displayed reduced body fat mass, diminished hepatic gluconeogenesis as well as enhanced BAT and hepatic insulin sensitivity [315]. Grk5 inhibition, reduction of gene expression or knock out led to a similar phenotype [316], possibly offering an explanation for the mode of action. However, supported by recent observations that Grk5 deficient mice display a decreased level of lipid metabolism and adipogenic gene transcripts in WAT, MEFs, and pre-adipocytes derived from SVFs of GRK5$^{-/-}$ mice, lean corpora after high fat diet (HFD) condition, a large decrease in white adipose tissue (WAT) as well as increased Grk5 mRNA levels during differentiation and increased expression of PPAR-γ, adiponectin, aP2, C/EBPβ, and C/EBPγ after Grk5-overexpressing 3T3-L1 cells [316] and the detection of Grk5 as diabetic loci in Chinese Hans [317], we are highlighting Grk5 as negative regulator of insulin release and glucose uptake.

The aarF domain containing kinase 1 (Adck1) is a member of the Adck protein kinase family and belongs to the class atypical kinases with a protein kinase domain (STYKc). In humans, the Adck family encloses five isoforms (Adck1-5). Whereas Adck3 and Adck4 are highly similar and seem to derive from a gene duplication in vertebrates, Adck1, Adck2 and Adck5, in contrast, seem to have split from Adck3 and 4 very early during evolution, highlighting that all eukaryotes and several, but not all, gram-negative bacteria possess at least one representative of each subgroup [318]. Yeast ABC1/Coq8 is the ortholog of ADCK3 and 4, whereas bacterial UbiB is more similar to the ADCK1–ADCK5 subgroup. The universal core structure of ADCKs comprises a highly conserved lysine that binds the alpha phosphate and two highly conserved aspartates that bind the magnesium ions chelated by ATP. Moreover, all ADCK proteins share a common N-terminal domain (with invariable residues Lys276,

Glu278, and Gln279), which is absent from all other protein and non-protein kinases and appears specifically related with ubiquinone metabolism [318]. However, due to the lack of information concerning Adck1, we postulate an anti-diabetic effect by increasing insulin release in beta-TC6 cells, while the mechanism remains elusive.

The ephrin receptor A4 (EphA4) belongs to the ephrin receptor subfamily and is involved in various aspects of cell-cell communication [319, 320]. Recently, Ephrin-EphA interactions have been connected to be mediators in the insulin secretion pathway by providing beta-cell communication via ephrin-As and EphAs [321]. Here, the proposed model suggests two modes of action: a) at a low glucose concentration, EphA forward signaling is predominant and suppresses insulin secretion, b) at a high glucose concentration, EphAs are dephosphorylated via PTP activity, which shifts the balance from EphA forward signaling toward ephrin-A reverse signaling, which enhances insulin secretion [321]. EphA4 is involved in the PIP2/PIP3 signaling as well as GDP/GTP exchange, both connected to regulate insulin secretion in pancreatic beta cells [322, 323]. Moreover, EphA4 leads to a transient activation of MAP-kinases, which has also been connected to insulin secretion. Genome-wide association studies (GWASs) and expression quantitative trait loci (eQTL) analyses of type 2 diabetes in Mexican population identified Epha4 SNPs as risk loci for type 2 diabetes in muscle and adipose tissues [324]. In line with this finding, we detected an insulin release increase after gene depletion and therefore we a propose EphA4 as a possible anti-diabetic target.

Recommending Scyl1, Gprk5, Adck1 and EphA4 as new negatively regulating kinases in triggering insulin release, we investigated parameters like insulin release after parallel reduction of gene expression, insulin secretion in a low glucose environment (prevention of hypoglycemia), glucose uptake, Akt/PKB phosphorylation, and connection of mRNA levels after sunitinib treatment as well as target binding affinity to sunitinib.

The double knock-down, including that of Csnk2A1 as a positive control [267, 325], revealed three possible kinase pairs (Scyl1 and Adck1; Adck1 and EphA4 and Csnk2A1 and EphA4) out

of ten possible combinations which displayed additive effects on insulin release. This indicates that Scyl1 and Adck1; Adck1 and EphA4 and Csnk2A1 and EphA4, respectively, are involved in different signaling cascades of insulin release and thus could lead to beneficial effects. Regarding the requirements of an anti-diabetic target to prevent hypoglycemia [326], we tested if the identified negatively regulating kinases were glucose dependent. After a 1.125 mM glucose treatment, we monitored a slight decrease of insulin release after reduction of gene expression for the three most promising candidates Scyl1, Gprk5 and Adck1 in low glucose media, suggesting that the kinases themselves are glucose dependent, inversely triggering factors of insulin signaling and as a result should prevent hypoglycemia. In contrast to already used sulfonylureas that carry the side-effect to induce hypoglycemia [111], the targets should have a more promising safety profile. Focusing on peripheral tissue like muscles (C2C12 cells) and adipose tissue (3T3-L1 cells), we examined significantly improved glucose uptake upon gene depletion for Grk5 and, however more slightly but insignificantly for Scyl1 and Adck1. The identified targets also seem to act on peripheral tissue by improving glucose uptake by a so far elusive mechanism, proposing a second anti-diabetic mode of action comparable to Metformin [98]. The enhanced glucose uptake, also displayed in beta-TC6 cells for Scyl1 and Grk5 inhibitors, could be an explanation for the increased insulin release due to increased glucose metabolism. Interestingly, reduction of Gprk2 has been recently linked to play a significant role in mediating desensitization of the glucose-dependent insulin-tropic polypeptide receptor (GIPR) function, which has been connected to display reduced GIP-stimulated insulin release in the rat by elevated serum GIP levels [309, 327]. Focusing on Akt/PKB phosphorylation which is connected to GLUT4 translocation and increased glucose uptake [27, 261, 266], we monitored a clearly increased phosphorylation level of Akt/PKB after reduction of gene expression of Scyl1 and Gprk5. This coincides with the previously described observation of 2-NBDG uptake and insulin release and supports the data of glucose dependent mode of action for both targets. Nevertheless, the exact role of Grk5 still remains elusive.

Beside the influence of the identified targets Scly1, Gprk5, Adck1 and EphA4 on beta-TC6, C2C12 and 3T3-L1 cells, we were able to connect the targets or their family members to the multiple-kinase inhibitor sunitinib by a KINOMEscan[TM], suggesting a more or less equal binding for the targets themselves. Here, EphA4 as well as the Adck1 family members Adck3 and Adck4 displayed a low sunitinib binding efficiency, whereas the Gprk5 family members Gprk1, Gprk4 and Gprk7 depicted a high sunitinib binding efficiency. The inhibition of Scyl1 was determined in parallel to the compound library screen with a rather low efficiency. However, as sunitinib has been revealed to be a rather unspecific kinase inhibitor, a combined effect as displayed for the double knock down of target candidates due to multi kinase inhibition seems to be possible. In addition to the direct inhibition of the target candidates by sunitinib, we monitored decreased mRNA levels after 24 h for all of them, offering a second mode of action of sunitinib by chronically reducing mRNA levels.

6.2 SCYL1 INHIBITOR COMPOUNDS AS ANTI-DIABETIC DRUGS

As Scyl1 appeared to have no active kinase domain *in vitro* [300] and phosphorylation of substrates, respectively auto-phosphorylation, have not been observed, no enzymatic assay could be established. In order to identify compounds that bind to Scyl1 and subsequently inhibit interaction with other proteins, a Scyl1 binding assay based on the Proteros Reporter Displacement Technology was established. For cell based assays we chose five Scyl1 inhibitors, ranging between 92 – 100 % inhibition and an IC_{50}-value of 0.5 – 3.0 µM, as well as non-inhibiting structures as controls. Likewise to the previously performed knock-down of Scyl1, the inhibition by selected compound structures displayed a concentration dependent increase in insulin released up to the 3-fold (Cpd 10) to the DMSO treated control, which was even stronger than the previously observed effect upon reduction of target gene expression. A similar effect for non-inhibiting control compounds was not monitored. The observed increased release of insulin in a high glucose 4.5 mM (81 mg/dL) media was not detectable

in a low glucose 1.125 mM (20 mg/dL) environment; rendering Scyl1 inhibitors as glucose dependent agents for insulin release that might also prevent hypoglycemia. Interestingly, an insulin independent uptake of 2-NBDG after Scyl1 inhibitor treatment was monitored. Investigating peripheral tissue models *in vitro*, inhibition of Scyl1 by the identified compound structures displayed a significant increase of 2-NBDG in C2C12 and beta-TC6 cells, while the negative control compounds did not. Due to the non-inhibiting control compounds in glucose uptake and insulin release, we assumed a target specific effect. However, regarding the different core structures of Scyl1 inhibitors and non-inhibitors, an unspecific compound based impact could not be excluded. In general, the enhanced insulin release could possibly be explained by simulating higher external glucose levels due to improved glucose uptake after target inhibition or reduction of target gene expression. Meeting the impact of the compound structures on inhibition of proliferation and thus toxicology characteristics, we detected a controversial picture for C2C12 and beta-TC6 cells, probably caused by the different doubling times of beta-TC6 (36 - 48 h) [274] and C2C12 (~ 13 h) [275] cells. Nevertheless, compound structures 10, 11 and 12, respectively, have the less toxic influence on proliferation but still need to be further investigated due to a hit to lead conversion and animal models. In summary, the compound structures 10, 11 and 12 are the most promising Scyl1 inhibitors which increase the uptake of 2-NBDG glucose analog as well as, dependent or independent, increase the release of insulin without causing hypoglycemia. Thus, targeting Scyl1 possibly combines the benefits of peripheral tissue sensitizing like e.g. with Metformin as well as improving the release of insulin like e.g. sulfonylureas and consequently is a promising new objective for the treatment of type 2 diabetes.

6.3 GRK5 INHIBITOR COMPOUNDS AS ANTI-DIABETIC DRUGS

Grk5, respectively the mouse homolog Gprk5 (max. ident. 96 %), encodes for a guanine nucleotide-binding protein (G protein)-coupled receptor kinase and acting by specifically phosphorylating agonist-occupied G protein-coupled receptors on the cytoplasmic loops and C terminus of the receptors. Despite the fact that Grk5 is a well characterized kinase, the connection to diabetes was not investigated so far. However, the first indication of the impact of Grk5 was published this year, connecting GRK5$^{-/-}$ deficient mice to improved fat metabolism and balance [316]. In parallel, we revealed Grk5 as negative regulator of insulin release as well as glucose uptake. In order to identify compounds that inhibit Grk5 phosphorylation, an ADP Glo™ Kinase Assay for Grk5 was established. For cell based assays, we decided on five Grk5 inhibitors, ranging between 51 – 68 % inhibition and an IC50-value of 71 – 111 µM, as well as non-inhibiting structures. In spite of the high IC50-values, we could display a cellular assay based effect for 5 µM, which could be explained by enhanced membrane transfer of the compound, improved solvation as well as possible unspecific binding as demonstrated for Scyl1, here highlighting compound structures 3 and 4. The identified compounds displayed a clear concentration dependent increase of insulin release after inhibiting Grk5, whereas the non-inhibiting control compounds did not. Even more significantly than upon Scyl1 inhibitor treatment, the observed increased release of insulin in high glucose 4.5 mM (81 mg/dL) media was not detectable in low glucose 1.125 mM (20 mg/dL) media. Moreover, the release of insulin was down-regulated after Grk5 inhibitor treatment to one-tenth compared to the DMSO control, suggesting a mechanism activation of Grk5 by high glucose levels that due to inhibition led to an increased insulin release, respectively, a deactivation or basal activity of Grk5 in low glucose environment, enhanced by Grk5 inhibitors that led to a decrease in insulin release. Furthermore, the improved 2-NBDG uptake seemed to be insulin independent. Testing the peripheral tissue for glucose uptake by Grk5 inhibitor compounds, we obtained an equal picture as for the Scyl1 inhibitors. Grk5 inhibitor compounds 1 – 3 displayed a significant increase in 2-NBDG uptake,

which inclines with the previously described insulin release and supports the hypothesis of improved insulin release due to increased glucose sensitization.

Due to a missing kinase profile for the most promising structures of both targets, we cannot tell if the effect of an improved glucose uptake via 2-NBDG was based on the targets Grk5 and Scyl1. Thinking of the high background fluorescence of the non-inhibitor structures, a compound related effect could be assumed. But as the reduction of target gene expression led to an increased uptake of 2-NBDG as well and the no insulin release in beta-TC6 cells was monitored for the non-inhibitor controls, we propose a target specific effect. Focusing on the toxicological effect of the used Grk5 inhibitors, we observed an impaired proliferation for all compound structures but compound 5, which in turn had not displayed any effect on glucose uptake or insulin secretion. If this toxic side effect is based on the structures or the inhibition of Grk5 itself, needs to be further investigated. Structure based toxicity should be covered by a hit to lead conversion and animal models. In conclusion, the compound structures 1, 2 and 3 are the most promising Grk5 inhibitors, that increase the uptake of 2-NBDG glucose analog as well as increase the release of insulin without causing hypoglycemia. Like Scyl1, Grk5 possibly combines the benefits of peripheral tissue sensitizing like Metformin as well as improving the release of insulin like sulfonylureas. Grk5 is therefore a promising new target for the development of novel treatments for type 2 diabetes.

7 LITERATURE

1. Paul, L., Beitrage zur mikroscopischen Anatomie der Bauchspeicheldrüse. Inaugural-dissertation Gustav Lange University Berlin, 1869

2. Karamitsos, D.T., The story of insulin discovery. Diabetes Res Clin Pract, 2011. 93 Suppl 1: p. S2-8.

3. Murray, I., Paulesco and the isolation of insulin. J Hist Med Allied Sci, 1971. 26(2): p. 150-7.

4. Sanger, F., Some chemical investigations on the structure of insulin. Cold Spring Harb Symp Quant Biol, 1950. 14: p. 153-60.

5. Ullrich, A., et al., Rat insulin genes: construction of plasmids containing the coding sequences. Science, 1977. 196(4296): p. 1313-9.

6. Villa-Komaroff, L., et al., A bacterial clone synthesizing proinsulin. Proc Natl Acad Sci U S A, 1978. 75(8): p. 3727-31.

7. Crea, R., et al., Chemical synthesis of genes for human insulin. Proc Natl Acad Sci U S A, 1978. 75(12): p. 5765-9.

8. Sures, I., et al., Nucleotide sequence of human preproinsulin complementary DNA. Science, 1980. 208(4439): p. 57-9.

9. Genentech, First Successful Laboratory Production of Human Insulin. Genentech Press Release, 1978.

10. Edition, I.D.A.t., IDF Diabetes Atlas 4th edition. 2009.

11. Centre, W.M., Diabetes: Key facts. Fact sheet N°312, 2011.

12. Kahn, S.E., R.L. Hull, and K.M. Utzschneider, Mechanisms linking obesity to insulin resistance and type 2 diabetes. Nature, 2006. 444(7121): p. 840-6.

13. MacDonald, P.E., J.W. Joseph, and P. Rorsman, Glucose-sensing mechanisms in pancreatic beta-cells. Philos Trans R Soc Lond B Biol Sci, 2005. 360(1464): p. 2211-25.

14. Schuit, F.C., et al., Glucose sensing in pancreatic beta-cells: a model for the study of other glucose-regulated cells in gut, pancreas, and hypothalamus. Diabetes, 2001. 50(1): p. 1-11.

15. Saltiel, A.R. and C.R. Kahn, Insulin signalling and the regulation of glucose and lipid metabolism. Nature, 2001. 414(6865): p. 799-806.

16. Pessin, J.E. and A.R. Saltiel, Signaling pathways in insulin action: molecular targets of insulin resistance. J Clin Invest, 2000. 106(2): p. 165-9.

17. Boulton, T.G., et al., ERKs: a family of protein-serine/threonine kinases that are activated and tyrosine phosphorylated in response to insulin and NGF. Cell, 1991. 65(4): p. 663-75.

18. Chiang, S.H., et al., Insulin-stimulated GLUT4 translocation requires the CAP-dependent activation of TC10. Nature, 2001. 410(6831): p. 944-8.

19. Kessler, A., et al., Diversification of cardiac insulin signaling involves the p85 alpha/beta subunits of phosphatidylinositol 3-kinase. Am J Physiol Endocrinol Metab, 2001. 280(1): p. E65-74.

20. Lazar, D.F., et al., Mitogen-activated protein kinase kinase inhibition does not block the stimulation of glucose utilization by insulin. J Biol Chem, 1995. 270(35): p. 20801-7.

21. Lietzke, S.E., et al., Structural basis of 3-phosphoinositide recognition by pleckstrin homology domains. Mol Cell, 2000. 6(2): p. 385-94.

22. Mackay, D.J. and A. Hall, Rho GTPases. J Biol Chem, 1998. 273(33): p. 20685-8.

23. Toker, A., Protein kinases as mediators of phosphoinositide 3-kinase signaling. Mol Pharmacol, 2000. 57(4): p. 652-8.

24. Ziegler, S.F., et al., Molecular cloning and characterization of a novel receptor protein tyrosine kinase from human placenta. Oncogene, 1993. 8(3): p. 663-70.

25. Cho, H., et al., Insulin resistance and a diabetes mellitus-like syndrome in mice lacking the protein kinase Akt2 (PKB beta). Science, 2001. 292(5522): p. 1728-31.

26. Cho, H., et al., Akt1/PKBalpha is required for normal growth but dispensable for maintenance of glucose homeostasis in mice. J Biol Chem, 2001. 276(42): p. 38349-52.

27. Kohn, A.D., et al., Expression of a constitutively active Akt Ser/Thr kinase in 3T3-L1 adipocytes stimulates glucose uptake and glucose transporter 4 translocation. J Biol Chem, 1996. 271(49): p. 31372-8.

28. Park, S.Y., et al., Crystal structures of Human TBC1D1 and TBC1D4 (AS160) RabGAP domains reveal critical elements for GLUT4 translocation. J Biol Chem, 2011.

29. Bandyopadhyay, G., et al., Dependence of insulin-stimulated glucose transporter 4 translocation on 3-phosphoinositide-dependent protein kinase-1 and its target threonine-410 in the activation loop of protein kinase C-zeta. Mol Endocrinol, 1999. 13(10): p. 1766-72.

30. Standaert, M.L., et al., RO 31-8220 activates c-Jun N-terminal kinase and glycogen synthase in rat adipocytes and L6 myotubes. Comparison to actions of insulin. Endocrinology, 1999. 140(5): p. 2145-51.

31. Desbois-Mouthon, C., et al., Insulin differentially regulates SAPKs/JNKs and ERKs in CHO cells overexpressing human insulin receptors. Biochem Biophys Res Commun, 1998. 243(3): p. 765-70.

32. Miller, B.S., et al., Activation of cJun NH2-terminal kinase/stress-activated protein kinase by insulin. Biochemistry, 1996. 35(26): p. 8769-75.

33. Wild, S., et al., Global prevalence of diabetes: estimates for the year 2000 and projections for 2030. Diabetes Care, 2004. 27(5): p. 1047-53.

34. Association, A.D., Summary of revisions for the 2010 Clinical Practice Recommendations. Diabetes Care, 2010. 33 Suppl 1: p. S3.

35. Alberti, K.G. and P.Z. Zimmet, Definition, diagnosis and classification of diabetes mellitus and its complications. Part 1: diagnosis and classification of diabetes mellitus provisional report of a WHO consultation. Diabet Med, 1998. 15(7): p. 539-53.

36. ASSOCIATION, A.D., Gestational diabetes mellitus. Diabetes Care, 2004. 27 Suppl 1: p. S88-90.

37. Reaven, G.M., Banting lecture 1988. Role of insulin resistance in human disease. Diabetes, 1988. 37(12): p. 1595-607.

38. Usher-Smith, J.A., et al., Factors associated with the presence of diabetic ketoacidosis at diagnosis of diabetes in children and young adults: a systematic review. BMJ, 2011. 343: p. d4092.

39. Foulis, A.K., et al., The histopathology of the pancreas in type 1 (insulin-dependent) diabetes mellitus: a 25-year review of deaths in patients under 20 years of age in the United Kingdom. Diabetologia, 1986. 29(5): p. 267-74.

40. Gepts, W. and P.M. Lecompte, The pancreatic islets in diabetes. Am J Med, 1981. 70(1): p. 105-15.

41. Redondo, M.J., et al., Genetic determination of islet cell autoimmunity in monozygotic twin, dizygotic twin, and non-twin siblings of patients with type 1 diabetes: prospective twin study. BMJ, 1999. 318(7185): p. 698-702.

42. Verge, C.F., et al., Late progression to diabetes and evidence for chronic beta-cell autoimmunity in identical twins of patients with type I diabetes. Diabetes, 1995. 44(10): p. 1176-9.

43. Dean L, M.J., The Genetic Landscape of Diabetes. National Center for Biotechnology Information (US), 2004.

44. Todd, J.A., J.I. Bell, and H.O. McDevitt, HLA-DQ beta gene contributes to susceptibility and resistance to insulin-dependent diabetes mellitus. Nature, 1987. 329(6140): p. 599-604.

45. Bosi, E., et al., Mechanisms of autoimmunity: relevance to the pathogenesis of type I (insulin-dependent) diabetes mellitus. Diabetes Metab Rev, 1987. 3(4): p. 893-923.

46. Cucca, F., et al., A correlation between the relative predisposition of MHC class II alleles to type 1 diabetes and the structure of their proteins. Hum Mol Genet, 2001. 10(19): p. 2025-37.

47. Todd, J.A., et al., Robust associations of four new chromosome regions from genome-wide analyses of type 1 diabetes. Nat Genet, 2007. 39(7): p. 857-64.

48. Steck, A.K., et al., Association of non-HLA genes with type 1 diabetes autoimmunity. Diabetes, 2005. 54(8): p. 2482-6.

49. Bennett, S.T., et al., Susceptibility to human type 1 diabetes at IDDM2 is determined by tandem repeat variation at the insulin gene minisatellite locus. Nat Genet, 1995. 9(3): p. 284-92.

50. Bennett, S.T. and J.A. Todd, Human type 1 diabetes and the insulin gene: principles of mapping polygenes. Annu Rev Genet, 1996. 30: p. 343-70.

51. Vafiadis, P., et al., Class III alleles of the variable number of tandem repeat insulin polymorphism associated with silencing of thymic insulin predispose to type 1 diabetes. J Clin Endocrinol Metab, 2001. 86(8): p. 3705-10.

52. Kristiansen, O.P., Z.M. Larsen, and F. Pociot, CTLA-4 in autoimmune diseases--a general susceptibility gene to autoimmunity? Genes Immun, 2000. 1(3): p. 170-84.

53. Marron, M.P., et al., Insulin-dependent diabetes mellitus (IDDM) is associated with CTLA4 polymorphisms in multiple ethnic groups. Hum Mol Genet, 1997. 6(8): p. 1275-82.

54. Nistico, L., et al., The CTLA-4 gene region of chromosome 2q33 is linked to, and associated with, type 1 diabetes. Belgian Diabetes Registry. Hum Mol Genet, 1996. 5(7): p. 1075-80.

55. Fairweather, D. and N.R. Rose, Type 1 diabetes: virus infection or autoimmune disease? Nat Immunol, 2002. 3(4): p. 338-40.

56. Navratil, V., et al., When the human viral infectome and diseasome networks collide: towards a systems biology platform for the aetiology of human diseases. BMC Syst Biol, 2011. 5: p. 13.

57. Strycharz, M., K. Bartecka, and M. Polz-Dacewicz, The role of viruses in the etiopathogenesis of diabetes mellitus. Ann Univ Mariae Curie Sklodowska Med, 2004. 59(1): p. 257-60.

58. Saudek, F., et al., [Islet transplantation for treatment of type-1 diabetes mellitus]. Cas Lek Cesk, 2011. 150(1): p. 49-55.

59. Almind, K., A. Doria, and C.R. Kahn, Putting the genes for type II diabetes on the map. Nat Med, 2001. 7(3): p. 277-9.

60. Bonnefond, A., P. Froguel, and M. Vaxillaire, The emerging genetics of type 2 diabetes. Trends Mol Med, 2010. 16(9): p. 407-16.

61. Ounissi-Benkalha, H. and C. Polychronakos, The molecular genetics of type 1 diabetes: new genes and emerging mechanisms. Trends Mol Med, 2008. 14(6): p. 268-75.

62. Glamoclija, U. and A. Jevric-Causevic, Genetic polymorphisms in diabetes: influence on therapy with oral antidiabetics. Acta Pharm, 2010. 60(4): p. 387-406.

63. Weedon, M.N., et al., Combining information from common type 2 diabetes risk polymorphisms improves disease prediction. PLoS Med, 2006. 3(10): p. e374.

64. Buchanan, T.A., et al., Insulin sensitivity and B-cell responsiveness to glucose during late pregnancy in lean and moderately obese women with normal glucose tolerance or mild gestational diabetes. Am J Obstet Gynecol, 1990. 162(4): p. 1008-14.

65. Casey, G., The glucose [corrected] disease--understanding type 2 diabetes mellitus. Nurs N Z, 2011. 17(2): p. 16-21.

66. Defronzo, R.A., Glucose intolerance and aging: evidence for tissue insensitivity to insulin. Diabetes, 1979. 28(12): p. 1095-101.

67. Moran, A., et al., Insulin resistance during puberty: results from clamp studies in 357 children. Diabetes, 1999. 48(10): p. 2039-44.

68. Greenberg, A.S. and M.L. McDaniel, Identifying the links between obesity, insulin resistance and beta-cell function: potential role of adipocyte-derived cytokines in the pathogenesis of type 2 diabetes. Eur J Clin Invest, 2002. 32 Suppl 3: p. 24-34.

69. Scheen, A.J., From obesity to diabetes: why, when and who? Acta Clin Belg, 2000. 55(1): p. 9-15.

70. Wellen, K.E. and G.S. Hotamisligil, Inflammation, stress, and diabetes. J Clin Invest, 2005. 115(5): p. 1111-9.

71. Steppan, C.M., et al., The hormone resistin links obesity to diabetes. Nature, 2001. 409(6818): p. 307-12.

72. Boden, G., Role of fatty acids in the pathogenesis of insulin resistance and NIDDM. Diabetes, 1997. 46(1): p. 3-10.

73. Mohamed-Ali, V., et al., Subcutaneous adipose tissue releases interleukin-6, but not tumor necrosis factor-alpha, in vivo. J Clin Endocrinol Metab, 1997. 82(12): p. 4196-200.

74. Peraldi, P. and B. Spiegelman, TNF-alpha and insulin resistance: summary and future prospects. Mol Cell Biochem, 1998. 182(1-2): p. 169-75.

75. Kern, P.A., et al., Adipose tissue tumor necrosis factor and interleukin-6 expression in human obesity and insulin resistance. Am J Physiol Endocrinol Metab, 2001. 280(5): p. E745-51.

76. Scherer, P.E., Adipose tissue: from lipid storage compartment to endocrine organ. Diabetes, 2006. 55(6): p. 1537-45.

77. Psaltopoulou, T., I. Ilias, and M. Alevizaki, The role of diet and lifestyle in primary, secondary, and tertiary diabetes prevention: a review of meta-analyses. Rev Diabet Stud, 2010. 7(1): p. 26-35.

78. Raina Elley, C. and T. Kenealy, Lifestyle interventions reduced the long-term risk of diabetes in adults with impaired glucose tolerance. Evid Based Med, 2008. 13(6): p. 173.

79. Orozco, L.J., et al., Exercise or exercise and diet for preventing type 2 diabetes mellitus. Cochrane Database Syst Rev, 2008(3): p. CD003054.

80. Ripsin, C.M., H. Kang, and R.J. Urban, Management of blood glucose in type 2 diabetes mellitus. Am Fam Physician, 2009. 79(1): p. 29-36.

81. Lebovitz HE, V.A.D.A., Combination therapy for hyperglycemia. herapy for diabetes mellitus and related disorders, 3rd ed., 1998. 211–9.

82. Lebovitz, H.E., Type 2 diabetes: an overview. Clin Chem, 1999. 45(8 Pt 2): p. 1339-45.

83. Metzger, B.E. and D.R. Coustan, Summary and recommendations of the Fourth International Workshop-Conference on Gestational Diabetes Mellitus. The Organizing Committee. Diabetes Care, 1998. 21 Suppl 2: p. B161-7.

84. Engelgau, M.M., et al., The epidemiology of diabetes and pregnancy in the U.S., 1988. Diabetes Care, 1995. 18(7): p. 1029-33.

85. Alexander, G.R., et al., A United States national reference for fetal growth. Obstet Gynecol, 1996. 87(2): p. 163-8.

86. Gloyn, A.L., Glucokinase (GCK) mutations in hyper- and hypoglycemia: maturity-onset diabetes of the young, permanent neonatal diabetes, and hyperinsulinemia of infancy. Hum Mutat, 2003. 22(5): p. 353-62.

87. Bjorkhaug, L., et al., Hepatocyte nuclear factor-1 alpha gene mutations and diabetes in Norway. J Clin Endocrinol Metab, 2003. 88(2): p. 920-31.

88. Yoshiuchi, I., et al., Analysis of a non-functional HNF-1alpha (TCF1) mutation in Japanese subjects with familial type 1 diabetes. Hum Mutat, 2001. 18(4): p. 345-51.

89. Fajans, S.S., G.I. Bell, and K.S. Polonsky, Molecular mechanisms and clinical pathophysiology of maturity-onset diabetes of the young. N Engl J Med, 2001. 345(13): p. 971-80.

90. Malecki, M.T., et al., Mutations in NEUROD1 are associated with the development of type 2 diabetes mellitus. Nat Genet, 1999. 23(3): p. 323-8.

91. Horikawa, Y., et al., Mutation in hepatocyte nuclear factor-1 beta gene (TCF2) associated with MODY. Nat Genet, 1997. 17(4): p. 384-5.

92. Stoffel, M. and S.A. Duncan, The maturity-onset diabetes of the young (MODY1) transcription factor HNF4alpha regulates expression of genes required for glucose transport and metabolism. Proc Natl Acad Sci U S A, 1997. 94(24): p. 13209-14.

93. Jonsson, J., et al., Insulin-promoter-factor 1 is required for pancreas development in mice. Nature, 1994. 371(6498): p. 606-9.

94. Banatvala, J.E., et al., Coxsackie B, mumps, rubella, and cytomegalovirus specific IgM responses in patients with juvenile-onset insulin-dependent diabetes mellitus in Britain, Austria, and Australia. Lancet, 1985. 1(8443): p. 1409-12.

95. Yoon, J.W., et al., Isolation of a virus from the pancreas of a child with diabetic ketoacidosis. N Engl J Med, 1979. 300(21): p. 1173-9.

96. Gamble, D.R. and K.W. Taylor, Seasonal incidence of diabetes mellitus. Br Med J, 1969. 3(5671): p. 631-3.

97. Hermann, L.S., Metformin: a review of its pharmacological properties and therapeutic use. Diabete Metab, 1979. 5(3): p. 233-45.

98. Klip, A. and L.A. Leiter, Cellular mechanism of action of metformin. Diabetes Care, 1990. 13(6): p. 696-704.

99. Zhou, G., et al., Role of AMP-activated protein kinase in mechanism of metformin action. J Clin Invest, 2001. 108(8): p. 1167-74.

100. Basu, R., et al., Effects of pioglitazone and metformin on NEFA-induced insulin resistance in type 2 diabetes. Diabetologia, 2008. 51(11): p. 2031-40.

101. Kim, Y.D., et al., Metformin inhibits hepatic gluconeogenesis through AMP-activated protein kinase-dependent regulation of the orphan nuclear receptor SHP. Diabetes, 2008. 57(2): p. 306-14.

102. Collier, C.A., et al., Metformin counters the insulin-induced suppression of fatty acid oxidation and stimulation of triacylglycerol storage in rodent skeletal muscle. Am J Physiol Endocrinol Metab, 2006. 291(1): p. E182-9.

103. Sohda, T., K. Meguro, and Y. Kawamatsu, Studies on antidiabetic agents. IV. Synthesis and activity of the metabolites of 5-[4-(1-methylcyclohexylmethoxy)benzyl]-2,4-thiazolidinedione (ciglitazone). Chem Pharm Bull (Tokyo), 1984. 32(6): p. 2267-78.

104. Auwerx, J., PPARgamma, the ultimate thrifty gene. Diabetologia, 1999. 42(9): p. 1033-49.

105. Dragica Soldo-Jureša, Ž.M., PPARγ – A NEW CONCEPT OF TREATMENT? Diabetologia Croatica, 2009. 38-2.

106. Moller, D.E., Potential role of TNF-alpha in the pathogenesis of insulin resistance and type 2 diabetes. Trends Endocrinol Metab, 2000. 11(6): p. 212-7.

107. Robinson, E. and D.J. Grieve, Significance of peroxisome proliferator-activated receptors in the cardiovascular system in health and disease. Pharmacol Ther, 2009. 122(3): p. 246-63.

108. Diez, J.J. and P. Iglesias, The role of the novel adipocyte-derived hormone adiponectin in human disease. Eur J Endocrinol, 2003. 148(3): p. 293-300.

109. Meirhaeghe, A., et al., A genetic polymorphism of the peroxisome proliferator-activated receptor gamma gene influences plasma leptin levels in obese humans. Hum Mol Genet, 1998. 7(3): p. 435-40.

110. Winkler, G. and L. Gero, [Pharmacogenetics of insulin secretagogue antidiabetics]. Orv Hetil, 2011. 152(41): p. 1651-60.

111. Wilensky, A.S., The Action of Sulfonylureas in Producing Hypoglycemia. Ala J Med Sci, 1964. 1: p. 83-91.

112. Gribble, F.M., et al., Tissue specificity of sulfonylureas: studies on cloned cardiac and beta-cell K(ATP) channels. Diabetes, 1998. 47(9): p. 1412-8.

113. Zawalich, W.S. and K.C. Zawalich, Glucagon-like peptide-1 stimulates insulin secretion but not phosphoinositide hydrolysis from islets desensitized by prior exposure to high glucose or the muscarinic agonist carbachol. Metabolism, 1996. 45(2): p. 273-8.

114. Zawalich, W.S., K.C. Zawalich, and H. Rasmussen, Influence of glucagon-like peptide-1 on beta cell responsiveness. Regul Pept, 1993. 44(3): p. 277-83.

115. Cvetkovic, R.S. and G.L. Plosker, Exenatide: a review of its use in patients with type 2 diabetes mellitus (as an adjunct to metformin and/or a sulfonylurea). Drugs, 2007. 67(6): p. 935-54.

116. Kerr, B.D., P.R. Flatt, and V.A. Gault, Effects of gamma-glutamyl linker on DPP-IV resistance, duration of action and biological efficacy of acylated glucagon-like peptide-1. Biochem Pharmacol, 2010. 80(3): p. 396-401.

117. McIntosh, C.H., et al., Dipeptidyl peptidase IV inhibitors: how do they work as new antidiabetic agents? Regul Pept, 2005. 128(2): p. 159-65.

118. Manning, G., Genomic overview of protein kinases. WormBook, 2005: p. 1-19.

119. Deininger, M., E. Buchdunger, and B.J. Druker, The development of imatinib as a therapeutic agent for chronic myeloid leukemia. Blood, 2005. 105(7): p. 2640-53.

120. Rini, B.I., et al., Hypothyroidism in patients with metastatic renal cell carcinoma treated with sunitinib. J Natl Cancer Inst, 2007. 99(1): p. 81-3.

121. Talpaz, M., et al., Dasatinib in imatinib-resistant Philadelphia chromosome-positive leukemias. N Engl J Med, 2006. 354(24): p. 2531-41.

122. Billemont, B., et al., Blood glucose levels in patients with metastatic renal cell carcinoma treated with sunitinib. Br J Cancer, 2008. 99(9): p. 1380-2.

123. Breccia, M., et al., Imatinib mesylate may improve fasting blood glucose in diabetic Ph+ chronic myelogenous leukemia patients responsive to treatment. J Clin Oncol, 2004. 22(22): p. 4653-5.

124. Breccia, M., et al., Fasting glucose improvement under dasatinib treatment in an accelerated phase chronic myeloid leukemia patient unresponsive to imatinib and nilotinib. Leuk Res, 2008. 32(10): p. 1626-8.

125. Costa, D.B. and M.S. Huberman, Improvement of type 2 diabetes in a lung cancer patient treated with Erlotinib. Diabetes Care, 2006. 29(7): p. 1711.

126. Tsapas, A., et al., Restoration of insulin sensitivity following treatment with imatinib mesylate (Gleevec) in non-diabetic patients with chronic myelogenic leukemia (CML). Leuk Res, 2008. 32(4): p. 674-5.

127. Veneri, D., M. Franchini, and E. Bonora, Imatinib and regression of type 2 diabetes. N Engl J Med, 2005. 352(10): p. 1049-50.

128. Templeton, A., et al., Remission of diabetes while on sunitinib treatment for renal cell carcinoma. Ann Oncol, 2008. 19(4): p. 824-5.

129. Oh, J.J., et al., Impact of sunitinib treatment on blood glucose levels in patients with metastatic renal cell carcinoma. Jpn J Clin Oncol, 2012. 42(4): p. 314-7.

130. Hagerkvist, R., et al., Imatinib mesylate (Gleevec) protects against streptozotocin-induced diabetes and islet cell death in vitro. Cell Biol Int, 2006. 30(12): p. 1013-7.

131. Hagerkvist, R., et al., Amelioration of diabetes by imatinib mesylate (Gleevec): role of beta-cell NF-kappaB activation and anti-apoptotic preconditioning. FASEB J, 2007. 21(2): p. 618-28.

132. Atkinson, M.A. and E.H. Leiter, The NOD mouse model of type 1 diabetes: as good as it gets? Nat Med, 1999. 5(6): p. 601-4.

133. Han, M.S., et al., Imatinib mesylate reduces endoplasmic reticulum stress and induces remission of diabetes in db/db mice. Diabetes, 2009. 58(2): p. 329-36.

134. Hagerkvist, R., L. Jansson, and N. Welsh, Imatinib mesylate improves insulin sensitivity and glucose disposal rates in rats fed a high-fat diet. Clin Sci (Lond), 2008. 114(1): p. 65-71.

135. Louvet, C., et al., Tyrosine kinase inhibitors reverse type 1 diabetes in nonobese diabetic mice. Proc Natl Acad Sci U S A, 2008. 105(48): p. 18895-900.

136. Kikuchi, Y., et al., A Rho-kinase inhibitor, fasudil, prevents development of diabetes and nephropathy in insulin-resistant diabetic rats. J Endocrinol, 2007. 192(3): p. 595-603.

137. Leiter, E.H., Multifactorial Control of Autoimmune Insulin-Dependent Diabetes in Nod Mice - Lessons for Ibd. Canadian Journal of Gastroenterology, 1995. 9(3): p. 153-159.

138. Bairlein, M., Characterization of the Small Molecule Kinase Inhibitor SU11248 (Sunitinib/SUTENT) in vitro and in vivo - Towards Response Prediction in Cancer Therapy with Kinase Inhibitors. PhD Thesis, 2010.

139. Kulkarni, R.N., Receptors for insulin and insulin-like growth factor-1 and insulin receptor substrate-1 mediate pathways that regulate islet function. Biochem Soc Trans, 2002. 30(2): p. 317-22.

140. Kulkarni, R.N., et al., Tissue-specific knockout of the insulin receptor in pancreatic beta cells creates an insulin secretory defect similar to that in type 2 diabetes. Cell, 1999. 96(3): p. 329-39.

141. Ueki, K., et al., Total insulin and IGF-I resistance in pancreatic beta cells causes overt diabetes. Nat Genet, 2006. 38(5): p. 583-8.

142. Engelman, J.A., J. Luo, and L.C. Cantley, The evolution of phosphatidylinositol 3-kinases as regulators of growth and metabolism. Nat Rev Genet, 2006. 7(8): p. 606-19.

143. Vanhaesebroeck, B., et al., The emerging mechanisms of isoform-specific PI3K signalling. Nat Rev Mol Cell Biol, 2010. 11(5): p. 329-41.

144. Kaneko, K., et al., Class IA phosphatidylinositol 3-kinase in pancreatic beta cells controls insulin secretion by multiple mechanisms. Cell Metab, 2010. 12(6): p. 619-32.

145. Sumara, G., et al., Regulation of PKD by the MAPK p38delta in insulin secretion and glucose homeostasis. Cell, 2009. 136(2): p. 235-48.

146. Koistinen, H.A., A.V. Chibalin, and J.R. Zierath, Aberrant p38 mitogen-activated protein kinase signalling in skeletal muscle from Type 2 diabetic patients. Diabetologia, 2003. 46(10): p. 1324-8.

147. de Alvaro, C., et al., Tumor necrosis factor alpha produces insulin resistance in skeletal muscle by activation of inhibitor kappaB kinase in a p38 MAPK-dependent manner. J Biol Chem, 2004. 279(17): p. 17070-8.

148. Kaneto, H., et al., Involvement of oxidative stress in the pathogenesis of diabetes. Antioxid Redox Signal, 2007. 9(3): p. 355-66.

149. Kaneto, H., et al., Involvement of oxidative stress and the JNK pathway in glucose toxicity. Rev Diabet Stud, 2004. 1(4): p. 165-74.

150. Kaneto, H., et al., Involvement of c-Jun N-terminal kinase in oxidative stress-mediated suppression of insulin gene expression. J Biol Chem, 2002. 277(33): p. 30010-8.

151. Kaneto, H., et al., Possible novel therapy for diabetes with cell-permeable JNK-inhibitory peptide. Nat Med, 2004. 10(10): p. 1128-32.

152. Hirosumi, J., et al., A central role for JNK in obesity and insulin resistance. Nature, 2002. 420(6913): p. 333-6.

153. Langelueddecke, C., et al., Effect of the AMP-kinase modulators AICAR, metformin and compound C on insulin secretion of INS-1E rat insulinoma cells under standard cell culture conditions. Cell Physiol Biochem, 2012. 29(1-2): p. 75-86.

154. Rutter, G.A. and I. Leclerc, The AMP-regulated kinase family: enigmatic targets for diabetes therapy. Mol Cell Endocrinol, 2009. 297(1-2): p. 41-9.

155. Viollet, B., et al., AMPK inhibition in health and disease. Crit Rev Biochem Mol Biol, 2010. 45(4): p. 276-95.

156. Towler, M.C. and D.G. Hardie, AMP-activated protein kinase in metabolic control and insulin signaling. Circ Res, 2007. 100(3): p. 328-41.

157. da Silva Xavier, G., et al., Role for AMP-activated protein kinase in glucose-stimulated insulin secretion and preproinsulin gene expression. Biochem J, 2003. 371(Pt 3): p. 761-74.

158. Leclerc, I., et al., Metformin, but not leptin, regulates AMP-activated protein kinase in pancreatic islets: impact on glucose-stimulated insulin secretion. Am J Physiol Endocrinol Metab, 2004. 286(6): p. E1023-31.

159. Tsuboi, T., et al., 5'-AMP-activated protein kinase controls insulin-containing secretory vesicle dynamics. J Biol Chem, 2003. 278(52): p. 52042-51.

160. Chang, T.J., et al., Serine-385 phosphorylation of inwardly rectifying K+ channel subunit (Kir6.2) by AMP-dependent protein kinase plays a key role in rosiglitazone-induced closure of the K(ATP) channel and insulin secretion in rats. Diabetologia, 2009. 52(6): p. 1112-21.

161. Dufer, M., et al., Activation of the AMP-activated protein kinase enhances glucose-stimulated insulin secretion in mouse beta-cells. Islets, 2010. 2(3): p. 156-63.

162. Wang, C.Z., et al., 5-amino-imidazole carboxamide riboside acutely potentiates glucose-stimulated insulin secretion from mouse pancreatic islets by KATP channel-dependent and -independent pathways. Biochem Biophys Res Commun, 2005. 330(4): p. 1073-9.

163. Wollheim, C.B. and P. Maechler, Beta-cell mitochondria and insulin secretion: messenger role of nucleotides and metabolites. Diabetes, 2002. 51 Suppl 1: p. S37-42.

164. Easom, R.A., CaM kinase II: a protein kinase with extraordinary talents germane to insulin exocytosis. Diabetes, 1999. 48(4): p. 675-84.

165. Easom, R.A., et al., Correlation of the activation of Ca2+/calmodulin-dependent protein kinase II with the initiation of insulin secretion from perifused pancreatic islets. Endocrinology, 1997. 138(6): p. 2359-64.

166. Wang, Y., et al., Proteomic analysis reveals novel molecules involved in insulin signaling pathway. J Proteome Res, 2006. 5(4): p. 846-55.

167. Aspinwall, C.A., et al., Roles of insulin receptor substrate-1, phosphatidylinositol 3-kinase, and release of intracellular Ca2+ stores in insulin-stimulated insulin secretion in beta -cells. J Biol Chem, 2000. 275(29): p. 22331-8.

168. Roper, M.G., et al., Effect of the insulin mimetic L-783,281 on intracellular Ca2+ and insulin secretion from pancreatic beta-cells. Diabetes, 2002. 51 Suppl 1: p. S43-9.

169. Persaud, S.J., H. Asare-Anane, and P.M. Jones, Insulin receptor activation inhibits insulin secretion from human islets of Langerhans. FEBS Lett, 2002. 510(3): p. 225-8.

170. Zawalich, W.S., G.J. Tesz, and K.C. Zawalich, Are 5-hydroxytryptamine-preloaded beta-cells an appropriate physiologic model system for establishing that insulin stimulates insulin secretion? J Biol Chem, 2001. 276(40): p. 37120-3.

171. Zawalich, W.S. and K.C. Zawalich, Effects of glucose, exogenous insulin, and carbachol on C-peptide and insulin secretion from isolated perifused rat islets. J Biol Chem, 2002. 277(29): p. 26233-7.

172. Meng, R., et al., CK2 phosphorylation of Pdx-1 regulates its transcription factor activity. Cell Mol Life Sci, 2010. 67(14): p. 2481-9.

173. Mosley, A.L., J.A. Corbett, and S. Ozcan, Glucose regulation of insulin gene expression requires the recruitment of p300 by the beta-cell-specific transcription factor Pdx-1. Mol Endocrinol, 2004. 18(9): p. 2279-90.

174. Boini, K.M., et al., Serum- and glucocorticoid-inducible kinase 1 mediates salt sensitivity of glucose tolerance. Diabetes, 2006. 55(7): p. 2059-66.

175. Jeyaraj, S., et al., Role of SGK1 kinase in regulating glucose transport via glucose transporter GLUT4. Biochem Biophys Res Commun, 2007. 356(3): p. 629-35.

176. Palmada, M., et al., SGK1 kinase upregulates GLUT1 activity and plasma membrane expression. Diabetes, 2006. 55(2): p. 421-7.

177. Grahammer, F., et al., Intestinal function of gene-targeted mice lacking serum- and glucocorticoid-inducible kinase 1. Am J Physiol Gastrointest Liver Physiol, 2006. 290(6): p. G1114-23.

178. Dieter, M., et al., Regulation of glucose transporter SGLT1 by ubiquitin ligase Nedd4-2 and kinases SGK1, SGK3, and PKB. Obes Res, 2004. 12(5): p. 862-70.

179. Lang, F., et al., (Patho)physiological significance of the serum- and glucocorticoid-inducible kinase isoforms. Physiol Rev, 2006. 86(4): p. 1151-78.

180. Ullrich, S., et al., Serum- and glucocorticoid-inducible kinase 1 (SGK1) mediates glucocorticoid-induced inhibition of insulin secretion. Diabetes, 2005. 54(4): p. 1090-9.

181. Ullrich, S., et al., Dexamethasone increases Na+/K+ ATPase activity in insulin secreting cells through SGK1. Biochem Biophys Res Commun, 2007. 352(3): p. 662-7.

182. Friedrich, B., et al., Variance of the SGK1 gene is associated with insulin secretion in different European populations: results from the TUEF, EUGENE2, and METSIM studies. PLoS One, 2008. 3(11): p. e3506.

183. Edelman, A.M., D.K. Blumenthal, and E.G. Krebs, Protein serine/threonine kinases. Annu Rev Biochem, 1987. 56: p. 567-613.

184. Cohen, P., The role of protein phosphorylation in human health and disease. The Sir Hans Krebs Medal Lecture. Eur J Biochem, 2001. 268(19): p. 5001-10.

185. Manning, D.W., R Martinez, T Hunter, S Sudarsanam, Full complement of human protein kinases (the human kinome). Science 2002.

186. Manning, G., et al., The protein kinase complement of the human genome. Science, 2002. 298(5600): p. 1912-34.

187. Robinson, D.R., Y.M. Wu, and S.F. Lin, The protein tyrosine kinase family of the human genome. Oncogene, 2000. 19(49): p. 5548-57.

188. Dhanasekaran, N. and E. Premkumar Reddy, Signaling by dual specificity kinases. Oncogene, 1998. 17(11 Reviews): p. 1447-55.

189. Saito, H., Histidine phosphorylation and two-component signaling in eukaryotic cells. Chem Rev, 2001. 101(8): p. 2497-509.

190. Schlessinger, J. and A. Ullrich, Growth factor signaling by receptor tyrosine kinases. Neuron, 1992. 9(3): p. 383-91.

191. Grant, S.K., Therapeutic protein kinase inhibitors. Cell Mol Life Sci, 2009. 66(7): p. 1163-77.

192. Shawver, L.K., D. Slamon, and A. Ullrich, Smart drugs: tyrosine kinase inhibitors in cancer therapy. Cancer Cell, 2002. 1(2): p. 117-23.

193. Eisenhauer, E.A., From the molecule to the clinic--inhibiting HER2 to treat breast cancer. N Engl J Med, 2001. 344(11): p. 841-2.

194. Cobleigh, M.A., et al., Multinational study of the efficacy and safety of humanized anti-HER2 monoclonal antibody in women who have HER2-overexpressing metastatic breast cancer that has progressed after chemotherapy for metastatic disease. J Clin Oncol, 1999. 17(9): p. 2639-48.

195. Yang, J.C., et al., A randomized trial of bevacizumab, an anti-vascular endothelial growth factor antibody, for metastatic renal cancer. N Engl J Med, 2003. 349(5): p. 427-34.

196. Saltz, L.B., et al., Phase II trial of cetuximab in patients with refractory colorectal cancer that expresses the epidermal growth factor receptor. J Clin Oncol, 2004. 22(7): p. 1201-8.

197. Curigliano, G., et al., Breast cancer vaccines: a clinical reality or fairy tale? Ann Oncol, 2006. 17(5): p. 750-62.

198. Disis, M.L., et al., Effect of dose on immune response in patients vaccinated with an her-2/neu intracellular domain protein--based vaccine. J Clin Oncol, 2004. 22(10): p. 1916-25.

199. Stix, G., Shutting down a gene. Antisense drug wins approval. Sci Am, 1998. 279(5): p. 46, 50.

200. Grossman, S.A., et al., Efficacy and toxicity of the antisense oligonucleotide aprinocarsen directed against protein kinase C-alpha delivered as a 21-day continuous intravenous infusion in patients with recurrent high-grade astrocytomas. Neuro Oncol, 2005. 7(1): p. 32-40.

201. Villalona-Calero, M.A., et al., A phase I/II study of LY900003, an antisense inhibitor of protein kinase C-alpha, in combination with cisplatin and gemcitabine in patients with advanced non-small cell lung cancer. Clin Cancer Res, 2004. 10(18 Pt 1): p. 6086-93.

202. Hau, P., et al., Inhibition of TGF-beta2 with AP 12009 in recurrent malignant gliomas: from preclinical to phase I/II studies. Oligonucleotides, 2007. 17(2): p. 201-12.

203. Mullen, P., et al., Antisense oligonucleotide targeting of Raf-1: importance of raf-1 mRNA expression levels and raf-1-dependent signaling in determining growth response in ovarian cancer. Clin Cancer Res, 2004. 10(6): p. 2100-8.

204. Liu, Y. and N.S. Gray, Rational design of inhibitors that bind to inactive kinase conformations. Nat Chem Biol, 2006. 2(7): p. 358-64.

205. Traxler, P. and P. Furet, Strategies toward the design of novel and selective protein tyrosine kinase inhibitors. Pharmacol Ther, 1999. 82(2-3): p. 195-206.

206. Zhang, J., P.L. Yang, and N.S. Gray, Targeting cancer with small molecule kinase inhibitors. Nat Rev Cancer, 2009. 9(1): p. 28-39.

207. Liu, Y., et al., Structural basis for selective inhibition of Src family kinases by PP1. Chem Biol, 1999. 6(9): p. 671-8.

208. Gray, N.S., et al., Exploiting chemical libraries, structure, and genomics in the search for kinase inhibitors. Science, 1998. 281(5376): p. 533-8.

209. Schindler, T., et al., Structural mechanism for STI-571 inhibition of abelson tyrosine kinase. Science, 2000. 289(5486): p. 1938-42.

210. Lawrie, A.M., et al., Protein kinase inhibition by staurosporine revealed in details of the molecular interaction with CDK2. Nat Struct Biol, 1997. 4(10): p. 796-801.

211. Vesely, J., et al., Inhibition of cyclin-dependent kinases by purine analogues. Eur J Biochem, 1994. 224(2): p. 771-86.

212. Arcaro, A. and M.P. Wymann, Wortmannin is a potent phosphatidylinositol 3-kinase inhibitor: the role of phosphatidylinositol 3,4,5-trisphosphate in neutrophil responses. Biochem J, 1993. 296 (Pt 2): p. 297-301.

213. Motzer, R.J., et al., Sunitinib efficacy against advanced renal cell carcinoma. J Urol, 2007. 178(5): p. 1883-7.

214. Motzer, R.J., et al., Sunitinib versus interferon alfa in metastatic renal-cell carcinoma. N Engl J Med, 2007. 356(2): p. 115-24.

215. Millauer, B., et al., Glioblastoma growth inhibited in vivo by a dominant-negative Flk-1 mutant. Nature, 1994. 367(6463): p. 576-9.

216. (FDA), U.F.a.D.A., FDA approves Sutent for advanced pancreatic tumors (NET). 2011.

217. Barrios, C.H., et al., Phase II trial of continuous once-daily dosing of sunitinib as first-line treatment in patients with metastatic renal cell carcinoma. Cancer, 2012. 118(5): p. 1252-9.

218. (FDA), U.F.a.D.A., FDA approves new treatment for gastrointestinal and kidney cancer. 2006.

219. Abrams, T.J., et al., SU11248 inhibits KIT and platelet-derived growth factor receptor beta in preclinical models of human small cell lung cancer. Mol Cancer Ther, 2003. 2(5): p. 471-8.

220. Mendel, D.B., et al., In vivo antitumor activity of SU11248, a novel tyrosine kinase inhibitor targeting vascular endothelial growth factor and platelet-derived growth factor receptors: determination of a pharmacokinetic/pharmacodynamic relationship. Clin Cancer Res, 2003. 9(1): p. 327-37.

221. O'Farrell, A.M., et al., SU11248 is a novel FLT3 tyrosine kinase inhibitor with potent activity in vitro and in vivo. Blood, 2003. 101(9): p. 3597-605.

222. O'Farrell, A.M., et al., An innovative phase I clinical study demonstrates inhibition of FLT3 phosphorylation by SU11248 in acute myeloid leukemia patients. Clin Cancer Res, 2003. 9(15): p. 5465-76.

223. Sun, L., et al., Discovery of 5-[5-fluoro-2-oxo-1,2- dihydroindol-(3Z)-ylidenemethyl]-2,4-dimethyl-1H-pyrrole-3-carboxylic acid (2-diethylaminoethyl)amide, a novel tyrosine kinase inhibitor targeting vascular endothelial and platelet-derived growth factor receptor tyrosine kinase. J Med Chem, 2003. 46(7): p. 1116-9.

224. Osusky, K.L., et al., The receptor tyrosine kinase inhibitor SU11248 impedes endothelial cell migration, tubule formation, and blood vessel formation in vivo, but has little effect on existing tumor vessels. Angiogenesis, 2004. 7(3): p. 225-33.

225. Gu, T.L., et al., Survey of activated FLT3 signaling in leukemia. PLoS One, 2011. 6(4): p. e19169.

226. Masson, K. and L. Ronnstrand, Oncogenic signaling from the hematopoietic growth factor receptors c-Kit and Flt3. Cell Signal, 2009. 21(12): p. 1717-26.

227. Naoe, T. and H. Kiyoi, Normal and oncogenic FLT3. Cell Mol Life Sci, 2004. 61(23): p. 2932-8.

228. Tornillo, L. and L.M. Terracciano, An update on molecular genetics of gastrointestinal stromal tumours. J Clin Pathol, 2006. 59(6): p. 557-63.

229. Duensing, A., et al., Biology of gastrointestinal stromal tumors: KIT mutations and beyond. Cancer Invest, 2004. 22(1): p. 106-16.

230. Lin, C.C., RET mutations and medullary thyroid cancer. J Formos Med Assoc, 2011. 110(11): p. 731; author reply 732.

231. Sharma, B.P. and D. Saranath, RET gene mutations and polymorphisms in medullary thyroid carcinomas in Indian patients. J Biosci, 2011. 36(4): p. 603-11.

232. Murakumo, Y., et al., RET and neuroendocrine tumors. Pituitary, 2006. 9(3): p. 179-92.

233. Sapi, E., The role of CSF-1 in normal physiology of mammary gland and breast cancer: an update. Exp Biol Med (Maywood), 2004. 229(1): p. 1-11.

234. Sapi, E. and B.M. Kacinski, The role of CSF-1 in normal and neoplastic breast physiology. Proc Soc Exp Biol Med, 1999. 220(1): p. 1-8.

235. Murray, L.J., et al., SU11248 inhibits tumor growth and CSF-1R-dependent osteolysis in an experimental breast cancer bone metastasis model. Clin Exp Metastasis, 2003. 20(8): p. 757-66.

236. Morimoto, A.M., et al., Gene expression profiling of human colon xenograft tumors following treatment with SU11248, a multitargeted tyrosine kinase inhibitor. Oncogene, 2004. 23(8): p. 1618-26.

237. Yee, K.W., et al., Synergistic effect of SU11248 with cytarabine or daunorubicin on FLT3 ITD-positive leukemic cells. Blood, 2004. 104(13): p. 4202-9.

238. Rini, B.I., Sunitinib. Expert Opin Pharmacother, 2007. 8(14): p. 2359-69.

239. Huynh, H., et al., Sunitinib (SUTENT, SU11248) suppresses tumor growth and induces apoptosis in xenograft models of human hepatocellular carcinoma. Curr Cancer Drug Targets, 2009. 9(6): p. 738-47.

240. Delbaldo, C., et al., Sunitinib in advanced pancreatic neuroendocrine tumors: latest evidence and clinical potential. Ther Adv Med Oncol, 2012. 4(1): p. 9-18.

241. Theou-Anton, N., et al., Benefit-risk assessment of sunitinib in gastrointestinal stromal tumours and renal cancer. Drug Saf, 2009. 32(9): p. 717-34.

242. Choong, N.W., et al., Phase II study of sunitinib malate in head and neck squamous cell carcinoma. Invest New Drugs, 2010. 28(5): p. 677-83.

243. Zhu, A.X., et al., Efficacy, safety, and potential biomarkers of sunitinib monotherapy in advanced hepatocellular carcinoma: a phase II study. J Clin Oncol, 2009. 27(18): p. 3027-35.

244. Faivre, S., et al., Safety, pharmacokinetic, and antitumor activity of SU11248, a novel oral multitarget tyrosine kinase inhibitor, in patients with cancer. J Clin Oncol, 2006. 24(1): p. 25-35.

245. Demetri, G.D., et al., Efficacy and safety of sunitinib in patients with advanced gastrointestinal stromal tumour after failure of imatinib: a randomised controlled trial. Lancet, 2006. 368(9544): p. 1329-38.

246. Kassem, M.G., A.F. Motiur Rahman, and H.M. Korashy, Sunitinib malate. Profiles Drug Subst Excip Relat Methodol, 2012. 37: p. 363-88.

247. Kulke, M.H., et al., Activity of sunitinib in patients with advanced neuroendocrine tumors. J Clin Oncol, 2008. 26(20): p. 3403-10.

248. Pfizer, I., SUTENT (sunitinib malate) prescribing information. 2007.

249. JM., S., SU-11248 SUGEN. Curr Op in Investig. Drugs, 2004. 5:1329^39.

250. Zou, C., Y. Wang, and Z. Shen, 2-NBDG as a fluorescent indicator for direct glucose uptake measurement. J Biochem Biophys Methods, 2005. 64(3): p. 207-15.

251. J. Sambrook, E.F.F., T. Maniatis, Molecular Cloning: A Laboratory Manual. (2nd Edn.)Cold Spring Harbor Laboratory Press, Cold Spring Harbor, NY (1989), 1990.

252. Gershoni, J.M. and G.E. Palade, Protein blotting: principles and applications. Anal Biochem, 1983. 131(1): p. 1-15.

253. Green, H. and O. Kehinde, An established preadipose cell line and its differentiation in culture. II. Factors affecting the adipose conversion. Cell, 1975. 5(1): p. 19-27.

254. Scheen, A.J., [From obesity to diabetes or the natural history of abnormalities in the secretion and action of insulin]. Rev Med Liege, 1992. 47(7): p. 325-37.

255. Nishioka, C., et al., Sunitinib, an orally available receptor tyrosine kinase inhibitor, induces monocytic differentiation of acute myelogenous leukemia cells that is enhanced by 1,25-dihydroxyvitamin D(3). Leukemia, 2009. 23(11): p. 2171-3.

256. Cernkovich, E.R., et al., Midkine is an autocrine activator of signal transducer and activator of transcription 3 in 3T3-L1 cells. Endocrinology, 2007. 148(4): p. 1598-604.

257. Magun, R., et al., Expression of a constitutively activated form of protein kinase B (c-Akt) in 3T3-L1 preadipose cells causes spontaneous differentiation. Endocrinology, 1996. 137(8): p. 3590-3.

258. Harrell, N.B., et al., Essential role of p38 MAPK for activation of skeletal muscle glucose transport by lithium. Arch Physiol Biochem, 2007. 113(4-5): p. 221-7.

259. Yang, S.N. and P.O. Berggren, CaV2.3 channel and PKClambda: new players in insulin secretion. J Clin Invest, 2005. 115(1): p. 16-20.

260. Arkhammar, P., et al., Protein kinase C modulates the insulin secretory process by maintaining a proper function of the beta-cell voltage-activated Ca2+ channels. J Biol Chem, 1994. 269(4): p. 2743-9.

261. Schultze, S.M., et al., PI3K/AKT, MAPK and AMPK signalling: protein kinases in glucose homeostasis. Expert Rev Mol Med, 2012. 14: p. e1.

262. Lee, S.J., et al., Involvement of Ca2+/calmodulin kinase II (CaMK II) in genistein-induced potentiation of leucine/glutamine-stimulated insulin secretion. Mol Cells, 2009. 28(3): p. 167-74.

263. Couto, F.M., et al., Exenatide blocks JAK1-STAT1 in pancreatic beta cells. Metabolism, 2007. 56(7): p. 915-8.

264. Roccisana, J., et al., Targeted inactivation of hepatocyte growth factor receptor c-met in beta-cells leads to defective insulin secretion and GLUT-2 downregulation without alteration of beta-cell mass. Diabetes, 2005. 54(7): p. 2090-102.

265. Bernal-Mizrachi, E., et al., Defective insulin secretion and increased susceptibility to experimental diabetes are induced by reduced Akt activity in pancreatic islet beta cells. J Clin Invest, 2004. 114(7): p. 928-36.

266. Leibiger, B., et al., Insulin-feedback via PI3K-C2alpha activated PKBalpha/Akt1 is required for glucose-stimulated insulin secretion. FASEB J, 2010. 24(6): p. 1824-37.

267. Walther, R.G.W.A., 17498 Neuenkirchen, DE), MODULATION OF THE SYNTHESIS OF INSULIN, 2007, Ernst-moritz-arndt-universität, Greifswald (Domstr. 14, 17487 Greifswald, DE).

268. Wilkerson, H.L. and B. Glenn, A preliminary report on a study of blood sugar screening levels. Am J Public Health Nations Health, 1951. 41(4): p. 440-6.

269. Cassmeyer, V.L., Preventing, recognizing, and treating diabetic shock (continuing education credit). Nurs Life, 1987. 7(1): p. 33-40.

270. Poitout, V., et al., Morphological and functional characterization of beta TC-6 cells--an insulin-secreting cell line derived from transgenic mice. Diabetes, 1995. 44(3): p. 306-13.

271. Neumann, L., K. von Konig, and D. Ullmann, HTS reporter displacement assay for fragment screening and fragment evolution toward leads with optimized binding kinetics, binding selectivity, and thermodynamic signature. Methods Enzymol, 2011. 493: p. 299-320.

272. Neumann, L., et al., Fragment-based lead generation: identification of seed fragments by a highly efficient fragment screening technology. J Comput Aided Mol Des, 2009.

273. Cheng, H.C., The power issue: determination of KB or Ki from IC50. A closer look at the Cheng-Prusoff equation, the Schild plot and related power equations. J Pharmacol Toxicol Methods, 2001. 46(2): p. 61-71.

274. Mataga, N., et al., Establishment of a novel chondrocyte-like cell line derived from transgenic mice harboring the temperature-sensitive simian virus 40 large T-antigen gene. J Bone Miner Res, 1996. 11(11): p. 1646-54.

275. Bardouille, C., et al., Growth and differentiation of permanent and secondary mouse myogenic cell lines on microcarriers. Appl Microbiol Biotechnol, 2001. 55(5): p. 556-62.

276. Cuenda, A. and A.R. Nebreda, p38delta and PKD1: kinase switches for insulin secretion. Cell, 2009. 136(2): p. 209-10.

277. Jiang, Y., et al., Characterization of the structure and function of the fourth member of p38 group mitogen-activated protein kinases, p38delta. J Biol Chem, 1997. 272(48): p. 30122-8.

278. Goke, R., et al., Exendin-4 is a high potency agonist and truncated exendin-(9-39)-amide an antagonist at the glucagon-like peptide 1-(7-36)-amide receptor of insulin-secreting beta-cells. J Biol Chem, 1993. 268(26): p. 19650-5.

279. Siiteri, P.K., Adipose tissue as a source of hormones. Am J Clin Nutr, 1987. 45(1 Suppl): p. 277-82.

280. Falcao-Pires, I., et al., Physiological, pathological and potential therapeutic roles of adipokines. Drug Discov Today, 2012.

281. Cariou, B., B. Charbonnel, and B. Staels, Thiazolidinediones and PPARgamma agonists: time for a reassessment. Trends Endocrinol Metab, 2012. 23(5): p. 205-15.

282. Voelker, R., Diabetes drug is linked with bladder cancer risk. JAMA, 2012. 307(24): p. 2577.

283. Ammon, H.P., C. Reiber, and E.J. Verspohl, Indirect evidence for short-loop negative feedback of insulin secretion in the rat. J Endocrinol, 1991. 128(1): p. 27-34.

284. Argoud, G.M., D.S. Schade, and R.P. Eaton, Insulin suppresses its own secretion in vivo. Diabetes, 1987. 36(8): p. 959-62.

285. Garvey, W.T., et al., Modulation of insulin secretion by insulin and glucose in type II diabetes mellitus. J Clin Endocrinol Metab, 1985. 60(3): p. 559-68.

286. Elahi, D., et al., Feedback inhibition of insulin secretion by insulin: relation to the hyperinsulinemia of obesity. N Engl J Med, 1982. 306(20): p. 1196-202.

287. Anderwald, C., et al., Insulin infusion during normoglycemia modulates insulin secretion according to whole-body insulin sensitivity. Diabetes Care, 2011. 34(2): p. 437-41.

288. Araki, E., et al., Alternative pathway of insulin signalling in mice with targeted disruption of the IRS-1 gene. Nature, 1994. 372(6502): p. 186-90.

289. Burks, D.J. and M.F. White, IRS proteins and beta-cell function. Diabetes, 2001. 50 Suppl 1: p. S140-5.

290. Nogueira, T.C., et al., Involvement of phosphatidylinositol-3 inase/AKT/PKCzeta/lambda pathway in the effect of palmitate on glucose-induced insulin secretion. Pancreas, 2008. 37(3): p. 309-15.

291. Araujo, E.P., et al., Restoration of insulin secretion in pancreatic islets of protein-deficient rats by reduced expression of insulin receptor substrate (IRS)-1 and IRS-2. J Endocrinol, 2004. 181(1): p. 25-38.

292. Zawalich, W.S., G.J. Tesz, and K.C. Zawalich, Inhibitors of phosphatidylinositol 3-kinase amplify insulin release from islets of lean but not obese mice. J Endocrinol, 2002. 174(2): p. 247-58.

293. Hagiwara, S., et al., An inhibitory role for phosphatidylinositol 3-kinase in insulin secretion from pancreatic B cell line MIN6. Biochem Biophys Res Commun, 1995. 214(1): p. 51-9.

294. Cui, X., et al., Akt signals upstream of L-type calcium channels to optimize insulin secretion. Pancreas, 2012. 41(1): p. 15-21.

295. Sorenson, R.L. and T.C. Brelje, Prolactin receptors are critical to the adaptation of islets to pregnancy. Endocrinology, 2009. 150(4): p. 1566-9.

296. Eberhard, D. and E. Lammert, The pancreatic beta-cell in the islet and organ community. Curr Opin Genet Dev, 2009. 19(5): p. 469-75.

297. Liu, S.C., W.S. Lane, and G.E. Lienhard, Cloning and preliminary characterization of a 105 kDa protein with an N-terminal kinase-like domain. Biochim Biophys Acta, 2000. 1517(1): p. 148-52.

298. Burman, J.L., J.N. Hamlin, and P.S. McPherson, Scyl1 regulates Golgi morphology. PLoS One, 2010. 5(3): p. e9537.

299. Burman, J.L., et al., Scyl1, mutated in a recessive form of spinocerebellar neurodegeneration, regulates COPI-mediated retrograde traffic. J Biol Chem, 2008. 283(33): p. 22774-86.

300. Andrade, M.A. and P. Bork, HEAT repeats in the Huntington's disease protein. Nat Genet, 1995. 11(2): p. 115-6.

301. Pelkmans, L., et al., Genome-wide analysis of human kinases in clathrin- and caveolae/raft-mediated endocytosis. Nature, 2005. 436(7047): p. 78-86.

302. Conner, S.D. and S.L. Schmid, CVAK104 is a novel poly-L-lysine-stimulated kinase that targets the beta2-subunit of AP2. J Biol Chem, 2005. 280(22): p. 21539-44.

303. Palczewski, K. and J.L. Benovic, G-protein-coupled receptor kinases. Trends Biochem Sci, 1991. 16(10): p. 387-91.

304. Lefkowitz, R.J., Seven transmembrane receptors: something old, something new. Acta Physiol (Oxf), 2007. 190(1): p. 9-19.

305. Kohout, T.A. and R.J. Lefkowitz, Regulation of G protein-coupled receptor kinases and arrestins during receptor desensitization. Mol Pharmacol, 2003. 63(1): p. 9-18.

306. Patial, S., et al., G-protein coupled receptor kinases mediate TNFalpha-induced NFkappaB signaling via direct interaction with and phosphorylation of IkappaBalpha. Biochem J, 2009.

307. Sorriento, D., et al., The G-protein-coupled receptor kinase 5 inhibits NFkappaB transcriptional activity by inducing nuclear accumulation of IkappaB alpha. Proc Natl Acad Sci U S A, 2008. 105(46): p. 17818-23.

308. Larsen, L., et al., Extracellular signal-regulated kinase is essential for interleukin-1-induced and nuclear factor kappaB-mediated gene expression in insulin-producing INS-1E cells. Diabetologia, 2005. 48(12): p. 2582-90.

309. Tseng, C.C. and X.Y. Zhang, Role of G protein-coupled receptor kinases in glucose-dependent insulinotropic polypeptide receptor signaling. Endocrinology, 2000. 141(3): p. 947-52.

310. Mayor, F., Jr., et al., G Protein-coupled receptor kinase 2 (GRK2): A novel modulator of insulin resistance. Arch Physiol Biochem, 2011. 117(3): p. 125-30.

311. Garcia-Guerra, L., et al., G protein-coupled receptor kinase 2 plays a relevant role in insulin resistance and obesity. Diabetes, 2010. 59(10): p. 2407-17.

312. Usui, I., et al., GRK2 is an endogenous protein inhibitor of the insulin signaling pathway for glucose transport stimulation. EMBO J, 2004. 23(14): p. 2821-9.

313. Chen, M., et al., G Protein-coupled receptor kinases phosphorylate LRP6 in the Wnt pathway. J Biol Chem, 2009. 284(50): p. 35040-8.

314. Mani, A., et al., LRP6 mutation in a family with early coronary disease and metabolic risk factors. Science, 2007. 315(5816): p. 1278-82.

315. Liu, W., et al., Low density lipoprotein (LDL) receptor-related protein 6 (LRP6) regulates body fat and glucose homeostasis by modulating nutrient sensing pathways and mitochondrial energy expenditure. J Biol Chem, 2012. 287(10): p. 7213-23.

316. Wang, F., et al., GRK5 deficiency decreases diet-induced obesity and adipogenesis. Biochem Biophys Res Commun, 2012. 421(2): p. 312-7.

317. Li, H., et al., A Genome-Wide Association Study Identifies GRK5 and RASGRP1 as Type 2 Diabetes Loci in Chinese Hans. Diabetes, 2012.

318. Lagier-Tourenne, C., et al., ADCK3, an ancestral kinase, is mutated in a form of recessive ataxia associated with coenzyme Q10 deficiency. Am J Hum Genet, 2008. 82(3): p. 661-72.

319. Himanen, J.P. and D.B. Nikolov, Eph signaling: a structural view. Trends Neurosci, 2003. 26(1): p. 46-51.

320. Pasquale, E.B., Eph receptor signalling casts a wide net on cell behaviour. Nat Rev Mol Cell Biol, 2005. 6(6): p. 462-75.

321. Konstantinova, I., et al., EphA-Ephrin-A-mediated beta cell communication regulates insulin secretion from pancreatic islets. Cell, 2007. 129(2): p. 359-70.

322. Hagren, O.I. and A. Tengholm, Glucose and insulin synergistically activate phosphatidylinositol 3-kinase to trigger oscillations of phosphatidylinositol 3,4,5-trisphosphate in beta-cells. J Biol Chem, 2006. 281(51): p. 39121-7.

323. Thore, S., A. Wuttke, and A. Tengholm, Rapid turnover of phosphatidylinositol-4,5-bisphosphate in insulin-secreting cells mediated by Ca2+ and the ATP-to-ADP ratio. Diabetes, 2007. 56(3): p. 818-26.

324. Below, J.E., et al., Genome-wide association and meta-analysis in populations from Starr County, Texas, and Mexico City identify type 2 diabetes susceptibility loci and enrichment for expression quantitative trait loci in top signals. Diabetologia, 2011. 54(8): p. 2047-55.

325. Isaeva, A.R. and V.I. Mitev, CK2 is acting upstream of MEK3/6 as a part of the signal control of ERK1/2 and p38 MAPK during keratinocytes autocrine differentiation. Z Naturforsch C, 2011. 66(1-2): p. 83-6.

326. Khavin, I.B., [Hypoglycemia in diabetes mellitus]. Klin Med (Mosk), 1967. 45(3): p. 106-10.

327. Tseng, C.C., et al., Chronic desensitization of the glucose-dependent insulinotropic polypeptide receptor in diabetic rats. Am J Physiol, 1996. 270(4 Pt 1): p. E661-6.

8 APPENDIX

8.1 ABBREVIATIONS

°C	degree celsius
2-NBDG	2-[N-7-nitrobenz-2-oxa-1,3-diazol-4-yl)-amino]-2-deoxy-d-glucose]
MTT	3-4,5-Dimethylthiazol-2-yl-2,5-diphenyltetrazolium bromide
ABL	c-abl oncogene 1, receptor tyrosine kinase
ADCK1	aarF-containing kinase 1
αGI	alpha-glycosidase inhibitors
AIM	adipogenesis initiation media
AKT1	thymoma viral proto-oncogene 1
AML	acute myeloid leukemia
AMPK	AMP-dependent protein kinase
APC	antigen-presenting cell
APM	adipogenesis progression media
APS	ammonium peroxodisulfate
ATP	adenosine triphosphate
CaMK	calcium/calmodulin-dependent protein kinases
CaMKK2	calcium/calmodulin-dependent protein kinase kinase 2
CASK	calcium/calmodulin-dependent protein serine kinase
Cbl	signal transduction protein Cbl
Cdk6/Crk2	cyclin-dependent kinase6
cDNA	complementary DNA
CERK	ceramide kinase
CHKB	choline kinase beta
CHX	cycloheximid
CK2/CSNK2A1	serine/threonine casein kinase 2, alpha 1 polypeptide
CMV	cytomegalovirus retinitis
Cpd	compound
CSF-1R	colony-stimulating factors type 1
CTLA4	cytotoxic T-lymphocyte-associated protein 4
CVBs	oxsackie b viruses
DAG	diacylglycerol
DMEM	Dulbecco's modified eagle medium
DMSO	dimethylsulfoxide
DPP-IV	dipeptidyl-peptidase-IV
EGF	epidermal growth factor
EGFR	epidermal growth factor receptor
ELISA	enzyme-linked immunosorbent assay
EPHA4	Eph receptor A4
eQTL	expression quantitative trait loci
ER	endoplasmatic reticulum
ERK1/2	mitogen-activated protein kinase 1 and 2
FACS	fluorescence activated cell sorting
FCS	fetal calf serum
FDA	Food and Drug Administration (USA)
FFA	free fatty acids
FLT3	fetal liver tyrosine kinase receptor 3

FP	fluorescence polarization
FUK	fucokinase
Gab-1	GRB2-associated binding protein 1
GCK	glucokinase
GDM	Gestational Diabetes Mellitus
GIST	gastrointestinal stromal tumor
GLP-1	glucagon-like peptide-1
GLUT4	glucose transporter type 4
Grb2	growth factor receptor-bound protein 2
GRK5 / GPRK5	G protein-coupled receptor kinase 5
GSK3A	glycogen synthase kinase 3 alpha
GWAS	genome-wide association studies
HLA	human leukocyte antigen
HNFs	hepatocyte nuclear factors
HPL	human placental lactogen
HTVS	high titer virus stocks
IBMX	3-Isobutyl-1-methylxanthin
IGF	insulin-like growth factor
InsR	insulin receptor
IP2	phospholipid-phosphatidyl-inositol-4,5-bisphosphate
IP3	inositol-1, 4, 5-triphosphate
IRS	insulin receptor substrate
ITPKA	inositol-trisphosphate 3-kinase A
JAK1	janus kinase 1
JNK	c-jun N-terminal kinase
JNK	JUN N-terminal kinas
KCNH2	potassium voltage-gated channel, subfamily H, member 2
kDa	kilodalton
KIT	proto-oncogene tyrosine-protein kinase
LCK	lymphocyte-specific protein tyrosine kinase
LGA	"large for gestational age infant"
M	molar
m	milli
MAP2K3	mitogen-activated protein kinase kinase 3
MAP3K9	mitogen-activated protein kinase kinase kinase 9
MAPK13/p38δ	mitogen-activated protein kinase 13
MET	met proto-oncogene kinase
MOA	modes of action
MODY	maturity-onset diabetes of young
mRCC	metastatic renal cell carcinoma
NCS	newborn calf serum
NDM	neonatal diabetes mellitus
NEFA	non esterified fatty acids
NET	neuroendocrine tumors
NET	pancreatic neuroendocrine tumors
NEUROD1	neurogenic differentiation 1 factor
NIH	National Institutes of Health
NOD	non-obese diabetic
NSCLC	non-small-cell lung cancer

OD	optical density
p38/MAPK14	mitogen-activated protein kinase 14
PBS	phosphate-buffered saline
PCR	polymerase chain reaction
PDGFR	platelet-derived growth factor receptor
PDK1	phosphoinositide-dependent kinase 1
PI3K	phosphoinositide-3-kinase
PIK3C3	phosphoinositide-3-kinase, class 3
PIP5K1C	phosphatidylinositol-4-phosphate 5-kinase, type I, gamma
PPARγ	peroxisome proliferator-activated receptor gamma
PRKCB	protein kinase C beta
PRKCN	protein kinase D3
PTK	protein tyrosine kinase
RET	neurotropic factor receptor
RIOK2	RIO kinase 2
RNAi	ribonucleic acid interference
ROR1	receptor tyrosine kinase-like orphan receptor 1
SCYL1	SCY1-like kinase 1
SDS	sodium dodecyl sulfate
SGK1	serum/glucocorticoid regulated kinase 1
SNPs	single-nucleotide polymorphism
STAT3	signal transducer and activator of transcription 3
stdev	standard deviation
stE	standard error
STK	serine/threonine protein kinases
TBC1D1	TBC1 domain family member 1
TEMED	N'N'N'N'-Tetramethylethylenediamine
TKIs	tyrosine kinase inhibitors
TLK2	tousled-like kinase 2
TNF-α	tumour necrosis factor-α
μ	Micro
UCLA	University of California
VEGF	vascular endolial growth factor
VEGFR	vascular endolial growth factor receptors
VNTRs	variable number of tandem repeats

9 ACKNOWLEDGEMENTS